

**INVESTIGATION OF ASYMMETRIC PLATINUM (IV)  
COMPLEXES AS ANTICANCER PRODRUGS**

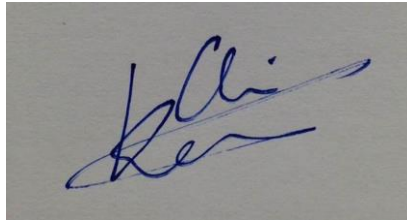
**CHIN CHEE FEI**  
*(B. Sci (Hons.), NUS)*

**A THESIS SUBMITTED**  
**FOR THE DEGREE OF DOCTOR OF PHILOSOPHY**  
**OF SCIENCE**  
**DEPARTMENT OF CHEMISTRY**  
**NATIONAL UNIVERSITY OF SINGAPORE**

**2014**

## DECLARATION

I hereby declare that this thesis is my original work and it has been written by me in its entirety. I have duly acknowledged all the sources of information which have been used in the thesis. This thesis has also not been submitted for any degree in any university previously.



---

Chin Chee Fei  
17 December 2014

## **ACKNOWLEDGEMENTS**

I am indebted to many people for the successful completion of my dissertation. First and foremost, to my PhD supervisor Dr Ang Wee Han for his continuous guidance, patience and faith with me during this 4.5 years journey. I am very thankful for the numerous opportunities he has given me in terms of projects and oversea conferences. He is also pivotal in assisting me to obtain the Solvay Graduate Fellowship in Science which allowed me to gain employment upon graduation. Dr Ang has been a role model for me during this period and his teachings will be beneficial for me when I entered the workforce. I would also like to thank my FYP supervisor Dr Huynh Han Vinh for teaching me synthetic skills when I was just an 'infant' in research. Without him, I would probably not have developed a passion for research and pursue PhD. In addition, I also thanked Dr Giorgia Pastorin for her guidance in my carbon nanotubes project.

I would also like to take this opportunity to thank Tian Quan and Siew Qi for showing me the rope in the biological arena. I would not be able to learn the biological aspects of my work in such a short time without them. Special thanks to Siew Qi for helping me out in some of the biological assays. My stay here would not have been made more enjoyable without my fellow PhD colleagues, Jun Xiang, Daniel Wong, Mun Juinn and Jian Yu. A significant chapter of the work reported here was contributed by Agnes Thng as part of her FYP project for which I gratefully acknowledged.

I am also grateful to the NUS Chemistry technical staffs, namely Mdm Han, Mdm Leng, Mdm Wong, Dr Wu, and Miss Tan for their assistance in the analytical aspects of my PhD studies. Special thanks to Miss Tan Geok Kheng who has been also been a trusted friend and confidant during my stay in NUS.

Lastly, I thank my family for their years of love, emotional support and encouragement that allowed me to come thus far in life. They have truly been my pillar of strength all these years and I dedicate this work to them. I would also like to thank my closest friends for encouraging me to take up the PhD scholarship four years ago and standing by me all these years.

Once again, thank you everyone who has played a part in my eight and a half years stay in NUS.

# TABLE OF CONTENTS

|   |             |
|---|-------------|
| <i>Acknowledgements</i> .....   | <i>i</i>    |
| <i>Table of Contents</i> .....  | <i>iii</i>  |
| <i>Summary</i> .....  | <i>vii</i>  |
| <i>List of Tables</i> .....   | <i>ix</i>   |
| <i>List of Figures</i> .....  | <i>x</i>    |
| <i>List of Schemes</i> .....  | <i>xiii</i> |
| <i>List of Abbreviations</i> .....  | <i>xiv</i>  |
| <br>  |             |
| <b>Chapter 1 - Introduction</b> .....   | <b>1</b>    |
| 1.1    Platinum(IV) Bis-Carboxylates as Anticancer Prodrugs.....                              | 5           |
| 1.2    Synthesis of Platinum(IV) Complexes .....  | 8           |
| 1.2.1    Classical Oxidation of Platinum(II) to Platinum(IV) complexes.....                   | 8           |
| 1.2.2    Non-Classical Oxidation of Platinum(II) to Platinum(IV) complexes .....              | 9           |
| 1.2.3    Classical Synthesis of Symmetric Bis-Ammine Platinum(IV) Complexes .....             | 11          |
| 1.2.4    Non-Classical Synthesis of Asymmetric Bis-Ammine Platinum(IV) Complexes .....        | 14          |
| 1.3    Applications of Platinum(IV) Bis-Carboxylates .....                                    | 16          |
| 1.3.1    Platinum(IV) Complexes with Lipophilic Axial Ligands.....                            | 16          |
| 1.3.2    Platinum(IV) Complexes with Bioactive Axial Ligands .....                            | 21          |
| 1.3.3    Targeted Delivery of Platinum(IV) Complexes using Drug Carriers .....                | 29          |
| 1.4    Summary .....  | 39          |
| <br>  |             |
| <b>Chapter 2 - Research Objectives and Thesis Layout</b> .....                                | <b>41</b>   |
| <br>  |             |
| <b>Chapter 3 - Developing a Novel Class of Asymmetric Platinum(IV) Bis-Carboxylates</b> ..... | <b>44</b>   |
| 3.1    Introduction .....   | 44          |

|     |   |    |
|-----|---|----|
| 3.2 | Synthetic Strategy to Develop Asymmetric Platinum(IV) Bis-Carboxylates.....             | 45 |
| 3.3 | Synthesis of Platinum(IV) Mono-Carboxylates <b>A-I</b> .....                            | 47 |
| 3.4 | Synthesis of Asymmetric Platinum(IV) Bis-Carboxylates <b>3-22</b> .....                 | 50 |
| 3.5 | Characterization of Synthesized Platinum(IV) Complexes <b>A-I</b> and <b>3-22</b> ..... | 54 |
| 3.6 | Summary .....   | 58 |
| 3.7 | Experimental Procedures.....  | 59 |

## **Chapter 4 – Tuning the Pharmacological Properties of Asymmetric Platinum(IV) Bis-Carboxylates ..... 73**

|       |   |    |
|-------|---|----|
| 4.1   | Introduction .....  | 73 |
| 4.2   | Evaluating the Tunable Pharmacological Properties of Asymmetric Platinum(IV) Bis-Carboxylates .....                           | 74 |
| 4.2.1 | Evaluating the Tunable Lipophilicity and Aqueous Solubility of Asymmetric Platinum(IV) Bis-Carboxylates.....                  | 75 |
| 4.2.2 | Evaluating the Tunable Anti-Proliferative Properties of Asymmetric Platinum(IV) Bis-Carboxylates .....                        | 78 |
| 4.3   | Evaluation of the Mechanism of Asymmetric Platinum(IV) Bis-Carboxylates .....   | 81 |
| 4.4   | Expanding the Scope of Investigation on Asymmetric Platinum(IV) Bis-Carboxylates .....  | 84 |
| 4.4.1 | Evaluating the Stability of the Expanded Asymmetric Platinum(IV) Bis-Carboxylates Series.....                                 | 86 |
| 4.4.2 | Evaluating the Reduction Rate of the Expanded Asymmetric Platinum(IV) Bis-Carboxylates Series.....                            | 87 |
| 4.4.3 | Evaluating the Lipophilicities and Aqueous Solubilities of the Expanded Asymmetric Platinum(IV) Bis-Carboxylates Series ..... | 91 |
| 4.4.4 | Evaluating the Anti-Proliferative Properties of the Expanded Asymmetric Platinum(IV) Bis-Carboxylates Series .....            | 93 |
| 4.4.5 | Investigation for Inter-Dependency Properties within the Expanded Asymmetric Platinum(IV) Bis-Carboxylates Series .....       | 95 |
| 4.5   | Summary .....   | 97 |
| 4.6   | Experimental Procedures.....  | 98 |

**Chapter 5 - Photoactivatable Properties of Asymmetric Platinum(IV) Bis-Carboxylates..... 103**

|     |  |     |
|-----|--|-----|
| 5.1 | Introduction .....   | 103 |
| 5.2 | Evaluating the Photoreducibility of Platinum(IV) Bis-Carboxylates .....                              | 105 |
| 5.3 | Evaluating the Photoactivation of Platinum(IV) Prodrugs by UV irradiation .....                      | 112 |
| 5.4 | Evaluating the Tunable Photoactivatable Properties Asymmetric of Platinum(IV) Bis-Carboxylates ..... | 115 |
| 5.5 | Evaluating the Photoactivation of Asymmetric Platinum(IV) Bis-Carboxylates by UV irradiation.....    | 116 |
| 5.6 | Summary .....  | 120 |
| 5.7 | Experimental Procedures.....   | 121 |

**Chapter 6 - Targeted Delivery of Dual-Drugs using Asymmetric Platinum(IV) Bis-Carboxylates Entrapped in Multi-Walled Carbon Nanotubes ..... 123**

|       |  |     |
|-------|--|-----|
| 6.1   | Introduction .....   | 124 |
| 6.2   | Synthesis and Characterization.....  | 128 |
| 6.2.1 | Asymmetric Platinum(IV) Bis-Carboxylate <b>23</b> .....                                | 128 |
| 6.2.2 | MWCNT-Platinum(IV) Prodrug Nanoconjugate [23·MWCNTc(RGDfK)] .....                      | 129 |
| 6.3   | Evaluating the Anticancer Properties of [23·MWCNTc(RGDfK)].....                        | 132 |
| 6.3.1 | Stability and Kinetic Properties .....   | 132 |
| 6.3.2 | Anti-Proliferative Property .....  | 133 |
| 6.3.3 | Platinum Uptake in Ishikawa Cells.....   | 135 |
| 6.3.4 | Evaluating the Internalization of [23·MWCNTc(RGDfK)] via Confocal Studies .....        | 136 |
| 6.3.5 | Investigating the Reduction of Asymmetric Platinum(IV) Bis-Carboxylate <b>23</b> ..... | 138 |
| 6.4   | Summary .....  | 139 |
| 6.5   | Experimental Procedures.....   | 140 |

**Chapter 7 - Conclusions ..... 149**

|     |  |     |
|-----|--|-----|
| 7.1 | Future Prospect of Platinum-Based Anticancer Drugs ..... | 151 |
|-----|--|-----|

|                               |     |
|-------------------------------|-----|
| <i>Bibliography</i> .....     | 153 |
| <i>Appendix</i> .....         | 182 |
| <i>Curriculum Vitae</i> ..... | 183 |



## SUMMARY

Platinum-based chemotherapeutic drug *Cisplatin* represents the first line of defence against many tumor malignancies, including lung, ovarian and testicular cancers. Cisplatin exhibits its anticancer activity through the binding to DNA strands, inhibits transcription and triggers apoptosis. However, its efficacy is limited by high toxicity and incidence of drug resistance, prompting the development of more effective platinum-based anticancer agents. One strategy to overcome these limitations is to develop kinetically stable and inert platinum(IV) prodrugs that can resist premature aquation and binding to essential plasma proteins. *Satraplatin* is currently the most successful platinum(IV) prodrug till date, and is currently undergoing various clinical evaluations against cancers. The development of platinum(IV) prodrugs allowed a more diverse anticancer strategies by varying the axial ligands while keeping the platinum(II) pharmacophores intact. These prodrugs strategies include the use of lipophilic ligands, bioactive ligands, targeted drugs delivery, and photoactivation of platinum(IV) complexes.

Classical symmetric platinum(IV) prodrug complexes are limited in their synthetic utility as their axial ligand sites for functionalization are identical and cannot fully exploit the vast potential of these prodrugs strategies. Hence, we developed a new class of asymmetric platinum(IV) bis-carboxylates based on the *cisplatin* template through the strategy of sequential carboxylation on a platinum(IV) bis-hydroxo precursor. This will allow us to access platinum(IV)

complexes with different axial ligands on the same scaffolds to achieve greater structural and functional diversity. We applied this strategy to develop functionalized platinum(IV) prodrug complexes in the context of tuning their pharmacological properties, developing photoactivatable prodrug complexes that can be triggered by UV irradiation, as well as achieving ratiometric delivery of drug combinations. In addition, the rationale and synthetic considerations for each of the design strategies are discussed.

## LIST OF TABLES

|  |     |
|--|-----|
| <b>Table 1.</b> Comparison of bond distances (Å) and angles (°) of <b>A</b> , <b>1</b> , <b>2</b> and <b>3</b> ..... | 58  |
| <b>Table 2.</b> Properties of platinum(IV) complexes .....   | 77  |
| <b>Table 3.</b> Stability and reduction rates of asymmetric platinum(IV) complexes...                                | 90  |
| <b>Table 4.</b> Properties of asymmetric platinum(IV) complexes .....  | 93  |
| <b>Table 5.</b> UV-Vis spectroscopy data of platinum(IV) complexes .....   | 115 |
| <b>Table 6.</b> IC <sub>50</sub> values (μM) against cancer cell lines .....   | 135 |
| <b>Table 7.</b> Selected X-ray crystallographic data for <b>A</b> and <b>3</b> .....                                 | 182 |

## LIST OF FIGURES

|  |    |
|--|----|
| <b>Figure 1.</b> Chemical structures of cisplatin and the anticancer agents used in combination therapy.....   | 1  |
| <b>Figure 2.</b> Schematic diagram showing the mode of action of cisplatin upon administration .....   | 2  |
| <b>Figure 3.</b> Chemical structures of FDA-approved platinum(II) anticancer agents .....  | 3  |
| <b>Figure 4.</b> Chemical structure of platinum(IV) complexes with differing axial ligands and their properties.....   | 7  |
| <b>Figure 5.</b> Chemical structure of clinically investigated platinum(IV) complexes... ..  | 8  |
| <b>Figure 6.</b> Chemical structures of symmetric platinum(IV) complexes bearing lipophilic axial ligands.....   | 18 |
| <b>Figure 7.</b> Chemical structures of asymmetric platinum(IV) complexes bearing lipophilic axial ligands.....  | 19 |
| <b>Figure 8.</b> Symmetrical platinum (IV) complexes with therapeutic active axial ligands.....  | 24 |
| <b>Figure 9.</b> Asymmetric platinum(IV) complexes with therapeutic active axial ligands.....  | 28 |
| <b>Figure 10.</b> Targeted delivery of asymmetric platinum(IV) complexes by Lippard <i>et al.</i> .....  | 36 |
| <b>Figure 11.</b> Chemical structure of platinum(IV) mono-carboxylates <b>A-I</b> .....  | 47 |
| <b>Figure 12.</b> Chemical structure of asymmetric platinum(IV) bis-carboxylates <b>3-22</b> .....   | 50 |
| <b>Figure 13.</b> Typical ammine peak in <sup>1</sup> H NMR spectra of platinum(IV) (A) bis-carboxylate and (B) mono-carboxylate in DMSO-d <sub>6</sub> solvent..... | 55 |
| <b>Figure 14.</b> Chemical structure of symmetric platinum(IV) bis-carboxylates <b>1-2</b> .....   | 56 |
| <b>Figure 15.</b> Molecular representation of platinum(IV) complexes <b>A</b> (left) and <b>3</b> (right); thermal ellipsoids are 50% equiprobability envelopes..... | 57 |

|  |     |
|--|-----|
| <b>Figure 16.</b> Chemical structure of platinum(IV) complexes evaluated for tunable pharmacological properties .....  | 74  |
| <b>Figure 17.</b> Dose-dependent drug efficacy studies for cisplatin, complexes <b>A-D</b> , <b>1</b> and <b>3-5</b> on A2780 and A2780/Cis tumor cells.....   | 81  |
| <b>Figure 18.</b> HPLC chromatograms showing 5'-dGMP; reaction of complex <b>A</b> with 5'-dGMP; reaction of complex <b>A</b> with 5'-dGMP in the presence of 3 mM ascorbic acid; and reaction of cisplatin with 5'-dGMP ..... | 84  |
| <b>Figure 19.</b> Chemical structure of asymmetric platinum(IV) complexes investigated for their structure activity relationships.....   | 85  |
| <b>Figure 20.</b> HPLC chromatograms depicting the stability of complex <b>6</b> after 72 h and instability of complex <b>10</b> after 24 h .....  | 87  |
| <b>Figure 21.</b> Graphs depicting the reduction asymmetric platinum(IV) complexes .....   | 90  |
| <b>Figure 22.</b> Dose-dependent drug efficacy studies for asymmetric platinum(IV) complexes <b>6-9</b> , <b>12-13</b> and <b>15-19</b> .....  | 95  |
| <b>Figure 23.</b> Chemical structure of platinum(IV) complexes investigated for their photoactivatable properties .....  | 105 |
| <b>Figure 24.</b> <sup>195</sup> Pt NMR spectra of cisplatin, and complex <b>1</b> before and after UV .....   | 107 |
| <b>Figure 25.</b> Effect of irradiation of UV light at 365 nm on <sup>1</sup> H NMR spectra of complex <b>1</b> after 0, 5, 15, 30, 45, and 60 min .....   | 108 |
| <b>Figure 26.</b> Effect of irradiation of UV light at 365 nm on <sup>1</sup> H NMR spectra of complex <b>3</b> after 0, 15, 30 and 120 min in D <sub>2</sub> O solvent.....   | 110 |
| <b>Figure 27.</b> Effect of irradiation of UV light at 365 nm on <sup>1</sup> H NMR spectra of complex <b>2</b> after 0, 15, 30, 45, 90 and 180 min in D <sub>2</sub> O solvent.....   | 111 |
| <b>Figure 28.</b> Standard curve depicting the increasing fluorescence intensity with increasing concentration of cisplatin .....  | 113 |
| <b>Figure 29.</b> Chart depicting the increase in fluorescence intensity of platinum(IV) complexes <b>1-3</b> upon UV irradiation at (a) 254 nm and (b) 365 nm.....  | 114 |
| <b>Figure 30.</b> UV absorption spectrum of complex <b>21</b> before and after UV irradiation at 365 nm.....   | 117 |

|   |     |
|---|-----|
| <b>Figure 31.</b> Fluorescence intensities at the maximum emission wavelength, 378nm, taken at specified times after initial UV irradiation of complexes <b>I</b> and <b>20-21</b> .....  | 119 |
| <b>Figure 32.</b> Photoactivation prodrug strategy using this class of asymmetric platinum(IV) bis-carboxylates .....   | 120 |
| <b>Figure 33.</b> Chemical structure of doxorubicin (Doxo), c(RGDfK), and asymmetric carboxylate platinum(IV)-Doxo conjugate, <b>23</b> .....   | 127 |
| <b>Figure 34.</b> Concept of ratiometric dual-drug delivery via hydrophobic entrapment using MWCNT as nanocarrier .....   | 127 |
| <b>Figure 35.</b> Release of Doxo from MWCNT <sub>TEG</sub> monitored using UV-vis spectroscopy ( $\lambda_{550}$ ).....  | 133 |
| <b>Figure 36.</b> Platinum content of Ishikawa cell extracts after treatment with MWCNT <sub>c(RGDfK)</sub> , <b>23</b> and [ <b>23</b> ·MWCNT <sub>c(RGDfK)</sub> ] .....  | 136 |
| <b>Figure 37.</b> Merged fluorescence image of Ishikawa cells (a) untreated (control), and exposed to (b) Doxo, (c) [ <b>23</b> ·MWCNT <sub>c(RGDfK)</sub> ] (d) [ <b>23</b> ·MWCNT <sub>c(RGDfK)</sub> ] added to fixed/stained untreated cells as background control..... | 137 |
| <b>Figure 38.</b> RP-HPLC Chromatograms depicting the reduction of complex <b>23</b> in 3 mM ascorbic acid.....   | 139 |

## LIST OF SCHEMES

|   |     |
|---|-----|
| <b>Scheme 1.</b> Chemical structure of platinum(IV) complex and its reduction to platinum(II) complex .....   | 6   |
| <b>Scheme 2.</b> Classical oxidation of bis-ammine platinum(II) complexes .....   | 9   |
| <b>Scheme 3.</b> Non-classical oxidation of bis-am(m)ine platinum(II) complexes .....   | 10  |
| <b>Scheme 4.</b> Synthesis of bis-ammine platinum(IV) complexes.....  | 13  |
| <b>Scheme 5.</b> Selective carboxylation of bis-am(m)ine platinum(IV) complex .....   | 15  |
| <b>Scheme 6.</b> Targeted delivery of symmetric platinum(IV) complex in NCPs with targeting peptide.....  | 30  |
| <b>Scheme 7.</b> Targeted delivery of symmetric platinum(IV) complex using NPs with targeting aptamers .....  | 31  |
| <b>Scheme 8.</b> Targeted delivery of symmetric platinum(IV) Complex using MWCNTs.....  | 32  |
| <b>Scheme 9.</b> Targeted delivery of asymmetric platinum(IV) complex in a polymer that can assemble into nanomicelles .....                            | 37  |
| <b>Scheme 10.</b> Targeted delivery of asymmetric platinum(IV) complex in NPs using near-infrared (NIR) light.....                                      | 39  |
| <b>Scheme 11.</b> General synthetic route to prepare platinum(IV) complexes .....   | 46  |
| <b>Scheme 12.</b> Synthetic route to prepare platinum(IV) mono-carboxylates <b>A-I</b> ....   | 49  |
| <b>Scheme 13.</b> Synthetic route to prepare asymmetric platinum(IV) bis-carboxylates <b>3-22</b> .....   | 53  |
| <b>Scheme 14.</b> Synthetic scheme for (a) preparation of <b>23</b> and (b) surface functionalization of MWCNT to yield MWCNT <sub>c(RGDFK)</sub> ..... | 131 |

## **LIST OF ABBREVIATIONS**

FDA - Food and Drug Administration

DNA - Deoxyribonucleic Acid

GpG – Guanosine pair Guanosine

ApG – Adenine pair Guanosine

HMGB1 – High Mobility Group Box 1

TEG - Triethylene Glycol

DMF - Dimethylformamide

DMSO - Dimethyl Sulfoxide

THF - Tetrahydrofuran

DCM - Dichloromethane

ESI/MS - Electrospray Ionization Mass Spectrometry

NMR - Nuclear Magnetic Resonance

RP-HPLC - Reversed Phase-High Performance Liquid Chromatography

ICP-OES - Inductively Coupled Plasma-Optical Emission Spectrometry

r.t. – Room Temperature

h – Hours

min - Minutes

UV-vis - Ultraviolet-visible light

DDTC - Diethyldithiocarbamate

Rho-DDTC - Rhodamine-Diethyldithiocarbamate

5'd-GMP - 5'-Guanosine-2'-deoxymonophosphate

PBS - Phosphate Buffered Saline



MTT - Methylthiazol Tetrazolium

IC<sub>50</sub> – Half maximal inhibitory concentration

HEPES - 4-(2-hydroxyethyl)-1-piperazineethanesulfonic acid

FBS – Fetal Bovine Serum

mg – Milligram

mL – Milliliter

v – Volume

nm – Nanometer

µm – Micrometer

W – Watt

w - Weight

TLC – Thin Layer Chromatography

R<sub>f</sub> – Retardation Factor

ppm – Parts Per Million

DIPEA - N,N-Diisopropylethylamine

# Chapter 1

## Introduction

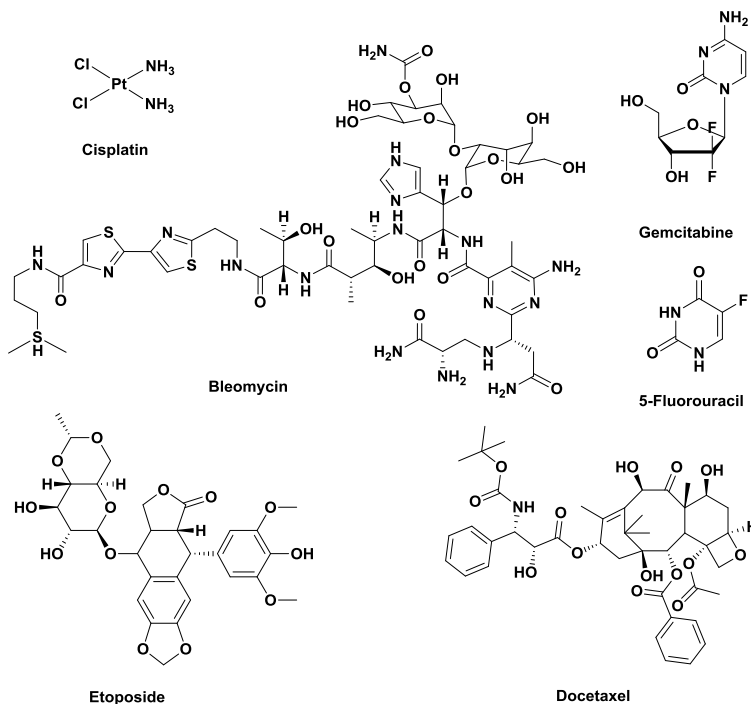


**Figure 1.** Chemical structures of cisplatin and the anticancer agents used in combination therapy

The discovery by Rosenberg that platinum complexes are capable of inhibiting cell division<sup>1</sup> has led to the establishment of a new discipline in medicinal chemistry: metal-based anticancer drugs.<sup>2</sup> Cisplatin, *cis*-diamminedichloroplatinum (II) (Figure 1), is the first platinum-based anti-cancer drug that has been used to treat a series of solid tumors such as testicular cancer, ovarian cancer and non-small cell lung cancer.<sup>3</sup> Since the introduction of cisplatin as a chemotherapeutic agent in combination chemotherapy, the survival rate for many cancer patients has increased significantly.<sup>4</sup> Together with bleomycin and

etoposide, it forms the first-line chemotherapy against testicular carcinoma.<sup>5</sup> It is also being investigated extensively with other FDA-approved drugs such as gemcitabine,<sup>6, 7, 8</sup> etoposide,<sup>9</sup> and docetaxel/fluorouracil<sup>10, 11</sup> (Figure 1).

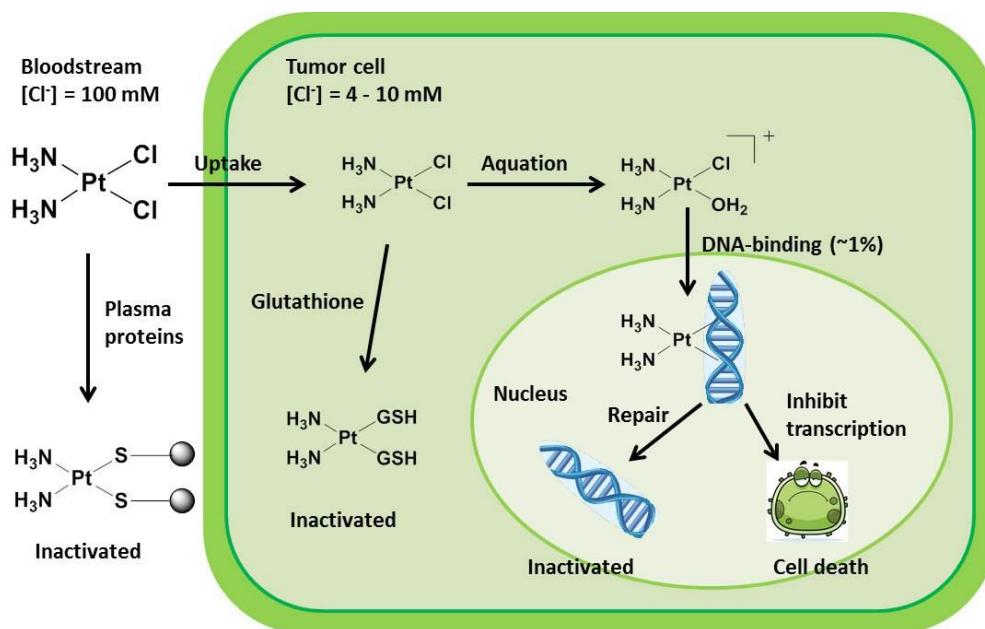


**Figure 2.** Schematic diagram showing the mode of action of cisplatin upon administration

Cisplatin enters the cell via passive diffusion and the copper transporter hCtrl pathway.<sup>12</sup> Upon reaching the cytoplasm, cisplatin undergoes aquation and loses one or both of its chloride ligands due to the high concentration of aqua ligands present. The resulting positively charged aquated platinum (II) species is very reactive and binds readily to nucleophilic purine bases in DNA to form platinated DNA cross-links adducts, such as 1,2-d(GpG) or 1,2-d(ApG) intrastrand cross links.<sup>13, 14</sup> The platinated DNA adducts bend and distort the DNA double helix

structure,<sup>15, 16</sup> inhibit transcription,<sup>17</sup> and lead to apoptosis or programmed cell death eventually (Figure 2).<sup>18</sup>

Despite the overall good success cure rate of cisplatin against certain cancers, its efficacy is limited by high toxicity and severe side-effects arising from premature aquation of the platinum(II) drugs and non-selective binding towards essential biomolecules, which lead to inactivation of the drug.<sup>19</sup> These side effects include nephrotoxicity, neurotoxicity, nausea and vomiting.<sup>20</sup> In addition, certain cancers develop resistance, either inherent or acquired during prolonged treatments, towards cisplatin chemotherapy.<sup>21</sup> This reduces the effectiveness of cisplatin, prompting for higher drug dosage for cancer patients.<sup>22</sup> Since the discovery of cisplatin, thousands of platinum complexes have been synthesized and their biological properties studied to screen for potential anticancer agents. However, less than 30 of them have made it to clinical trials in the last 30 years.<sup>23, 24</sup> Apart from cisplatin, only two other platinum complexes, carboplatin and oxaliplatin, have attained FDA approval as platinum-based therapeutic agents (Figure 3).

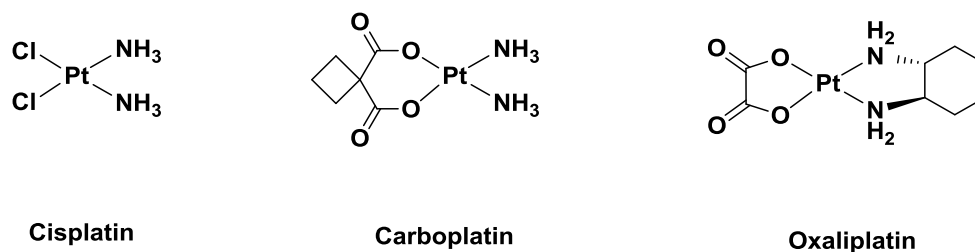


**Figure 3.** Chemical structures of FDA-approved platinum(II) anticancer agents

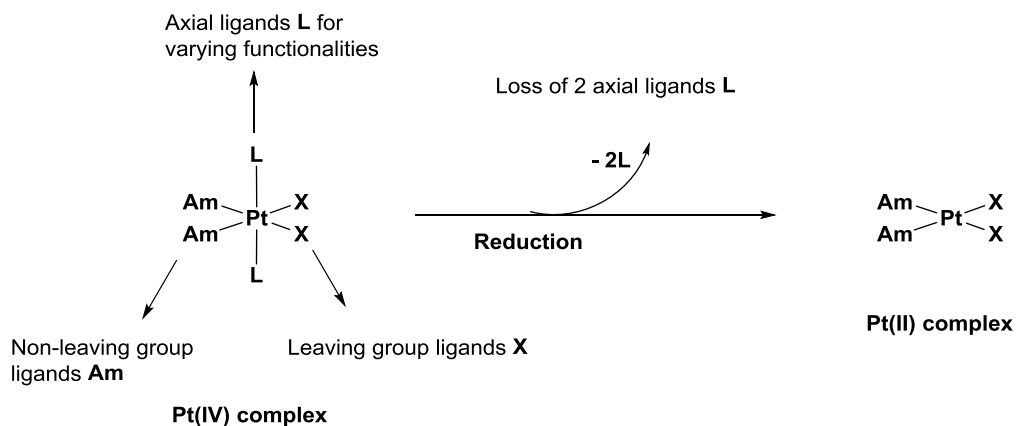
The toxicity of platinum-based drugs is dependent on the rate of hydrolysis of leaving groups as platinum complexes with labile leaving groups are more reactive and react indiscriminately with biological nucleophiles other than the putative DNA target.<sup>25</sup> Carboplatin displays higher stability and lower toxicity than cisplatin due to the presence of a stable chelating 1,1-cyclobutanedicarboxylato ligand as its leaving group. Due to its lower reactivity and toxicity profile, carboplatin can be administered in much higher dosage than cisplatin (400 mg/m<sup>2</sup> versus 40 mg/m<sup>2</sup>).<sup>26</sup> While carboplatin does not cause nephrotoxicity, its clinical use is limited by myelosuppression.<sup>24</sup> Carboplatin exhibits the same spectrum of activity as cisplatin as they yield the same [Pt(NH<sub>3</sub>)<sub>2</sub>(H<sub>2</sub>O)<sub>2</sub>] pharmacophore upon hydrolysis and therefore, results in the formation of the same platinated-DNA adducts.<sup>27, 28</sup> The second cisplatin analogue is oxaliplatin, the first FDA-approved platinum-based drug capable of overcoming tumors resistant to cisplatin and carboplatin, such as colorectal cancer.<sup>29</sup> In oxaliplatin, the bis-ammine ligands were replaced with a single bidentate 1,2-diaminocyclohexane (DACH) ligand.<sup>21</sup> Bearing a different pharmacophore from cisplatin, oxaliplatin overcome cisplatin resistance and exhibits different mechanism of action by binding DNA differently from cisplatin.<sup>30, 31</sup>

The ultimate intracellular target of cisplatin and its analogues is the DNA. After administration, the platinum drugs are prone to interactions with many reactive species, particularly sulfur containing molecules.<sup>32</sup> The species that compete with

DNA for the platinum complexes include protecting agents such as thiourea and glutathione, cell membrane ligands, peptides and proteins such as metallothionein, results in low yield of platinated-DNA adducts formed.<sup>33</sup> These limitations of cisplatin and its analogues lead to renewed interest in developing stable platinum(IV) complexes that are kinetically inert and resist rapid aquation under physiological conditions.<sup>34</sup>

### **1.1 Platinum(IV) Bis-Carboxylates as Anticancer Prodrugs**

Platinum(IV) complex is a six-coordinate metal complex with octahedral  $d^6$  metal configurations. Unlike platinum(II), platinum(IV) complexes consist of two additional axial ligands that allow the fine tuning of the properties and the attachment of functional or targeting groups, increasing the overall functionalities of the complex. They obey the 18 electrons rule and can undergo reduction to platinum(II) species that are four-coordinated square planar  $d^8$  metal configuration complexes with the concomitant dissociation of the two axial ligands (Scheme 1).<sup>34</sup> To exert their anticancer properties, the platinum(IV) complexes need to undergo intracellular reduction to platinum(II) analogues before they are able to bind to genomic DNA.<sup>35, 36</sup> This allows the prodrugs to remain inert and avoid undesirable side reactions. While the mechanism of action is similar to their platinum(II) precursors, platinum(IV) complexes are able to provide greater advantages, such as oral administration, reduced side effects and improved efficacy.



**Scheme 1.** Chemical structure of platinum(IV) complex and its reduction to platinum(II) complex

The ligands in the axial positions of platinum(IV) motifs allow wide range of structural variations that can affect the reduction potential ( $E_p$ ), lipophilicity, reactivity and cytotoxicity ( $IC_{50}$ ) of the prodrugs. Generally, platinum(IV) complexes that reduce too slowly will result in low activity profiles against cancer cell lines as the compounds remain in their inert platinum(IV) forms and pass through the body without exerting anticancer activity. On the other hand, platinum(IV) complexes that reduce readily will result in unfavorable side effects associated with platinum(II) species. Studies have shown that reduction of platinum(IV) complexes occurs most readily when the axial ligand is chloride and least readily when it is hydroxide, while platinum(IV) complexes with carboxylate ligands in the axial positions are found to have more favorable reduction rates under physiological conditions (Figure 4).<sup>37, 38, 39, 40</sup>

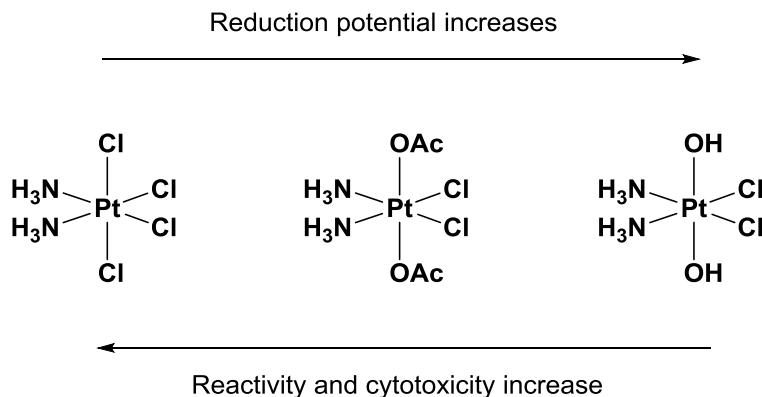


**Figure 4.** Chemical structure of platinum(IV) complexes with differing axial ligands and their properties

This result coincides with some of the clinical observations of platinum(IV) complexes that have entered clinical trials, i.e. tetraplatin, satraplatin and ipoplatin (Figure 5). Tetraplatin, bearing bis-chloro ligands in the axial positions, is too toxic as it reduces readily in the bloodstream, leading to various side effects such as neurotoxicity and myelosuppression.<sup>24</sup> Iproplatin, bearing bis-hydroxo ligands in the axial positions, is found to be ineffective in the treatment of many tumor types and less efficacy than cisplatin and carboplatin in tumors it is active in.<sup>24, 41, 42, 43, 44</sup> Satraplatin, bearing bis-acetate ligands in the axial positions, exhibits  $E_p$  between that of tetraplatin and ipoplatin. It is the most successful platinum(IV) drug to date as it is orally active, kinetically inert and exhibits anticancer activity against human carcinomas that are resistance to cisplatin.<sup>45, 46, 47</sup> Satraplatin is currently undergoing phase III clinical trial for the treatment of hormone refractory prostate cancer (HRPC) in combination with prednisone,<sup>48</sup> and a series of phase I/II/III clinical trials in conjunction with various drugs against prostate cancer and advanced solid tumors.<sup>24</sup>



Spurred by the positive evaluation of satraplatin in clinical trials, there is renewed interest in developing platinum(IV) anticancer agents, especially those with bis-carboxylate axial ligands. Other than the symmetric platinum(IV) complexes bearing identical axial ligands, asymmetric platinum(IV) complexes bearing different axial ligands have also been deployed and their prodrug strategies will be discussed in greater details in the ensuing sections.

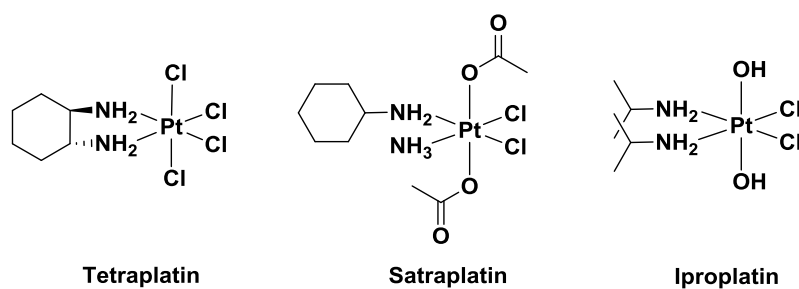
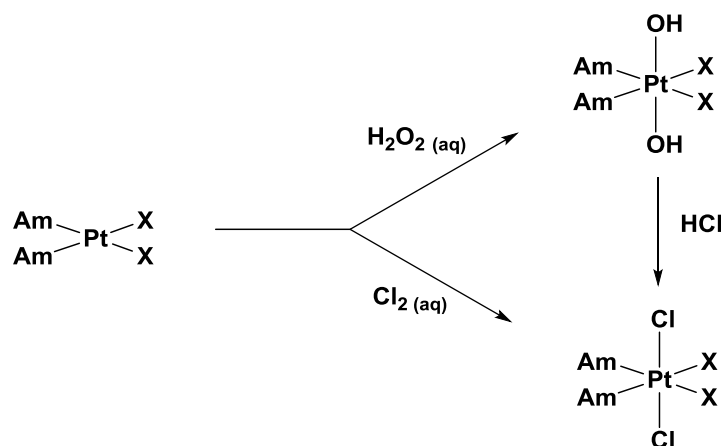


**Figure 5.** Chemical structure of clinically investigated platinum(IV) complexes

## 1.2 Synthesis of Platinum(IV) Complexes

### 1.2.1 Classical Oxidation of Platinum(II) to Platinum(IV) complexes

The most common synthetic route to the synthesis of platinum(IV) complexes involve a two-electron oxidation of its platinum(II) precursors using chlorine gas<sup>49, 50</sup> or hydrogen peroxide<sup>51</sup> in aqueous condition. This leads to the formation of platinum(IV) complexes bearing *trans*-chloro or *trans*-hydroxo ligands in the axial position (Scheme 2), the latter an important precursor for derivatized platinum(IV) complexes.<sup>52</sup> In the presence of chloride ligands, such as hydrogen chloride, displacement of the hydroxide ligands can take place to form the tetrachloro platinum(IV) complex (Scheme 2).<sup>53</sup>

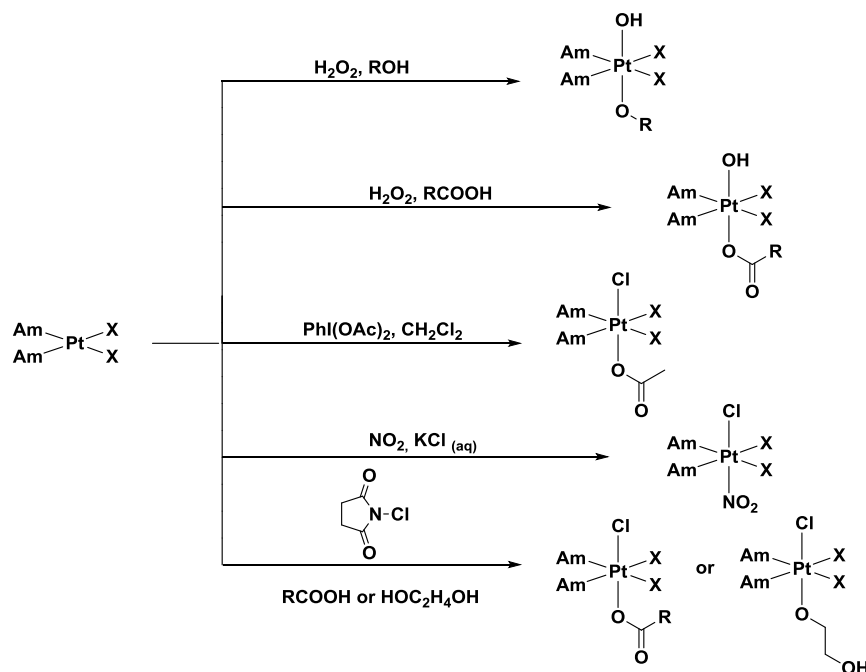


**Scheme 2.** Classical oxidation of bis-ammine platinum(II) complexes

### 1.2.2 Non-Classical Oxidation of Platinum(II) to Platinum(IV) complexes

The use of hydrogen peroxide in coordinating solvents results in asymmetric mono-hydroxo platinum(IV) products (Scheme 3). In the presence of alcohols,<sup>54, 55</sup> and glycols,<sup>56, 57</sup> the oxidation yields asymmetrical *trans*-alkoxo-hydroxo platinum(IV) complexes. When hydrogen peroxide is reacted with platinum(II) complexes in the presence of carboxylic acid, such as acetic or ethanoic acid,<sup>58, 59</sup> asymmetrical *trans*-carboxylato-hydroxo platinum(IV) complexes are obtained. However, this methodology does not apply to carboxylic acids with low pKa, such as formic<sup>60</sup> and bromoacetic acid,<sup>59</sup> as the stronger carboxylic acid is capable of protonating the second hydroxo ligand to form *trans* bis-carboxylate platinum(IV) complexes.<sup>52</sup> Other non-classical methods of oxidizing bis-ammine platinum(II) to platinum(IV) complexes include the use of  $\text{PhI}(\text{OAc})_2$  as an oxidant in dichloromethane to obtain a *trans*-chloro-acetato platinum(IV) complex,<sup>61</sup> and nitrogen dioxide gas as an oxidant in aqueous potassium chloride

solution to yield *trans*-chloro-nitrito platinum(IV) complex (Scheme 3).<sup>62</sup> While these methods provide novel synthetic pathways to access platinum(IV) complexes from platinum(II) precursors, they leave little room for structural variations of the scaffolds. A recently developed methodology that makes use of *N*-chlorosuccinimide in the presence of carboxylic acids or ethane-1,2-diol to synthesize *trans*-chloro-carboxylato or *trans*-chloro-alkoxo asymmetric platinum(IV) complexes via oxidative chlorination can overcome this (Scheme 3 last).<sup>63</sup> The synthesized *trans*-chloro-alkoxo platinum(IV) complex has a free alcohol group that allows further derivation of the structure by reacting with acids, amines, or amino acids. However, the other chloro ligand in the axial position remains non-functionalizable and limits further structural maneuver.

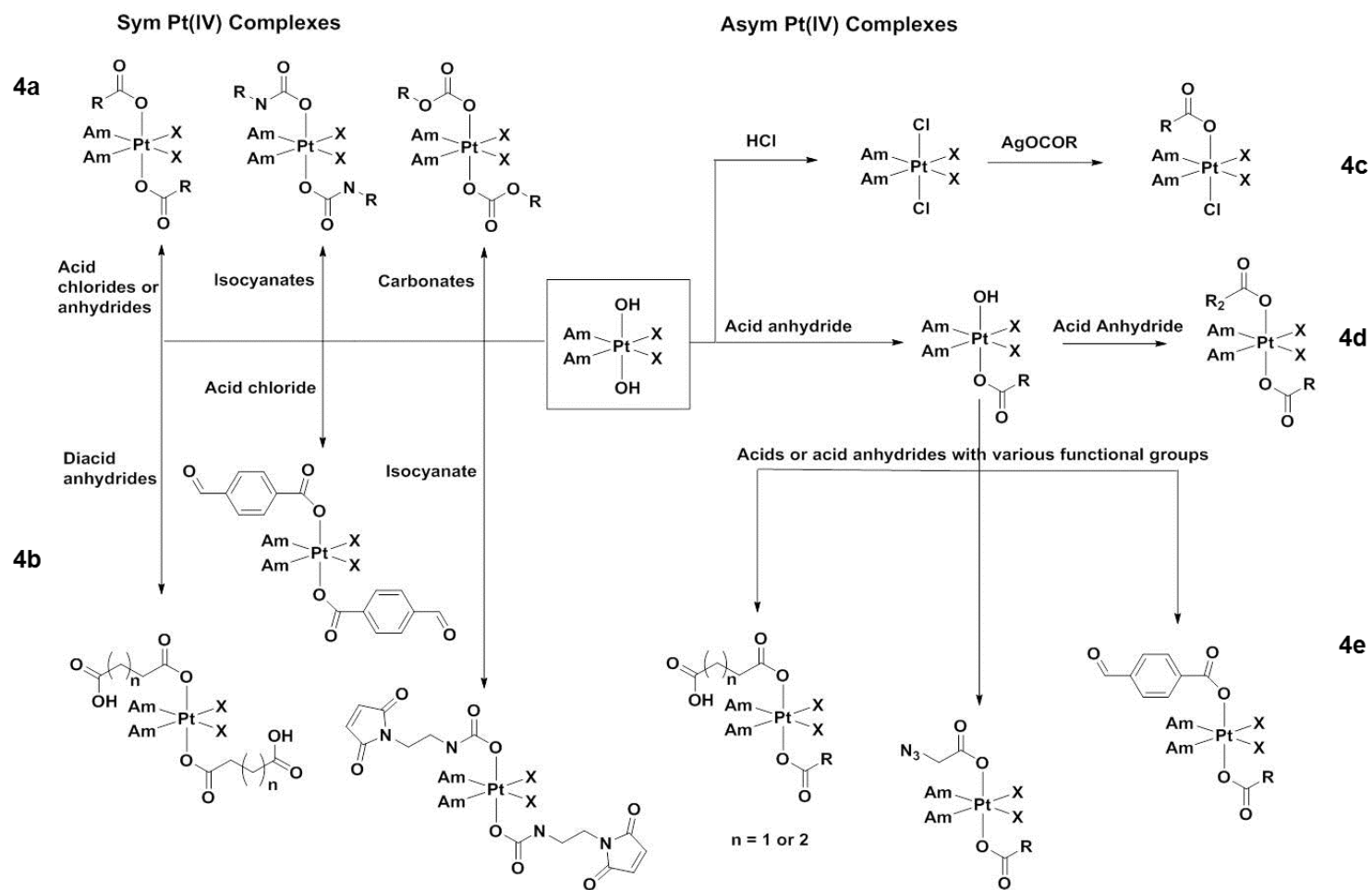


**Scheme 3.** Non-classical oxidation of bis-am(m)ine platinum(II) complexes

### 1.2.3 Classical Synthesis of Symmetric Bis-Ammine Platinum(IV) Complexes

Most of the synthesis of platinum(IV) complexes initiate from platinum(IV) bis-hydroxo complex precursor, *cis,cis,trans*-Pt(Am)<sub>2</sub>(X)<sub>2</sub>(OH)<sub>2</sub>. The coordinated hydroxo ligand acts as nucleophile to ‘attack’ electrophilic agents such as acid anhydrides, acid chlorides, isocyanates and pyrocarbonates to yield platinum(IV) carboxylate, carbamate or carbonate products (Scheme 4a).<sup>37, 64, 65, 66, 67</sup> The use of excess electrophiles in these reactions will generate the bis-symmetric platinum(IV) complexes. These methodologies allow structural variations in the platinum(IV) scaffolds that affect their chemical, physical and biological properties which will be discussed further in the later part of the chapter. Another strategy that has gained increasing popularity in recent years is the reactions of diacid anhydrides with platinum(IV) bis-hydroxo complex (Scheme 4b).<sup>68, 69</sup> The resulting platinum(IV) complexes formed have two terminal uncoordinated carboxylic acid groups that could couple readily with molecules with amine or alcohol functional groups.<sup>70</sup> This allows the attachment of small molecules to tune the lipophilicity and cytotoxic potency via structural variations,<sup>71</sup> or the attachment of bioactive ligands for co-administrations of drugs.<sup>72, 73</sup> Other than exploiting terminal carboxylic acid groups for conjugations, two new conjugation methods have also been developed. The first method makes use of aldehyde<sup>74</sup> or ketone<sup>75</sup> functional groups in the axial positions of platinum(IV) complexes that allow facile conjugations with short chain peptide or polymeric nanoparticle respectively. The carbonyl groups react readily with hydrazines and hydroxylamines to form stable hydrazones and oximes. The second method

attaches terminal maleimide functional groups in the axial positions of platinum(IV) complex.<sup>76</sup> Being thiol-selective, it is used as a precursor to bind thiol-containing tumor-targeting molecules such as human serum albumin.

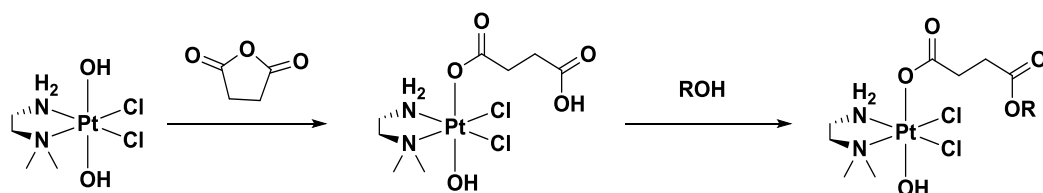


Scheme 4. Synthesis of bis-ammine platinum(IV) complexes

### 1.2.4 Non-Classical Synthesis of Asymmetric Bis-Ammine Platinum(IV) Complexes

The synthesis of asymmetrical platinum(IV) complexes requires sequential steps, a departure from classical one pot reaction designed to generate symmetrical platinum(IV) complexes. It is reported when *trans*-dichloro(1*R*,2*R*-dach)oxalato-platinum(IV) is treated with stoichiometric amount of silver carboxylate, it will undergo ligand substitution with an axial chloro ligand to generate *trans*-chloro-carboxylato platinum(IV) complex (Scheme 4c).<sup>77</sup> Another method involves the use of acid anhydride to generate mono *trans*-carboxylato-hydroxo platinum(IV) complex as acid chlorides are too reactive and favor the formation of *trans* bis-carboxylato platinum(IV) complexes. Excessive washing with water is required to quench the reaction and remove unwanted side-products when acid chlorides are used, decreasing the yield of mono-carboxylato platinum(IV) complex.<sup>65, 78</sup> To obtain the mono-carboxylato platinum(IV) complex in greater yield, the reaction needs to be carried out in dilute polar solvent conditions such as DMSO solvent.<sup>79</sup> The mono-carboxylato platinum(IV) complex can also be synthesized via direct oxidation of bis-ammine platinum(II) complex precursors with carboxylic acid (Scheme 3).<sup>58, 59</sup> Another method to selectively synthesize mono-carboxylato platinum(IV) complex can be achieved by using bulky *N,N*-dimethyl-ethane-1,2-diamine ligand on one end of the equatorial position (Scheme 5).<sup>80</sup> This allows the formation of only the mono-carboxylated product despite using excess succinic anhydride. While the free carboxylic group can be utilized for subsequent esterification, the unreacted hydroxo axial ligand is unable to undergo further

derivatization to form bis-carboxylato platinum(IV) complex due to steric hindrance.



**Scheme 5.** Selective carboxylation of bis-am(m)ine platinum(IV) complex

The mono-carboxylato platinum(IV) complexes are generally used as precursor to generate asymmetric bis-carboxylato platinum(IV) complexes through reactions with acid anhydrides or carboxylic acids (Scheme 4d).<sup>59, 79</sup> Asymmetric *trans*-alkoxo-carboxylato platinum(IV) complexes can also be synthesized from mono-alkoxo platinum(IV) complex using this strategy.<sup>55, 57</sup> In addition, the second carboxylation step can also proceed with acid anhydrides bearing terminal functional groups (Scheme 4e). The reaction of mono-carboxylato platinum(IV) complex with diacid anhydrides produces asymmetric platinum(IV) complexes with an uncoordinated terminal carboxylic acid group that can couple to bioactive organic molecule or delivery vehicle.<sup>55, 81, 82, 83</sup> Other than carboxylic acid function groups, asymmetric platinum(IV) complexes bearing a pendant azido or benzaldehyde functional groups have also been reported.<sup>59, 84</sup> Hambley *et al.* has previously reported an asymmetric platinum(IV) prodrug of oxaliplatin bearing an pendant azide on the axial position that is able to undergo copper(I)-catalyzed click reaction with anthraquinone bearing an alkyne group.<sup>59</sup> This is a feat our



group has previously attempted using platinum(IV) prodrug of cisplatin bearing aromatic azide group with limited success and is still under on-going investigation. This can be due simultaneous redox reaction that occurs when CuI is being oxidized to Cu(II) species, leading to the reduction of platinum(IV) to platinum(II) or platinum(0) species. The other conjugation method is through the previously mentioned chemoselective oxime ligation.<sup>74</sup> Through the development of asymmetric platinum(IV) complex bearing one benzaldehyde group, it allows our group to deliberately conjugate only one molecule of targeting peptide instead of two.<sup>84</sup>

Through various classical and non-classical synthetic methods, it allows a wide variety of symmetric and asymmetric bis-ammine platinum(IV) complexes to be synthesized, respectively. The careful design and synthesis of these platinum(IV) complexes are used in various anticancer prodrugs strategies which will be discussed further in the ensuing section.

### **1.3 Applications of Platinum(IV) Bis-Carboxylates**

#### **1.3.1 Platinum(IV) Complexes with Lipophilic Axial Ligands**

Lipophilicity is one of the most important physicochemical properties for a drug's success in the clinical development. It reflects the potential ability of a drug in aqueous forms to penetrate cell membranes that are hydrophobic in nature.<sup>85</sup>

Lipophilic molecules have been shown to improve uptake cellularly by facilitating transport across cell membranes.<sup>86, 87</sup> The increase in drugs' uptake can lead to

improved drugs' efficacies and lower dosage regimen. Structural-activity relationship studies have shown that the chemical and physical properties, such as the redox potential, rate of reduction, lipophilicity, cytotoxicity, and water solubility can be altered by varying the axial ligands while maintaining platinum(II) pharmacophore in the equatorial position.<sup>38, 39, 66, 71, 88</sup> Herein, the use of classical symmetric and non-classical asymmetric platinum(IV) complexes as a prodrug strategy to increase the lipophilicity and hence uptake will be discussed.

### 1.3.1.1 Symmetric Platinum(IV) Complexes with Lipophilic Axial Ligands

Dyson *et al.* has reported that the use of aromatic carboxylate ligands on the axial position of platinum(IV) prodrugs of cisplatin (Figure 6) can result in more than 10-fold increase in cytotoxicity against a panel of lung, colon and breast carcinoma cell lines compared to cisplatin. This is due to improved lipophilicity of the symmetric platinum(IV) bis-carboxylates, which leads to increased drugs uptake and hence, increased drug accumulation in the tumor sites.<sup>78</sup> Later on, Keppler *et al.* developed a series of symmetric platinum(IV) bis-carboxylates with different axial ligands using succinic and glutaric anhydride as carboxylation agents to study the relationship between lipophilicity, reduction potential, cellular accumulation and cytotoxicity of the prodrugs (Figure 6).<sup>70, 71, 89, 90</sup> This class of compounds is developed using various amine and alcohol molecules to yield the corresponding amides or esters with the existing uncoordinated carboxylic acid groups on the platinum(IV) complexes. The experimental results show a positive correlation between lipophilicity and cytotoxicity, whereby the more lipophilic

the complex, the more cytotoxic it is. More recently, Lippard *et al* reported a series of symmetric platinum(IV) bis-carbamates bearing alky or aryl substituents on the axial positions (Figure 6).<sup>66</sup> The platinum(IV) bis-carbamates are found to exhibit higher degree of structural variations by adopting different isomeric forms depending on the rotational orientation of the ligand. However, the cytotoxicities of these complexes are only comparable to cisplatin against lung carcinoma and normal lung tissue cell lines. This is possibly due to higher stability of the complexes based on the electrochemical studies results, which prevents the complexes from undergoing reduction intracellularly to the active platinum(II) species.

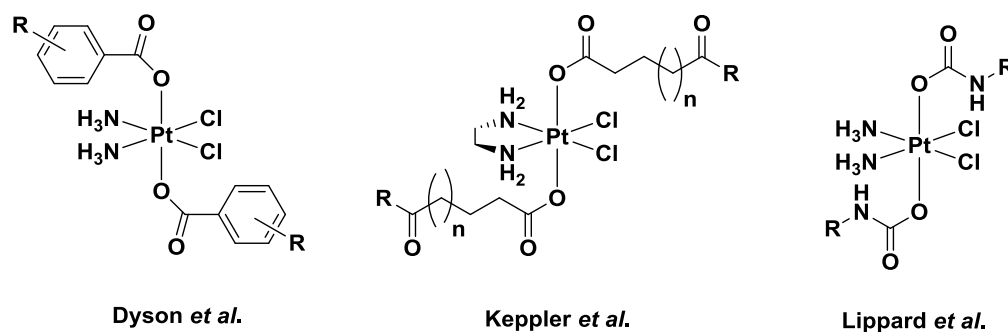


**Figure 6.** Chemical structures of symmetric platinum(IV) complexes bearing lipophilic axial ligands

Although the strategy of increasing the lipophilicity of the platinum(IV) complexes is successful in increasing the uptake and potency of the prodrugs, a major setback is the poor solubility in water, which is essential for DNA-binding metal compounds with anti-tumor activity and clinical efficacy.<sup>91</sup> On the other

hand, while the use of hydrophilic acetate ligands increases water solubility, it greatly reduces the drug's anti-proliferative efficacy.<sup>78, 92</sup> In addition, platinum(IV) complexes bearing acetate ligands are generally more stable as they are non-bulky and do not induce any steric hindrance on the structure.<sup>37</sup> Similarly, the presence of uncoordinated carboxylic group in the axial ligands can increase water solubility but decreases the drugs' potency significantly as the acidic proton can yield a negative charge upon dissociation and does not penetrate the cellular membrane easily.<sup>68, 71, 78</sup> Hence, there is a need to improve on this strategy to ensure a balance between lipophilicity and water solubility. One solution will be the development of asymmetrical platinum(IV) complexes bearing different axial ligands.

### 1.3.1.2 Asymmetric Platinum(IV) Complexes with Lipophilic Axial Ligands

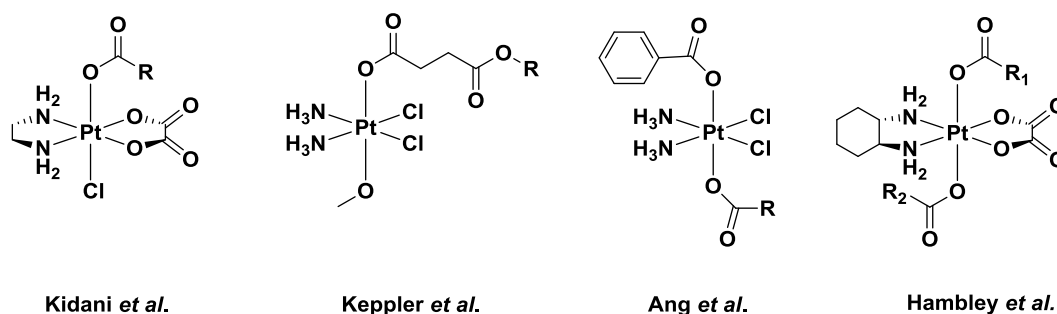


**Figure 7.** Chemical structures of asymmetric platinum(IV) complexes bearing lipophilic axial ligands

Many reports have shown that the redox potential, rate of reduction, lipophilicity, and cytotoxicity of platinum(IV) complexes can be altered by varying the axial

ligands.<sup>93, 94, 95, 96</sup> One of the early asymmetric platinum(IV) complexes was synthesized by Kidani *et al.* Using the FDA-approved platinum(II) anticancer drug, oxaliplatin, as the framework, the group found out that asymmetric *trans*-(carboxylato)chloro(1*R*,2*R*-cyclohexanediamine)(oxalate)platinum(IV) complexes (Figure 7) exhibit greater oral activity than the symmetric bis-carboxylato(1*R*,2*R*-cyclohexanediamine)(oxalate)platinum(IV) complexes *in-vitro*.<sup>77, 97</sup> Detailed studies revealed the use of asymmetric platinum(IV) motifs result in an increased rate of reduction using ascorbic acid and increased gastrointestinal absorption leading to an increased *in-vitro* activity. Evidently, the use of asymmetric platinum(IV) complexes allows the tuning of physical, chemical and biological properties, more effectively than the symmetric counterparts which is a promising discovery towards developing platinum(IV) anticancer drugs in a rational approach.

Subsequently, Keppler *et al.* reported the synthesis of a series of asymmetric *trans*-glycol-carboxylato platinum(IV) complexes (Figure 7).<sup>57, 80</sup> The group did not manage to find a distinct trend between the lipophilicity, drug uptake and cell cycle arrest for these complexes, likely due to limited structural variations. However they observed strong differences in *in-vitro* activity when the polarity of the terminal group R was varied between methyl ester and ethylene glycol ester. The former resulted in higher activity against various carcinoma cell lines and induced apoptosis stronger.

Later on, Our group Ang *et al.* showed it was possible to control the properties of platinum(IV) prodrugs using axial ligands with contrasting properties (Figure 7).<sup>79</sup> Through the simultaneous use of both hydrophilic and lipophilic ligands on the axial positions, we showed that various properties such as water solubility, lipophilicity and cytotoxicity could be controlled and tuned towards our desired properties (To be discussed further in Chapter 4). More recently, Hambley *et al.* developed a series of asymmetric mixed-carboxylato platinum(IV) prodrugs of oxaliplatin (Figure 7) through sequential acylation of the platinum(IV) complexes.<sup>59</sup> The compounds were obtained by synthesis and isolation of mono-carboxylato platinum(IV) complexes first through direct carboxylation of platinum(II) metal center<sup>80</sup> or coupling reaction with bis-hydroxido platinum(IV) complex, before undergoing further carboxylation to give the desired products.<sup>59</sup> These axial ligands include alky chains such as methyl, methyl azide and succinate group; and aromatic compound such as anthraquinone.

The ease of synthesizing asymmetric platinum(IV) complexes to give engineered properties that are of desired pharmacological standards can be pivotal in developing an effective platinum(IV) anticancer prodrug in the near future.

### **1.3.2 Platinum(IV) Complexes with Bioactive Axial Ligands**

Incidences of platinum associated drug resistance often nullify cisplatin's anti-proliferative efficacy.<sup>22</sup> Cancer drug resistance, the diminishing efficacy of specific chemotherapeutic agents towards their targets, is one of the most

challenging obstacles in modern cancer medicine.<sup>98, 99</sup> The underlying mechanisms upon which the resistance phenomena emerge is complex and differ across the spectrum of different cancer phenotypes.<sup>100</sup> Yet they point towards the interconnectivity and complexity of the various molecular pathways in cancer biology, giving rise to multiple redundancies by which these aberrant cells can survive and proliferate.<sup>101</sup> One strategy that is widely employed to combat chemoresistance is through combination therapy.<sup>102</sup> By administering a cocktail of different anticancer drugs working against different targets, combination therapy aims to deter the development of drug resistance by defeating cellular survival pathways in a multi-pronged assault and overcome the defence mechanisms through therapeutic synergism.<sup>103</sup> Since platinum(IV) complexes are kinetically inert to ligand substitution, the presence of the two axial ligands allow biocompatible molecules to be tethered on the outer-sphere without compromising the functionality of platinum(II) pharmacophore.<sup>60</sup> Upon intracellular reduction, stoichiometric equivalence of platinum(II) complex and bioactive ligands will be activated towards their respective targets.

### **1.3.2.1 Symmetric Platinum(IV) Complexes with Bioactive Axial Ligands**

Ethacrynic acid (EA) is an inhibitor of glutathione S-transferase (GST) P1-1, an enzyme that is overexpressed in cancer cells and nullifies the efficacies of anticancer drugs.<sup>104, 105</sup> To increase the potency of cisplatin, Dyson *et al.* synthesized ethacraplatin (Figure 8) by conjugating ethacrynic acid to cisplatin by acylation of *cis, cis, trans*-[Pt(NH<sub>3</sub>)<sub>2</sub>(Cl)<sub>2</sub>(OH)<sub>2</sub>], oxoplatin, with ethacrynic acyl

chloride.<sup>78</sup> Upon activation, two molecules of ethacrynic acid and one molecule of cisplatin were released simultaneously. This strategy decreased the GST activity of A549 lung carcinoma synergistically and more efficacious than ethacrynic acids.

In a similar strategy, Lippard *et al.* synthesized a series of symmetric platinum(IV) bis-estrogen carboxylates (Figure 8) by conjugating estrogen derivatives to functionalized platinum(IV) complexes via amide coupling.<sup>72</sup> Intracellular reduction afforded cisplatin and two equivalents of the modified estrogen ligands. The bis-estrogen carboxylated platinum(IV) compounds were effective in upregulating HMGB1, a protein that shields platinated DNA adducts from nucleotide excision repair (NER). This improves the efficacy of cisplatin as the platinated DNA will be more prone to apoptosis when NER cannot proceed.

Following the positive results, Lippard *et al.* proceeded to conjugate various targeting peptides to platinum(IV) complexes.<sup>73, 106</sup> The driving force for tumor cell proliferation is angiogenesis, the process of forming blood vessels from pre-existing ones. Hence, the ability to selectively target tumor endothelial cell offers an alternative route to treating cancer.<sup>107, 108</sup> Integrins are  $\alpha/\beta$  transmembrane receptors that bridges cell cytoskeleton to extracellular matrix, generating intracellular signals to allow cell proliferation.<sup>109</sup> The  $\alpha_v\beta_3$  and  $\alpha_v\beta_5$  integrins that are usually absent in resting endothelial cells are expressed in many tumor malignancies and crucial for the tumor cells' survivals. To target these receptors,



the group conjugated the peptide motifs RGD (Arg-Gly-Asp) and NGR (Asn-Gly Arg) to platinum(IV) complexes via amide coupling (Figure 8).<sup>73</sup> These peptides have high affinities with  $\alpha_v\beta_3$  and  $\alpha_v\beta_5$  integrins, and are used as targeting tools to direct the symmetric platinum(IV) prodrugs to selectively kill the angiogenic tumor endothelial cells. Other peptide chains such as AGR, Gly, (CRGDC)<sub>c</sub> and (RGDfk)<sub>c</sub> were also used.

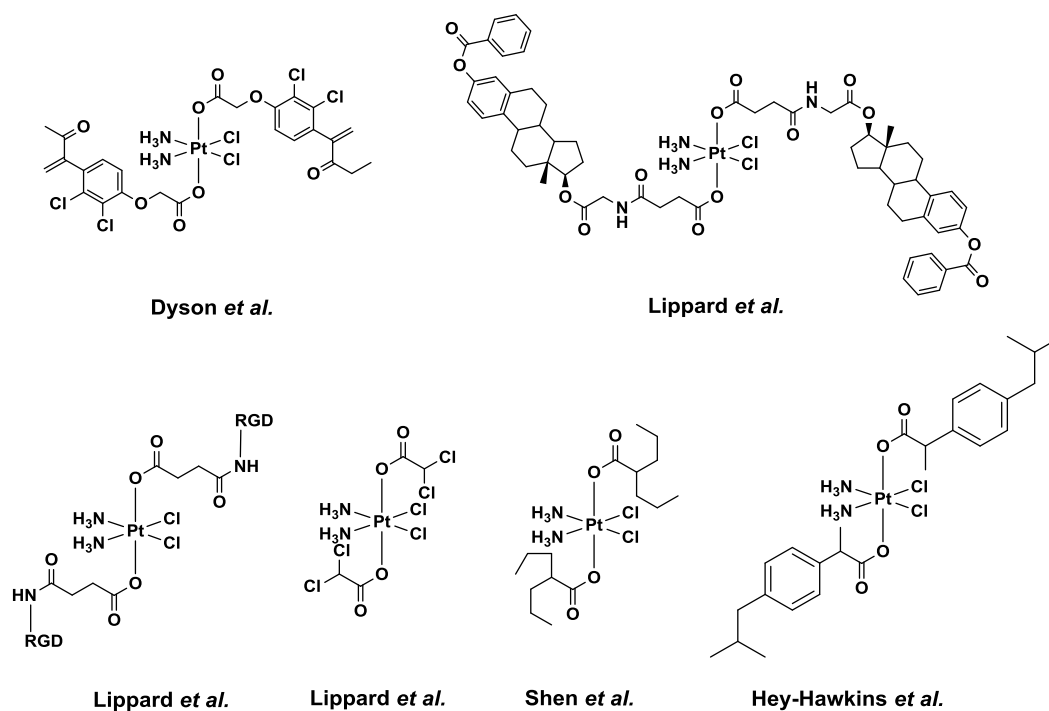


**Figure 8.** Symmetrical platinum (IV) complexes with therapeutic active axial ligands

The conjugation to platinum(IV) complexes using longer chain peptides such as CNGRC (cyclic peptide Cys-Asn-Gly-Arg-Cys) to target aminopeptidase N (CD13/APN);<sup>110</sup> TAT peptide (Gly-Arg-Lys-Lys-Arg-Arg-Gln-Arg-Arg-Arg-Pro-Gln) for better cell penetration;<sup>111</sup> and chlorotoxin,<sup>106</sup> a 36-amino-acid peptide

with four disulfide bridges, to selectively target tumor cells, have also resulted in more potent platinum(IV) complexes.

Other than peptides, small bioactive molecules can also be conjugated. Lippard *et al.* reported the synthesis of mitaplatin (Figure 8), a symmetric platinum(IV) prodrug of cisplatin comprising of dichloroacetate in the axial positions.<sup>112</sup> Dichloroacetate is a pyruvate dehydrogenase kinase (PDK) inhibitor that can reverse the glycolytic metabolism in the mitochondria of most solid tumors, known as the Warburg effect. Upon intracellular reduction of mitaplatin, cisplatin and two equivalents of dichloroacetate are released to target the DNA and mitochondria respectively. By inducing mitochondrial dysfunction, the tumor cells are more sensitive to cisplatin. However, further studies reveal that ligands with strong electron withdrawing groups on the axial positions of platinum(IV) complexes will destabilize the compound, leading to premature hydrolysis in aqueous conditions.<sup>113</sup> The electron-withdrawing dichloroacetate ligands will hence destabilize mitaplatin and be displaced with aqua molecules in aqueous biological conditions before reaching the tumor site. This result halted mitaplatin's progress towards clinical evaluation. Nevertheless, mitaplatin has proved the viability of developing synergistic platinum(IV) complexes to delivery two complementary drugs as anticancer prodrug strategy.

Subsequently, Shen *et al.* reported a symmetric platinum(IV) complex (VAAP) by conjugating valproic acid, a histone deacetylase inhibitor, to cisplatin using the

same synthetic method to yield mitaplatin (Figure 8).<sup>114</sup> VAAP was subsequently loaded in polyethylene glycol-polycaprolactone micelles (PEG-PCL) nanoparticles (NPs) as delivery vehicle. *In-vitro* results showed that PEG-PCL/VAAP and the free VAAP were significantly more potent against cisplatin and oxoplatin. *In-vivo* results based on A549 lung tumor xenograft model revealed that PEG-PCL/VAAP and the free VAAP were able to inhibit the rate of tumor growth more effectively than oxoplatin, with limited side effects.

Recently, Hey-Hawkins *et al.* covalently linked cyclooxygenase-2 (COX-2) inhibitor, ibuprofen, to cisplatin (Figure 8).<sup>115</sup> COX-2 is an enzyme involved in tumorigenesis, a process where normal cells are transformed to cancer cells. The platinum(IV) prodrugs bearing the COX-2 inhibitor in the axial positions exhibited significant increase in cytotoxicity in a series of tumor cells tested and was able to overcome cisplatin resistance tumor cells.

The tethering of bioactive ligands to the axial positions of platinum(IV) complexes have shown to be an effective prodrug strategy, as these complexes have displayed synergism with increased potency. However, it is not possible to vary the molecular ratio of the bioactive ligands to platinum(II) drug through the discussed methods as they only allowed a ratio of two bioactive molecules to one cisplatin molecule. To allow a ratiometric combinatorial drugs delivery, a different synthetic approach has to be adopted.

### 1.3.2.2 Asymmetric Platinum(IV) Complexes with Bioactive Axial Ligands

Through the development of asymmetric platinum(IV) complexes, it allows a step-wise sequential acylation of the axial ligands. Hence, it can allow the tethering of only one bioactive molecule in one of the two axial positions at a time. The remaining free axial position can be functionalized with simple organic molecule to alter its overall properties. It is also possible to covalently link another anticancer agent to the free axial position to further increase the functionalities of the prodrug in a triple drugs delivery approach, although there is no report on this till date.

Our group Ang *et al.* reported an asymmetric *trans*-doxorubicin-benzoate platinum(IV) prodrug of cisplatin (Figure 9) which will release one molecule of doxorubicin and one molecule of cisplatin upon activation.<sup>81</sup> Cisplatin and doxorubicin are currently combined in phase III clinical trials against endometrial adenocarcinoma, hence providing a compelling reason to link them together for combinatorial therapy. The presence of the benzoate ligand makes the compound more lipophilic to allow hydrophobic entrapment in carbon nanotubes (CNTs).<sup>116</sup> (To be discussed further in Chapter 6)

More recently, our group successfully designed an asymmetric multi-model platinum(IV) prodrug of cisplatin. The axial ligands consist of a dual functions peptide and acetate or hydroxo ligand in the *trans* position (Figure 9).<sup>84</sup> The peptides used in this work include annexin-1, WKYMVm (Trp-Lys-Tyr-Met-Val-

d-Met) and fMLFK (formyl-Met-Leu-Phe-Lys). The annexin-1 and WKYMVm peptides are able to target formyl peptide receptors (FPRs) to provide selectivity, while fMLFK peptide is non-targeting and used as control. As FPRs are overexpressed in certain malignant tumors, the selected peptides are aimed to target FPRs and simultaneously act as potent immune adjuvant to provoke an immune anticancer response to deliver therapeutic synergy. The presence of an acetate ligand in the other axial position is found to decrease the platinum(IV)'s reduction rate by 77-folds when compared with hydroxo ligand. This can prevent premature reduction before reaching the target tumor site and decrease the drug's efficacy. Against MC7-7 and MDA-MB-213 human breast cancer cell lines, the peptides conjugated platinum(IV) complexes exhibited comparable cytotoxicity with cisplatin, while the control with non-targeting fMLFK peptide resulted in negligible activity, validating the group's approach of active targeting via tethering targeting peptides in platinum(IV)'s axial positions.

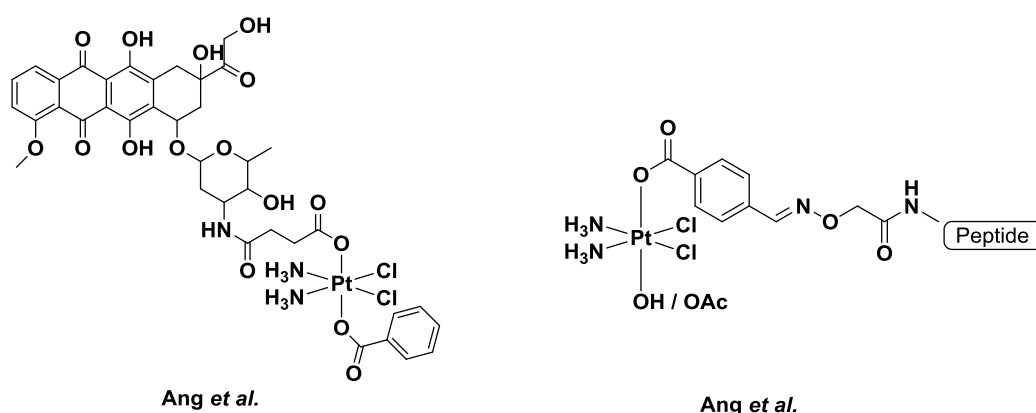


**Figure 9.** Asymmetric platinum(IV) complexes with therapeutic active axial ligands

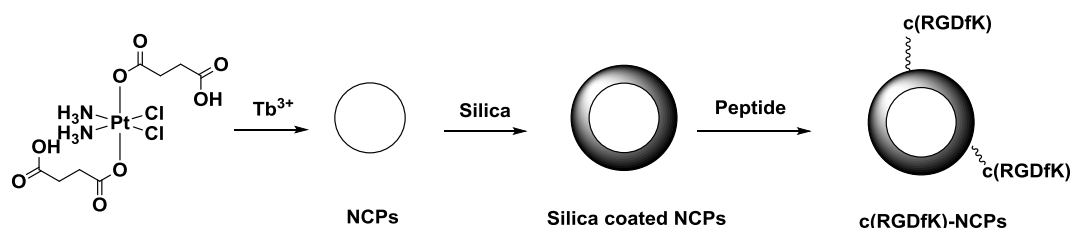
### 1.3.3 Targeted Delivery of Platinum(IV) Complexes using Drug Carriers

The strategy of delivering cytotoxic drugs selectively into cancerous cells has the potential to significantly improve the therapeutic efficacy of the carrier drugs.<sup>117</sup> Platinum-based chemotherapy often results in high toxicity and severe side-effects. Its limitations are often caused by non-specific binding with essential plasma proteins and its inability to differentiate between healthy and tumor cells. Hence it is the ultimate aim of platinum-based treatment to be able to target cancerous cells selectively, while leaving healthy cells unscathed. To overcome this selectivity issue, the use of macromolecular drug carriers has been utilized to deliver platinum drugs to the target tissue.<sup>118, 119, 120, 121, 122, 123</sup> The carriers can act as protective shells for the entrapped platinum drugs to prevent premature release and side reactions with essential plasma proteins. In addition, the surfaces of the carriers can be readily functionalized with passivating and targeting moieties. Furthermore, this can improve the drug accumulation in solid tumor due to better permeability and penetration of the carriers, and stay in the tumor sites which lack effective lymphatic drainage system.<sup>124</sup>

#### 1.3.3.1 Targeted Delivery of Symmetric Platinum(IV) Complexes using Drug Carriers

One of the early works of delivering platinum(IV) prodrugs in a nano-platform was reported by Lin *et al.*<sup>120</sup> The group formulated nanoscale coordination polymers (NCPs) from  $TbCl_3$  and bis-succinato platinum(IV) prodrug of cisplatin, obtained through precipitation. The NCPs formed were subsequently stabilized by

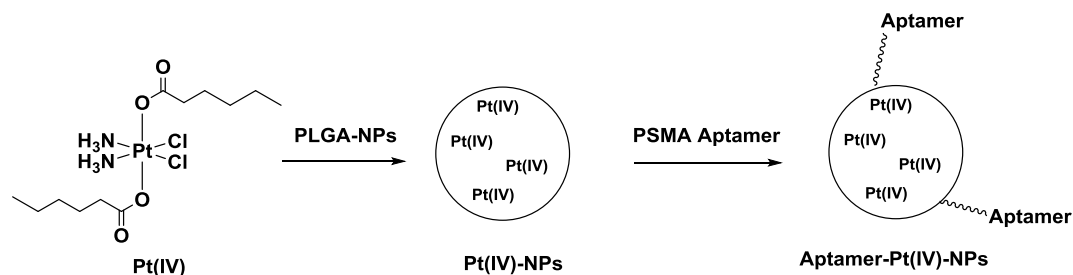
encapsulation in shells of amorphous silica when treated with polyvinylpyrrolidone and tetraethyl orthosilicate (Scheme 6). By varying the thickness of the silica shell, the rate of release of platinum(IV) prodrug could be controlled and ascertained. With dissolution half-lives up to 9 hours, this strategy allowed the platinum(IV) complex to be release slowly, circulate around the body, and accumulate into the tumor site.  $\alpha_v\beta_3$  integrins targeting peptide, c(RGDfK), was then grafted onto the silica surface to enhance accumulation and selectivity against angiogenic cancers. The c(RGDfK)-NCPs shows increased potency against HT-29 colon carcinoma cells that overexpresses the  $\alpha_v\beta_3$  integrins when compared to cisplatin, while the NCPs alone is non-efficacious.<sup>120</sup>



**Scheme 6.** Targeted delivery of symmetric platinum(IV) complex in NCPs with targeting peptide

In an alternate strategy with similar objective, Lippard *et al.* delivered cisplatin to prostate cancer cells by encapsulating hydrophobic bis-hexanoate platinum(IV) prodrug of cisplatin in pegylated poly(D,L-lactic-co-glycolic acid) (PLGA) nanoparticles (NPs) functionalized with prostate-specific membrane antigen (PSMA) targeting aptamers (Scheme 7).<sup>125</sup> Kinetic studies revealed slow controlled release of platinum(IV) payload over 60 hours, indicating the

feasibility of the NPs as the delivery vehicle. The aptamer-derivatized platinum(IV)-encapsulated in NPs was found to be 80 folds more superior than cisplatin against PSMA overexpressed prostate cancer cells, and 4 folds more superior than non-targeting platinum(IV)-encapsulated NPs.

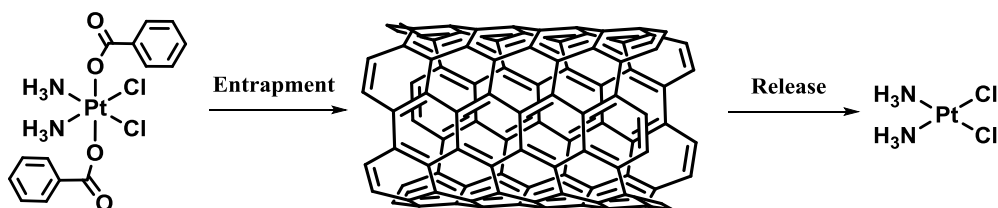


**Scheme 7.** Targeted delivery of symmetric platinum(IV) complex using NPs with targeting aptamers

Carbon nanotubes (CNTs) and nanohorns (CNHs) have also been reported as drug delivery platforms for platinum-based drugs.<sup>126, 127</sup> Their high aspect ratios allowed them to penetrate through the cellular membrane and release the platinum payloads directly at the tumor cells. One strategy is to load cisplatin or carboplatin within the inner cavity of CNTs and CNHs and subsequently release via diffusion. Due to the hydrophilicity of cisplatin and carboplatin, it is however not feasible to encapsulate the drugs in hydrophobic carriers as they can be displaced rapidly by aqua molecules before reaching the target site. To circumvent this, Ang and Pastorin *et al.* encapsulated an inert, hydrophobic and cytotoxic platinum(IV) prodrug of cisplatin within multi-walled CNTs (MWCNTs).<sup>122</sup> The hydrophobic-hydrophobic interactions between MWCNTs and platinum(IV) prodrug favored entrapment and also prevented release of the prodrug in an aqueous environment.



Upon interaction with intracellular reductants after cell penetration, the inert platinum(IV) prodrug was reduced to its active hydrophilic platinum(II) species, released from the MWCNTs, bound to DNA and eventually triggered apoptosis (Scheme 8).



**Scheme 8.** Targeted delivery of symmetric platinum(IV) Complex using MWCNTs

To study the *in-vivo* biodistribution, the MWCNTs encapsulating the platinum(IV) prodrug were functionalized with triethylene glycol (TEG) and delivered to female BALB/c mice.<sup>128</sup> Mice treated with platinum(IV)-MWCNTs were found to exhibit the highest platinum content in most tissues, indicating the effectiveness of delivering platinum(IV) prodrugs via hydrophobic entrapment. The free cisplatin and cisplatin-MWCNTs did not show significant differences in the platinum contents, likely due to cisplatin dissolving in aqueous solution and gets released from the MWCNTs before reaching the tumor sites. The free hydrophobic platinum(IV) prodrug displayed much lower platinum content in the tissues due to its poor solubility in aqueous solution. This indicated that through drug encapsulation, the poorly soluble platinum drugs could still be delivered to the tumors efficiently. Interestingly, the highest platinum content was detected in the kidney and liver when the mice were treated with free platinum(IV) prodrug,

while the platinum content in in the kidney tissue of the mice treated with platinum(IV)-MWCNTs decreased the most. These results show that delivery of platinum(IV) prodrug in nano-carriers can increase platinum accumulation and change the biodistribution profile significantly by selectively target tumor cells.

In an extension of the work, Ang and Pastorin *et al.* attached mitochondrial-targeting rhodamine-110 to the MWCNTs and loaded with platinum(IV) prodrug to yield MWCNTs-Rho-platinum(IV) to study the selectivity of MWCNTs.<sup>129</sup> Rhodamine-110 is cationic and uptakes into the mitochondria through negative mitochondrial membrane potential, resulting in preferential accumulation in cancer cells due to higher mitochondrial membrane potential in cancer cells as compared to normal cells. *In-vitro* results showed that the MWCNT-Rho-platinum(IV) exhibited 6-fold higher potency than the free platinum(IV) complex when tested against A2780 cancer cells, but not in IMR90 normal cells. These results validated the approach of selective targeting the tumor sites via delivery carriers resulting in increased anti-proliferative efficacies due to better selective and higher drug loading profiles.

### **1.3.3.2 Targeted Delivery of Asymmetric Platinum(IV) Complexes using Drug Carriers**

The use of asymmetric platinum(IV) prodrugs for targeted drug delivery adds a new dimensional approach to existing strategy by increasing the overall functionality of the compound. As mentioned earlier, the asymmetric platinum(IV) complexes can be tethered to two different molecules in the axial

positions. In some of the examples discussed in this section, platinum(IV) prodrugs are tethered to nano carriers instead of being loaded directly inside them.

Lippard *et al.* demonstrated this by conjugating asymmetric platinum(IV) complex, *cis,cis,trans*-[Pt(NH<sub>3</sub>)<sub>2</sub>Cl<sub>2</sub>(OEt)(O<sub>2</sub>CC<sub>2</sub>H<sub>4</sub>COOH)], bearing a single carboxylic functional group at one of its axial ligand site to single walled carbon nanotubes (SWCNTs) (Figure 10).<sup>55</sup> The SWCNTs, functionalized with amine groups joined by pegylated phospholipid chains, exhibited good aqua solubility and low toxicity against Ntera-2 testicular carcinoma cells. Upon conjugation to platinum(IV) complex, the SWCNT-platinum(IV) inhibited cell viability more than 2-fold and 10-fold higher than the free cisplatin and platinum(IV) prodrug respectively. In an extension to the work, Lippard *et al.* replaced the ethoxide (OEt) group with a folate receptor targeting group, folic acid (FA), conjugated via a PEG-amide linker to yield asymmetric SWCNT-platinum(IV)-FA conjugate (Figure 10).<sup>130</sup> Folate receptor (FR) is overexpressed in many tumor cells and the ability to target these receptors allow the platinum(IV) prodrug to be selective against the malignancies. As a proof of concept, the group tested SWCNT-platinum(IV)-FA and cisplatin against FR(+) human choriocarcinoma (JAR), FR(+) nasopharyngeal carcinoma (KB), and a control, FR(-) testicular (Ntera-2) carcinoma cell lines. The SWCNT-platinum(IV)-FA was found to be only significantly more efficacious than cisplatin in the FR(+) cell lines. This result demonstrates that targeting groups on the delivery vehicles can increase the overall selectivity of the delivered agents.

Other than CNTs, Lippard et al. also demonstrated the viability of delivering platinum(IV) complexes using polyvalent oligonucleotide gold nanoparticles (DNA-Au-NPs).<sup>82</sup> DNA-Au-NPs are attractive drug carriers as they offer high cellular uptake, low toxicity and low degradability under the influence of cellular enzymes. Platinum(IV) mono-carboxylate, *cis,cis,trans*-[Pt(NH<sub>3</sub>)<sub>2</sub>Cl<sub>2</sub>(OH)(O<sub>2</sub>CC<sub>2</sub>H<sub>4</sub>COOH)], bearing a single carboxylic group was conjugated to amine functionalized DNA-Au-NPs surface via amide linkage to yield asymmetric platinum(IV)-DNA-Au-NPs (Figure 10). The platinum(IV)-DNA-Au-NPs displayed significantly higher activity against a series of human carcinoma cells than cisplatin and unconjugated platinum(IV) mono-carboxylate. Fluorescence microscopy studies revealed localization of the particles in the vesicles and cytosol after 6 and 12 hours respectively. Further staining indicated colocalization of the platinum(IV)-DNA-Au-NPs with the microtubules in HeLa cervical cancer cells. Further immuno-fluorescence studies showed the formation of 1,2-d(GpG) intrastrand cross-links in the nuclei of the treated HeLa cells, supporting the hypothesis that the platinum(IV) complex undergo intracellular reduction to yield active platinum(II) species, which was discharged from the nano carriers.

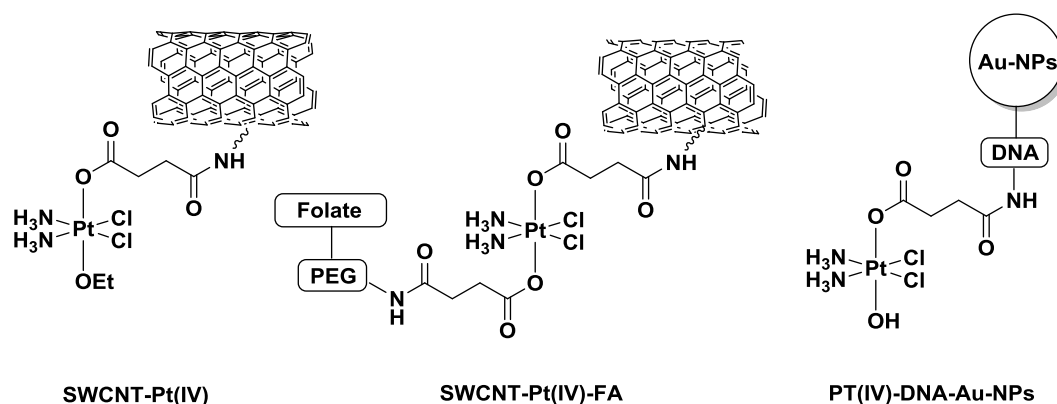
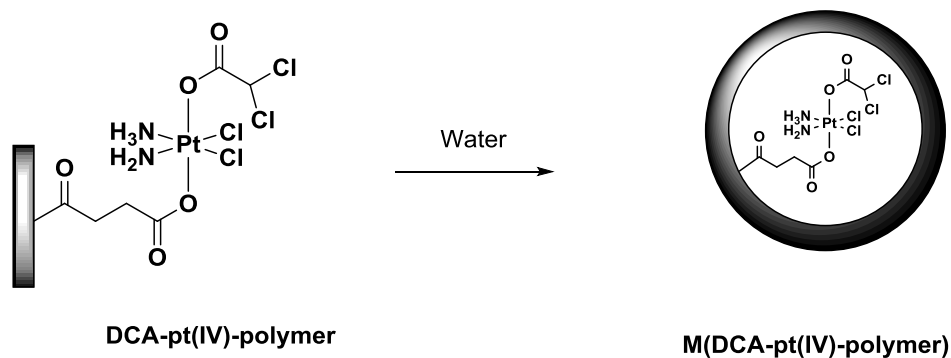


**Figure 10.** Targeted delivery of asymmetric platinum(IV) complexes by Lippard *et al.*

In another strategy, Zhang *et al.* conjugated symmetric bis-glutarate platinum(IV) prodrug of cisplatin to paclitaxel (Ptxl) via ester coupling. Due to steric hindrance of Ptxl, only one molecule of Ptxl could be attached to form the asymmetric Platinum(IV)-Ptxl conjugate, which was subsequently loaded into lipid-polymer hybrid nanoparticles to yield Ptxl-platinum(IV)-NPs.<sup>131</sup> Kinetic studies showed that up to 75% of platinum content was released from the NPs at pH 6.0 after 24 hours, which was likely due to hydrolysis of the ester linkage joining Ptxl and platinum(IV) complex. Against A2780 human ovarian carcinoma, the platinum(IV)-Ptxl-NPs exhibited comparable activity as cisplatin while the free platinum(IV)-Ptxl was ineffective. This demonstrates that the NPs are effective in delivering the platinum(IV)-Ptxl across the membrane diffusion barrier and enter the cancer cells.

To overcome setbacks of non-biocompatible small molecular drugs, Jing *et al.* developed an asymmetric multifunctional platinum(IV) prodrug of cisplatin that

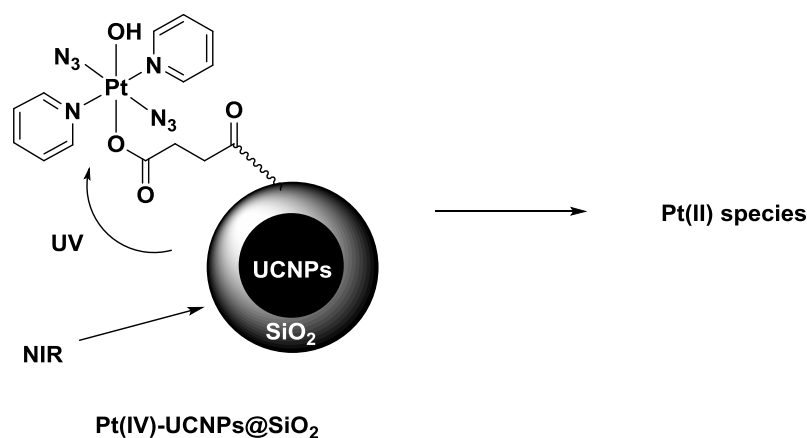
consisted of mitochondria-targeting dichloroacetate (DCA) molecule on one axial position, and a free carboxylic group on the other end. The platinum(IV) complex was conjugated to a biodegradable and amphiphilic polymer, MPEGb-PCL-b-PPL, which would assemble into nanomicelles to yield M(DCA-platinum(IV)-polymer) (Scheme 9).<sup>83</sup> Kinetic studies showed that the release of platinum from M(DCA-platinum(IV)-polymer) took place most readily in reducing agent such as ascorbic acid. Against SKOV-3 human ovarian carcinoma, M(DCA-platinum(IV)-polymer) exhibited lower cytotoxicity than cisplatin, but 5.7 folds more than free DCA-platinum(IV). Cellular uptake studies showed that the highest platinum content was obtained in cells treated with M(DCA-platinum(IV)-polymer), which was likely due to better internalization via endocytosis.



**Scheme 9.** Targeted delivery of asymmetric platinum(IV) complex in a polymer that can assemble into nanomicelles

Recently, Xing *et al.* conjugated an asymmetric photoactive platinum(IV) complex, *trans, trans, trans*-[Pt(N<sub>3</sub>)<sub>2</sub>(OH)(O<sub>2</sub>CCH<sub>2</sub>CH<sub>2</sub>CO<sub>2</sub>H)(py)<sub>2</sub>], to the surface of silica-coated upconversion luminescent nanoparticles (UCNPs@SiO<sub>2</sub>) to yield platinum(IV)-UCNPs@SiO<sub>2</sub>.<sup>132</sup> Photoactivation of platinum(IV)

complexes as a prodrug strategy has garnered considerable amount of attention in the late,<sup>133</sup> where photo-activatable platinum(IV) prodrug complexes are reduced using ultraviolet (UV) light to yield cytotoxic platinum(II) species.<sup>134, 135, 136</sup> These platinum(IV) complexes possess photoactive ligands such as azido or iodo (To be discussed further in Chapter 5). However UV radiation has very limited penetration depth in biological tissues as it is readily absorbed by aromatic amino acids and nucleic acids in the body.<sup>137</sup> Hence, this strategy allows the group to reduce the platinum(IV) prodrug to platinum(II) species by using UCNPs to absorb near-infrared (NIR) light and converting it to emissions that span a wide spectrum of wavelength, including UV light. Platinum content was released from platinum(IV)-UCNPs@SiO<sub>2</sub> upon NIR irradiation (Scheme 10), while the free platinum(IV) prodrug did not undergo reduction under the same condition. MTT assays experiment against A2780 and A2780 cisplatin resistant human ovarian carcinoma showed that the platinum(IV)-UCNPs@SiO<sub>2</sub> exhibited higher activity compared to cisplatin when irradiated with NIR, with up to 0.51±0.03 ng platinum per microgram of DNA observed in the DNA nucleus. This indicates the feasibility of using UCNPs as a drug carrier to overcome existing limitations of using UV to activate photoactivatable platinum(IV) prodrugs to enhance drug viability and selectivity against tumor cells.



**Scheme 10.** Targeted delivery of asymmetric platinum(IV) complex in NPs using near-infrared (NIR) light

## 1.4 Summary

Chemotherapeutic drug, cisplatin remains one of the most effectively and widely used anticancer drugs clinically. Despite its limitations, it is able to target the most fundamental aspect of cancer cells, their rapidly dividing nature. To overcome the drawbacks of cisplatin, platinum(IV) prodrug that would undergo intracellular reduction to yield cisplatin offer a direct solution as it is more inert and stable. Classical symmetric platinum(IV) complexes offered a variety of prodrug strategies that include using lipophilic molecules, bioactive molecules or delivery carriers that would eventually release cisplatin in the tumor sites. Non-classical asymmetric platinum(IV) complexes could also offer the same strategies but with more structural variations and functionalities than the classical prodrugs. While it is still at its infancy stage, the advantages of asymmetric platinum(IV) anticancer prodrugs of cisplatin over their symmetric counterparts were well



documented based on reported examples and would be the key focus in our investigation.

## Chapter 2

### Research Objectives and Thesis Layout

The key research objective is to investigate the development asymmetric platinum(IV) bis-carboxylates as anticancer prodrugs that are able to overcome different aspects of drug resistance and improve the pharmacological properties. The compounds developed were based on FDA-approved cisplatin as the focal point, since its activities and mechanisms have been well-documented. This would provide a good basis for evaluation as we seek to improve its efficacy and mitigate its limitations simultaneously. In this dissertation, three prodrug strategies based on asymmetric platinum(IV) bis-carboxylates would be investigated. Ultimately, the compounds of interest would undergo intracellular reduction to yield cisplatin and exhibit similar mechanistic actions.

In Chapter 3, the top-down approach of developing a novel class of asymmetric platinum(IV) bis-carboxylates bearing cisplatin pharmacophores through sequential carboxylation of oxoplatin was described. This synthetic methodology is a departure from classical methods used to generate only symmetric platinum(IV) bis-carboxylates. We were able to attach different ligands with contrasting properties simultaneously on the axial positions of platinum(IV) scaffolds, paving the way for rational development of cisplatin prodrugs.

In Chapter 4, the tunable pharmacological properties of asymmetric platinum(IV) bis-carboxylates were investigated. The studied compounds were compared against symmetric platinum(IV) bis-carboxylates in terms of lipophilicity, aqueous solubility, and cytotoxicity, to validate our hypothesis that the pharmacological properties could be tuned and engineered more effectively using the asymmetric scaffolds. Preliminary results identified asymmetric platinum(IV) bis-carboxylate **3** as a lead compound. To study structure activity relationships, minor structural variations of **3** in the axial positions whilst keeping the cisplatin pharmacophore generated a library of asymmetric platinum(IV) bis-carboxylates and the correlation between structural parameters and pharmacological attributes were analyzed. (*Reprinted 2015 with permission from C. F. Chin, Q. Tian, M. I. Setyawati, W. Fang, E. S. Q. Tan, D. T. Leong, W. H. Ang. Tuning the activity of platinum(IV) anticancer complexes through asymmetric acylation, J. Med. Chem., 2012, 55, 7571-7582 - Copyright 2012 American Chemical Society.*)

In Chapter 5, the photoactivatable property of platinum(IV) bis-carboxylates was investigated. This project depicts the use of aromatic chromophores in the axial positions to tune the wavelength for maximum absorption of light,  $\lambda_{\text{max}}$ , instead of using the conventional azido or iodo ligands on the equatorial positions. This allowed photoreducible prodrugs of cisplatin that can be triggered by UV irradiation to be developed.

In Chapter 6, an asymmetrical platinum(IV) prodrug of cisplatin bearing doxorubicin on one axial position was developed to achieve synergism in dual drugs delivery and overcome chemoresistance. Tuning of the lipophilic property of the prodrug was demonstrated using the free axial position as a handle. Benzoate ligand was attached on the free unconjugated axial position to improve lipophilicity to facilitate entrapment into tumor-targeting multi-walled carbon nanotubes (MWCNT). (*C. F. Chin, S. Q. Yap, J. Li, G. Pastorin, W. H. Ang. Ratiometric delivery of cisplatin and doxorubicin using tumour-targeting carbon-nanotubes entrapping platinum(IV) prodrugs, Chem. Sci., 2014, 5, 2265-2270 - Reproduced by permission of The Royal Society of Chemistry.*)

The dissertation is concluded with a discussion on the prospect of platinum-based anticancer drugs in the future.

## Chapter 3

### Developing a Novel Class of Asymmetric Platinum(IV) Bis-Carboxylates

#### 3.1 Introduction

The existing dilemma of employing platinum(IV) complexes with symmetrical axial bis-carboxylate ligands is too limited to fully exploit the vast potential of this prodrug strategy. Symmetric platinum(IV) bis-carboxylates that are lipophilic and cytotoxic exhibit poor aqueous solubility, and vice versa.<sup>138</sup> In addition, these scaffolds allow limited structural variations to vary the functionalities of the prodrugs. Since platinum(IV) prodrugs take on the properties of their coordinating ligands,<sup>139</sup> it should be practical to influence their properties by selectively “mixing-and-matching” the axial ligands. We surmise that it may be feasible to prepare stable asymmetric platinum(IV) bis-carboxylates that are lipophilic yet water-soluble, and hence more compatible with pharmaceutical applications, by combining carboxylate ligands with contrasting properties into the same scaffold. This class of asymmetric platinum(IV) carboxylate complexes will contain two different ligands at the axial sites which will serve as handles to fine-tune the pharmacological properties of the complex. Henceforth, we devised a practical method to carry out carboxylation onto a platinum(IV) scaffold in sequential steps, a departure from existing one pot procedures designed to generate symmetric bis-carboxylates. This synthetic strategy paves the

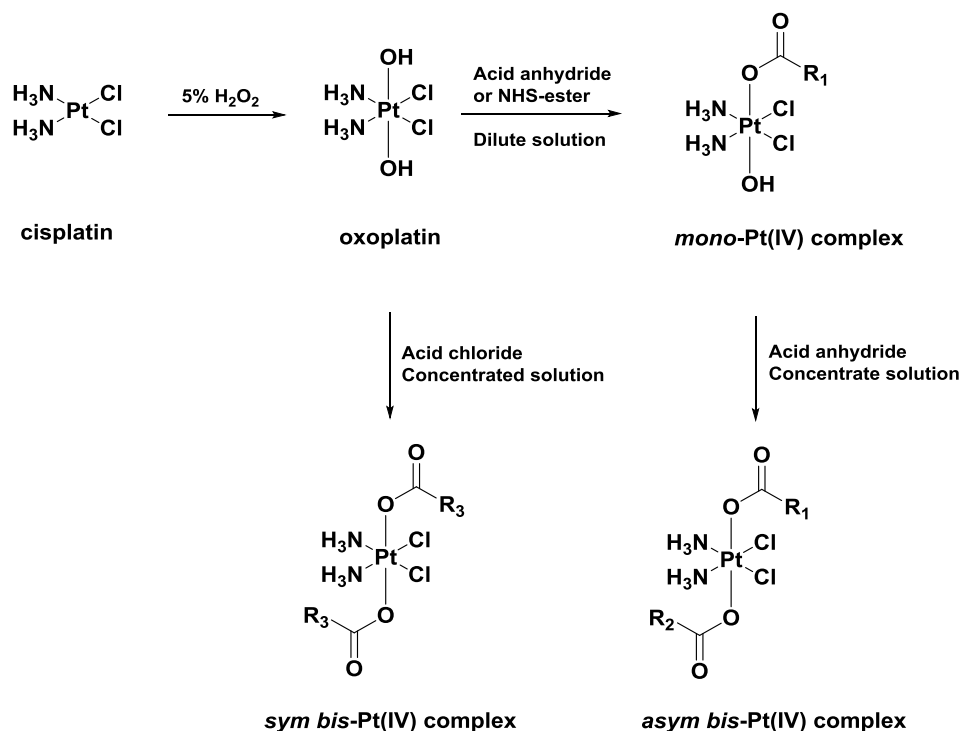
way for a rational development of asymmetric platinum(IV) bis-carboxylates containing the  $[cis-Pt(NH_3)_2Cl_2]$  cisplatin pharmacophore with engineered properties with the ultimate aim of enhancing their efficacies against cancer cells.

### 3.2 Synthetic Strategy to Develop Asymmetric Platinum(IV) Bis-Carboxylates

The strategy of preparing asymmetric platinum(IV) bis-carboxylates involved sequential carboxylation of oxoplatin at its axial ligand positions. Our approach was to limit the carboxylation reaction to only one hydroxyl ligand leaving remaining site for further systematic manipulations. The reaction was carried out using a less reactive carboxylating reagent and under high dilution conditions (Scheme 11). In previous reports, acylation using acid chlorides in concentrated conditions promoted the exclusive formation of symmetric platinum(IV) bis-carboxylates.<sup>78</sup> Reaction work-up also required extensive washing with water to remove the side-products which could dissolve water-soluble platinum(IV) mono-carboxylates.<sup>140, 141</sup> Treatment of oxoplatin with mildly reactive acid anhydrides or hydroxysuccinimide esters in a highly polar dilute solvent condition such as DMF and DMSO yielded mainly platinum(IV) mono-carboxylates. This strategy was also successfully applied in the mono-carboxylation of oxoplatin with succinic anhydride under high dilution conditions previously.<sup>142</sup>

The purified platinum(IV) mono-carboxylates were subsequently reacted with acid anhydrides in concentrated DMF solvent condition to synthesize asymmetric

platinum(IV) bis-carboxylates. DMF was used as solvent instead of DMSO for the reactions as acetic anhydrides and other acid anhydrides can activate DMSO to yield DMSO-electrophile adducts that are prone to nucleophilic attacks by the hydroxyl ligands and would not yield the target products.



**Scheme 11.** General synthetic route to prepare platinum(IV) complexes

To generate the products in good yields, the mono-carboxylation of oxoplatin was initiated with an aryl moiety first before carboxylating the other hydroxyl group with an alkyl moiety. The synthesis of platinum(IV) mono-aryl carboxylates generated higher yield than platinum(IV) mono-alkyl carboxylates, presumably due to steric hindrance of the aryl groups resulting in a more favorable formation of the mono-aryl products. In addition, asymmetric platinum(IV) complexes

exhibited similar solubility as aryl anhydrides since both were soluble in acetone and poorly soluble in diethyl ether. Purification work-up steps would require column chromatography if the synthetic sequence was reversed, which explained why our mono-carboxylation procedures always began with aromatic molecules first.

### 3.3 Synthesis of Platinum(IV) Mono-Carboxylates A-I

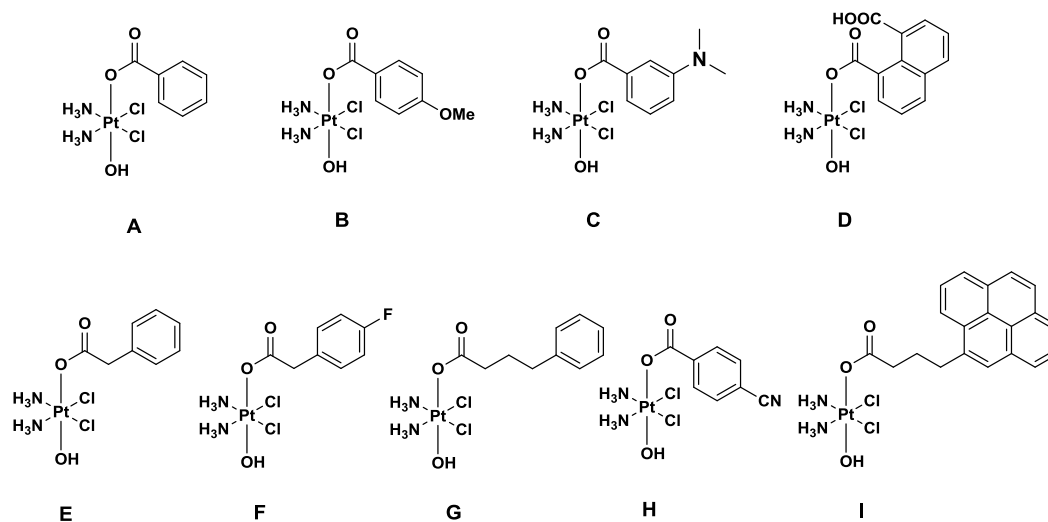
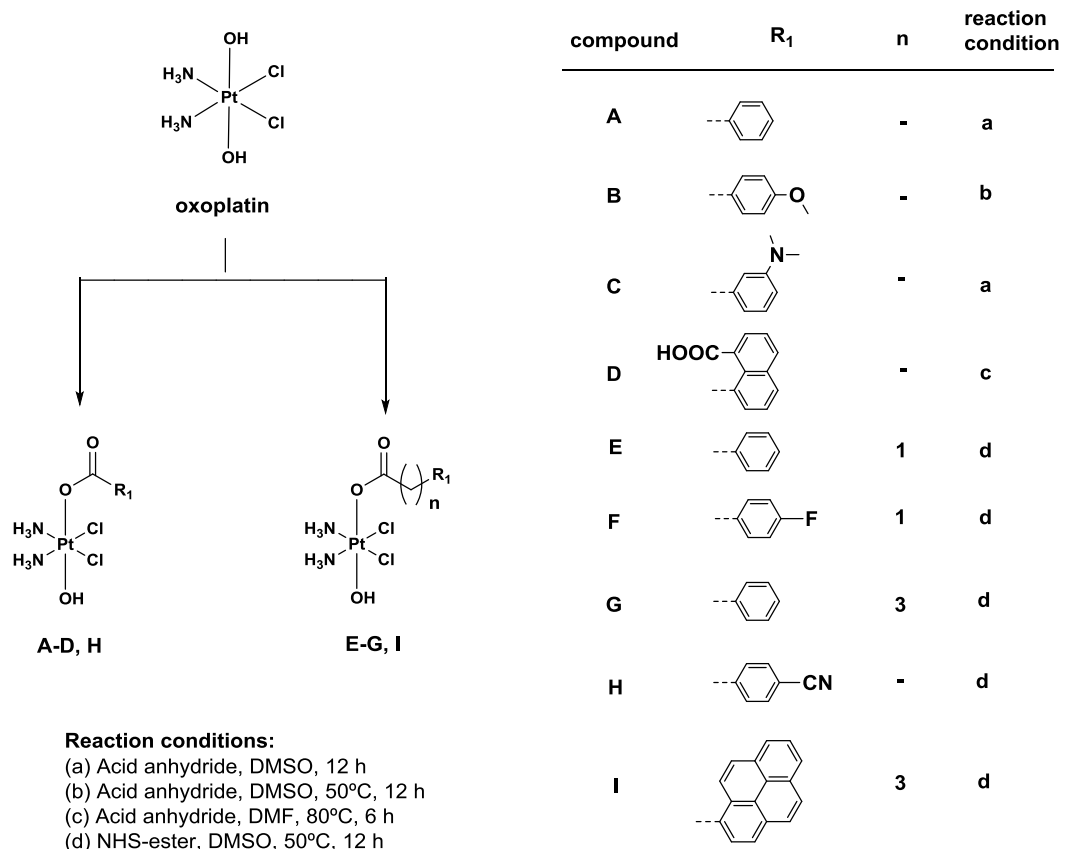


**Figure 11.** Chemical structure of platinum(IV) mono-carboxylates A-I

Mono-carboxylated platinum(IV) complexes A-I (Figure 11) were synthesized as shown in Scheme 12. Stirring oxoplatin with benzoic anhydride under high dilution conditions over 12 hours at room temperature generated the desired mono-carboxylated product A in good yields. Microwave heating at 75°C was initially found to be a rapid and reproducible method for preparing A, generating the desired product within 1 hour. However, the low reaction yields (10%) limited



its further applications. Mono-carboxylated platinum(IV) **B-I** were synthesized under the same high dilution conditions in DMSO with different temperature conditions due to different reactivities of the acid anhydrides and *N*-hydroxysuccinimide esters used (Scheme 12). The symmetric bis-carboxylated platinum(IV) derivatives were formed as the major side-product but they were readily removed by acetone washing. Acetone washing also helped to remove unreacted reagents and the platinum(IV) mono-carboxylates were purified by recrystallization from DMF and diethyl ether. Like their bis-carboxylate congeners, mono-carboxylate platinum(IV) complexes **A-I** were highly soluble in DMF and DMSO, and insoluble in chlorinated and non-polar solvents such as diethyl ether and hexane. Except **I**, complexes **A-H** were soluble in water indicating that the hydroxyl ligand was essential for improved hydrophilic properties. Solubility in other polar organic solvents such as acetone and THF also noticeably decreased. Reaction yields constituted the major challenge to this synthetic approach and repeated optimizations were required to achieve moderate recovery.



**Scheme 12.** Synthetic route to prepare platinum(IV) mono-carboxylates **A-I**

## 3.4 Synthesis of Asymmetric Platinum(IV) Bis-Carboxylates 3-22

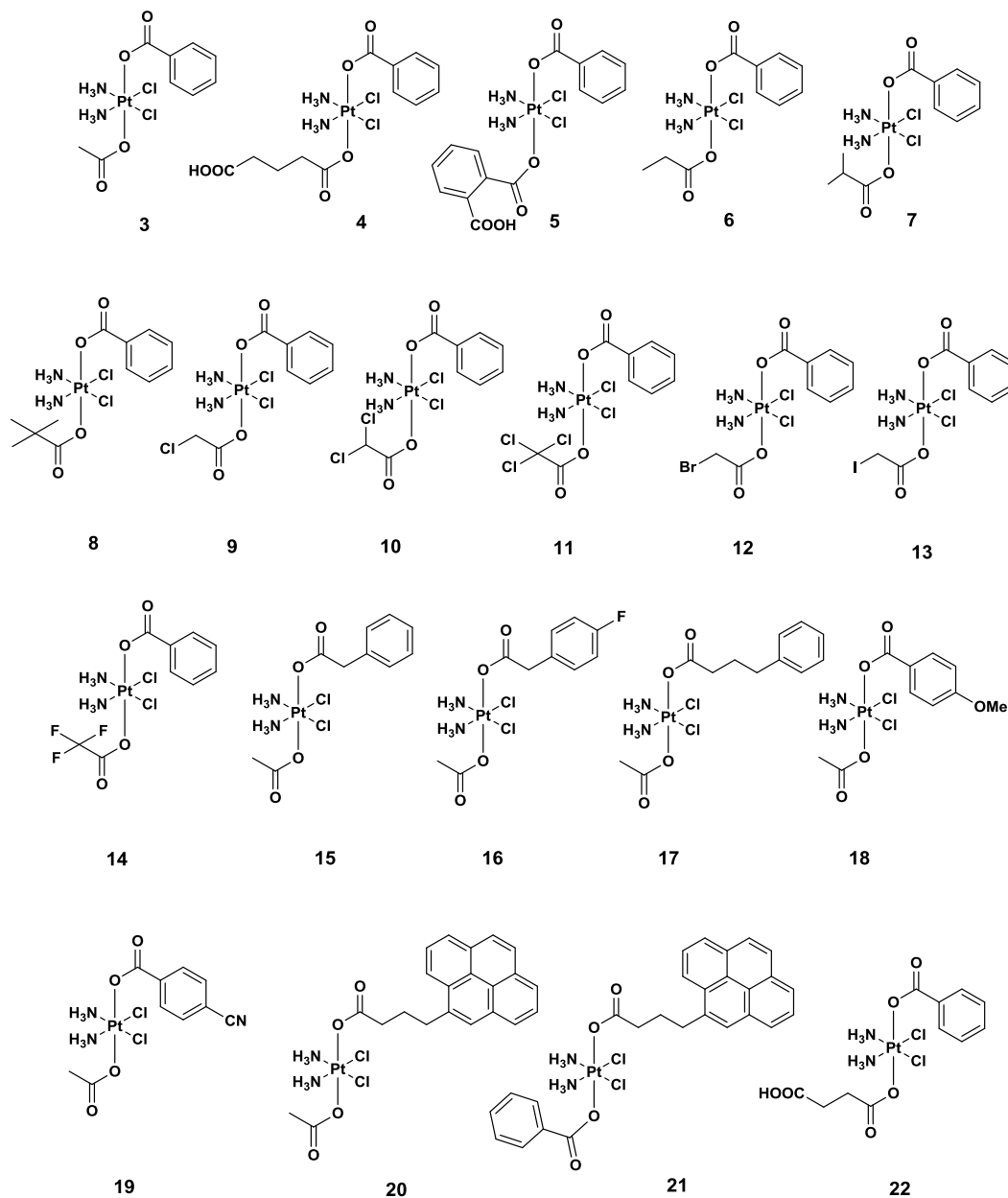


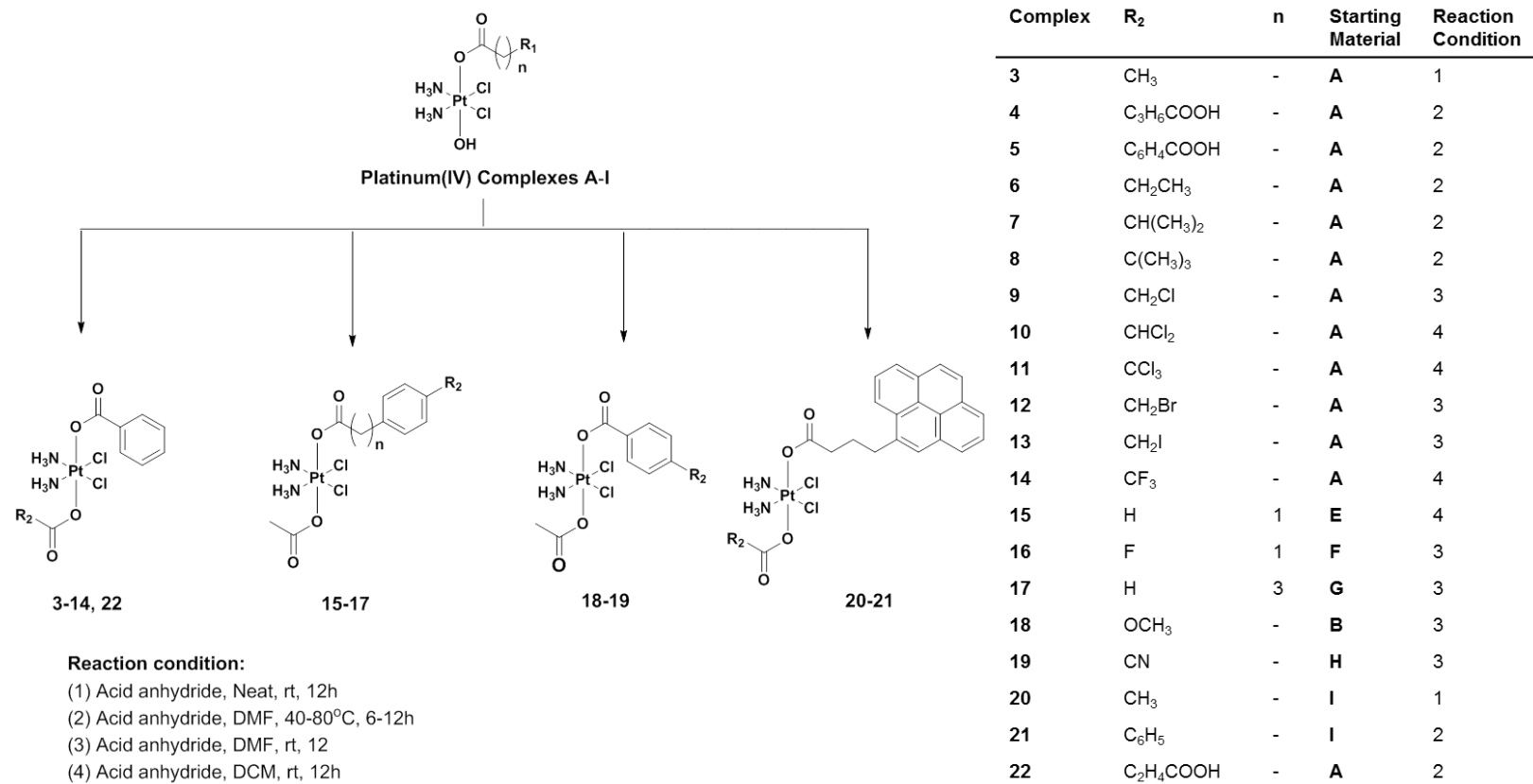
**Figure 12.** Chemical structure of asymmetric platinum(IV) bis-carboxylates 3-22

To generate asymmetric platinum(IV) bis-carboxylates 3-22 (Figure 12), the synthesized platinum(IV) mono-carboxylates were stirred with acid anhydrides in

DMF or DCM under different reaction conditions (Scheme 13). The reactions were generally facile and conversion was quantitative. For example, complex **A** was converted to **3** in neat acetic anhydride at r.t. for 24 hours and reaction completion was indicated by complete dissolution of the reactants. Reaction work-up was straightforward, involving lyophilizing the reaction mixture and triturating the residue with diethyl ether to remove the excess and unreacted acetic anhydride. Complexes **4** and **5** were obtained using a similar procedure using DMF as a solvent and excess of glutaric and phthalic anhydride at elevated temperatures, respectively, in good yields.

Different reaction conditions were used to activate the reactions to yield asymmetric platinum(IV) bis-carboxylates due to different reactivity of the acid anhydrides. To synthesize **6**, **A** was stirred in propionic anhydride/DMF mixture at 40°C overnight and the completion of the reaction was indicated by the dissolution of the reactants. However, this was not observed when **A** was reacted with isobutyric anhydride and trimethylacetic anhydride to synthesize **7** and **8** respectively. The reactions temperature were thus alleviated to 80°C and stirred overnight before homogeneous solutions could be obtained. This was likely due to the presence of more electron-donating methyl groups which decreased the activity of the acid anhydrides. Using this strategy, the asymmetric platinum(IV) bis-carboxylates could be synthesized and purified, except complexes **10**, **11** and **14**. The synthesis of **10**, **11** and **14** were not as facile, as undesirable side-products such as tetrachloro-platinum(IV) complex,  $\text{Pt}(\text{NH}_3)_2\text{Cl}_4$ , was observed on  $^1\text{H}$

NMR and ESI/MS when the same synthetic approach was used. This could be due to the high reactivity and acidic nature of the haloacetate anhydrides which resulted in the displacement of the carboxylate ligands. The reaction solvent was changed to DCM instead and the reactions were able to proceed heterogeneously to yield the targeted compounds. Reaction work-ups include filtering the reaction mixture and washing the residue with excess triethyl ether to remove unreacted acid anhydrides. In the synthesis of complex **21**, complex **I** was stirred with slight excess of benzoic anhydride in DMF at 70°C for 12 hours. The main challenge was to ascertain the conditions which would promote the consumption of **I** and removal of unreacted benzoic anhydride from the product. It was found that a higher temperature generated **21** in better yields and that washing the lyophilized reaction mixture extensively with diethyl ether could eliminate residual benzoic anhydride and also **21** partially, decreasing its overall yield. Nonetheless, these experimental work-up procedures allowed us to obtain the pure compounds for further studies.



**Scheme 13.** Synthetic route to prepare asymmetric platinum(IV) bis-carboxylates **3-22**

### 3.5 Characterization of Synthesized Platinum(IV) Complexes **A-I** and **3-22**

The synthesized platinum(IV) complexes were characterized using ESI-MS,  $^1\text{H}$ - and  $^{195}\text{Pt}$ -NMR spectroscopy, and their purity were determined by elemental analysis or RP-HPLC. Complex **A** and **3** were also characterized by single crystal X-ray diffraction. The  $[\text{M-H}]^+$  parent ion of the platinum(IV) complexes were readily observed using ESI-MS. Fragmentation analysis resulted in the loss of  $\text{NH}_3$ ,  $\text{HCl}$ , and carboxylate ligands, consistent with the proposed structures of the complexes.

In the  $^1\text{H}$  NMR spectra of platinum(IV) mono-carboxylates **A-I**, characteristic resonances could be observed at 5.90-6.10 ppm, which were assigned to the ammine ligands. After carboxylation to yield the asymmetric platinum(IV) bis-carboxylates **3-22**, these resonances were shifted downfield to 6.50-6.70 ppm (Figure 13). In deuterated  $\text{DMSO-d}_6$ , the ammine protons of the asymmetric platinum(IV) bis-carboxylates **3-22** appeared as a broadened peak in the  $^1\text{H}$  NMR spectra due to coupling to quadrupolar  $^{14}\text{N}$  nuclei and hence resulted in non-uniform charge distribution over the nuclear surface. When acetone- $\text{d}_6$  was used as the solvent, well resolved ammine resonances could be observed for the asymmetric platinum(IV) bis-carboxylates. However, well resolved ammine resonances were observed readily in platinum (IV) mono-carboxylates **A-I** where the spin-spin couplings for the ammine protons to quadrupolar  $^{14}\text{N}$  nuclei ( $^1J_{\text{NH}} =$

52–53 Hz) and  $^{195}\text{Pt}$  nucleus ( $^2J_{\text{HPt}} = 52$  Hz) in  $^1\text{H}$  NMR spectra when deuterated DMSO- $\text{d}_6$  was used, which could be due to the slow relaxation of the  $^{14}\text{N}$  nuclei.

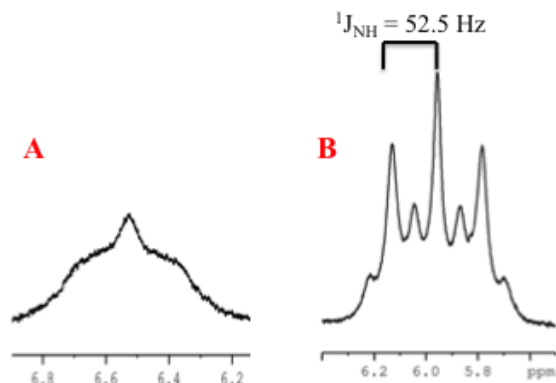


**Figure 13.** Typical ammine peak in  $^1\text{H}$  NMR spectra of platinum(IV) (A) bis-carboxylate and (B) mono-carboxylate in DMSO- $\text{d}_6$  solvent

$^{195}\text{Pt}$  NMR resonances of the platinum(IV) complexes were measured relative to an external  $\text{K}_2\text{PtCl}_4$  standard in  $\text{D}_2\text{O}$  that resonated at  $-1628\text{ppm}$ . The  $^{195}\text{Pt}$  chemical shifts of **A-I** were observed in the region of ca. 1015–1080 ppm, while the chemical shifts of **3-22** were observed in a more deshielded region of ca. 1100–1250 ppm, which could be due to the presence of an additional electron-withdrawing ligand resulting in greater deshielding effect on the platinum(IV) metal center. The  $^{195}\text{Pt}$  chemical shifts of the asymmetric platinum(IV) bis-carboxylates were consistent with the symmetric platinum(IV) bis-carboxylates **1-2** (Figure 14) obtained directly from their corresponding anhydrides, as well as other reported platinum(IV) alkyl and aryl carboxylates.<sup>140, 143, 144</sup>



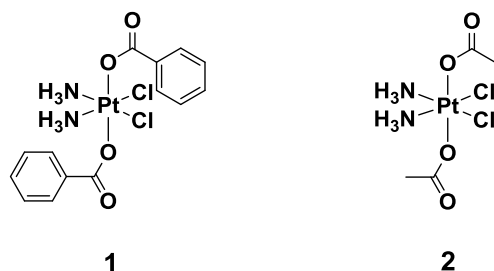


**Figure 14.** Chemical structure of symmetric platinum(IV) bis-carboxylates **1-2**

Single crystals of **A** and **3** suitable for X-ray diffraction studies were grown through vapor diffusion of acetone into DMSO solution of **A** and diethyl ether into acetone solution of **1**, respectively. To the best of our knowledge, complex **3** is the first reported example of *cis,cis,trans*-diamminedichlorobiscarboxylatoplatinum(IV) structure containing two different carboxylate ligands at the axial positions. In the crystallographic data of **A**, there are one molecule of **A** and one molecule of DMSO arranged in a monoclinic crystal system with  $C2/m$  space group. In the crystallographic data of **3**, there are two molecules of **1** and one molecule of acetone in a monoclinic unit cell with  $P2_1/c$  space group. Molecular representations of **A** and **3** are shown in Figure 15 and selected crystallographic structural data are given in Table 1, respectively. The co-ordination geometry about the platinum(IV) metal centers are octahedral. The average Pt-Cl and Pt-N bond lengths of 2.315(3) Å and 2.035(5) Å respectively are of typical values; they are held in a square-planar conformation similar to cisplatin. From the molecular structure of **A**, the Pt-O<sub>benzoate</sub> is 2.022(4) Å, while Pt-O<sub>hydroxyl</sub> is 1.975(4) Å, which is slightly shorter than Pt-O<sub>benzoate</sub>. This is likely to be due to lower electron withdrawing strength of hydroxyl ligand as

compared to the benzoate ligand, hence a shorter Pt-O bond length. From the molecular structure of **3**, the axial O-Pt-O bond across the acetate and benzoate ligands is slightly bent due to the intramolecular H-bonding between the ammine protons and the carboxylate oxygen atoms.<sup>140</sup> The Pt-O<sub>acetate</sub> bond length of is 2.021(5) Å which is slightly longer than Pt-O<sub>benzoate</sub> at 2.007(5) Å but consistent with reported values.<sup>140, 145</sup> In comparison, the average Pt-O bond length in symmetric platinum(IV) bis-benzoate **1** and bis-acetate **2** were reported to be 2.01(1) Å and 2.030(6) Å, respectively.

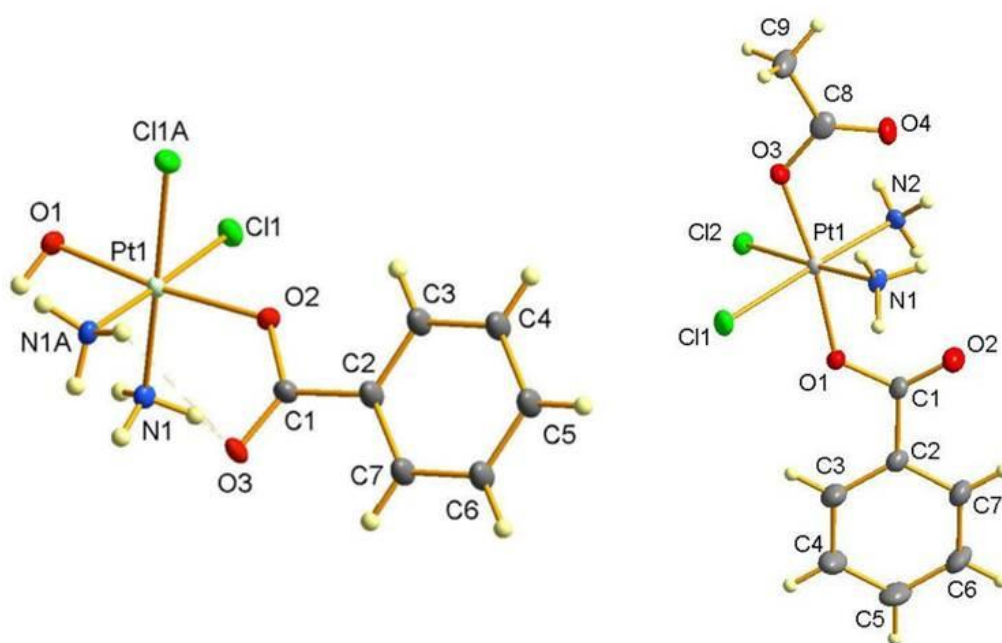


**Figure 15.** Molecular representation of platinum(IV) complexes **A** (left) and **3** (right); thermal ellipsoids are 50% equiprobability envelopes

**Table 1.** Comparison of bond distances (Å) and angles (°) of A, 1, 2 and 3

| Complex                  | A <sup>a</sup> | 1 <sup>b</sup> | 2 <sup>b</sup> | 3 <sup>a</sup> |
|--------------------------|----------------|----------------|----------------|----------------|
| Pt-O <sub>hydroxyl</sub> | 1.975(4)       | -              | -              | -              |
| Pt-O <sub>acetate</sub>  | -              | 2.01(1)        | -              | 2.007(5)       |
| Pt-O <sub>benzoate</sub> | 2.022(4)       | -              | 2.030(6)       | 2.021(5)       |
| Pt-N                     | 2.044(4)       | 2.05(1)        | 2.049(6)       | 2.035(5)       |
| Pt-Cl                    | 2.312(1)       | 2.30(1)        | 2.318(2)       | 2.316(2)       |
| C-O(Pt)                  | 1.300(8)       | 1.30(2)        | 1.303(11)      | 1.301(8)       |
| O=C(O)                   | 1.224(8)       | 1.22(2)        | 1.213(11)      | 1.230(8)       |
| C-C(O)                   | 1.504(7)       | 1.50(2)        | 1.502(14)      | 1.496(10)      |
| O-Pt-O                   | 173.3(2)       | 170.9(2)       | 176.7(3)       | 172.6(2)       |
| N-Pt-Cl                  | 178.4(1)       | 179.2(4)       | 177.1(2)       | 178.0(2)       |

<sup>a</sup> The bond parameters are average values between the two separate platinum(IV) molecules in the unit cell.

<sup>b</sup> The bond parameters listed are average values given the symmetrical nature of the complexes. The data was obtained from literature reports.<sup>140, 145</sup>

### 3.6 Summary

The development of a novel methodology to synthesize asymmetric platinum(IV) bis-carboxylates represents a new paradigm of platinum(IV) prodrugs strategy as it allows a greater structural variations that can provide greater variance in the pharmacological properties. This can potentially replace classical methodology of developing symmetric platinum(IV) bis-carboxylates and allow a more rational approach in platinum-based anticancer drugs design. In the ensuing chapters, the applications of asymmetric platinum(IV) bis-carboxylates will be explored and investigated.

### 3.7 Experimental Procedures

Unless otherwise noted, all procedures were carried out without taking precautions to exclude air and moisture. All solvents and chemicals were used as received without further treatment.  $\text{K}_2\text{PtCl}_4$  was obtained from both Precious Metals Online and Strem Chemicals. Cisplatin, oxoplatin, **1-2** were synthesized and purified accordingly to literature procedures.<sup>140, 141, 145, 146, 147</sup> The purities of asymmetric platinum(IV) precursors **E-I** were not performed as they were used subsequently in the synthesis of asymmetric platinum(IV) complexes. All other solvents and chemicals were of analytical grade or HPLC grade obtained from commercial sources.

**Instrumentation.**  $^1\text{H}$  and  $^{195}\text{Pt}$  NMR spectra were recorded on a Bruker ACF 300 and Bruker AMX 500 spectrometer and the chemical shifts ( $\delta$ ) were internally referenced by the residual solvent signals relative to tetramethylsilane for  $^1\text{H}$  and externally referenced using  $\text{K}_2\text{PtCl}_4$  for  $^{195}\text{Pt}$ . Mass spectra were measured using a Finnigan MAT LCQ or Bruker Ultimate 3000 ion trap ESI mass spectrometer. Elemental analyses of selected platinum compounds were carried out on the Perkin-Elmer PE 2400 elemental analyzer by CMMAC, NUS.

**X-ray Diffraction Studies.** X-ray data were collected with a Bruker AXS SMART APEX diffractometer using  $\text{Mo-K}\alpha$  radiation at 223(2) K with the SMART suite of Programs.<sup>148</sup> Data were processed and corrected for Lorentz and polarization effects using SAINT software,<sup>149</sup> and for absorption effects using the

SADABS software.<sup>150</sup> Structural solution and refinement were then carried out using the SHELXTL suite of programs.<sup>151</sup> The structure was solved by Direct Methods. Non-hydrogen atoms were located using difference maps and were given anisotropic displacement parameters in the final refinement. All H atoms were put at calculated positions using the riding model.

**Synthesis of *cis,cis,trans*-[Pt(NH<sub>3</sub>)<sub>2</sub>Cl<sub>2</sub>(CO<sub>2</sub>C<sub>6</sub>H<sub>5</sub>)OH] (A).** Benzoic anhydride (100 mg, 440 μmol) was added to *cis,cis,trans*-[Pt(NH<sub>3</sub>)<sub>2</sub>Cl<sub>2</sub>(OH)<sub>2</sub>] (100 mg, 300 μmol) in DMSO (20 mL). The reaction was stirred at r.t. for 12 h and filtered to remove unreacted starting materials. The filtrate was lyophilized and washed with acetone (3 x 10 mL) and cold DMF (1 x 5 mL), and dried *in vacuo* to yield the product as a white precipitate. Single crystals suitable for x-ray diffraction were grown from vapor diffusion of acetone into a solution of **A** in DMSO. Yield: 99 mg (75%). The purity of platinum(IV) compounds were conducted using analytical HPLC on a Shimadzu Prominence using a Shimpack VP-ODS C18 (5 μM, 120 Å, 250 x 4.60 mm i.d) column; 1.0 ml/min flow rate; 254 nm and 280 nm UV detection. The gradient eluent condition is as followed: 20% - 80% aqueous NH<sub>4</sub>OAc buffer (10 mM, pH 3.8) (solvent A) and MeCN (solvent B) over 20 minutes, followed by constant of 80% of solvent B for a further 5 minutes. <sup>1</sup>H NMR (300 MHz, DMSO-*d*<sub>6</sub>): δ 7.88 (d, 2 H, Ar-H), 7.47 (t, 1 H, Ar-H), 7.39 (t, 2 H, Ar-H), 6.06 (m, 6 H, NH<sub>3</sub>, <sup>1</sup>J<sub>HN</sub> = 52.2 Hz, <sup>2</sup>J<sub>HPt</sub> = 52.9 Hz). <sup>195</sup>Pt NMR (107.6 MHz, DMSO-*d*<sub>6</sub>): 1022.2 ppm. ESI-MS (neg. ion mode): *m/z* = 436.9 [M-H]<sup>-</sup>. Purity (HPLC): 94.1% at 254 nm and 93.4% at 280 nm

respectively; retention time ( $t_r$ ) = 6.9 min. Anal. Calcd. for **A**·1.25(DMF),  $C_7H_{12}Cl_2N_2O_3Pt$ : C, 24.35; H, 4.19; N, 8.59. Found: C, 24.71; H, 4.00; N, 8.60.

**Synthesis of *cis,cis,trans*-[Pt(NH<sub>3</sub>)<sub>2</sub>Cl<sub>2</sub>(CO<sub>2</sub>C<sub>6</sub>H<sub>4</sub>OCH<sub>3</sub>)OH] (B).** The compound **B** was prepared in accordance with the method used for **A** using 30 mg of 4-methoxy-benzoic anhydride. The reaction was stirred at 50°C overnight. Yield: 13 mg (30%). <sup>1</sup>H NMR (500 MHz, DMSO-*d*<sub>6</sub>): δ 7.83 (d, 2 H, Ar-H), 6.93 (d, 2 H, Ar-H), 6.05 (m, 6 H, NH<sub>3</sub>, <sup>1</sup>J<sub>HN</sub> = 51.1 Hz, <sup>2</sup>J<sub>HPt</sub> = 52.4 Hz), 3.80 (s, 3 H, Ar-OCH<sub>3</sub>) ppm. <sup>195</sup>Pt NMR (107.6 MHz, DMSO-*d*<sub>6</sub>): 1025.4 ppm. ESI-MS (neg. ion mode):  $m/z$  = 466.9 [M-H]<sup>-</sup>. Purity (HPLC): 95.1% at 254 nm and 95.3% at 280 nm;  $t_r$  = 8.6 min. Due to low yield of the compound, elemental analysis of the sample was not obtained.

**Synthesis of *cis,cis,trans*-[Pt(NH<sub>3</sub>)<sub>2</sub>Cl<sub>2</sub>(CO<sub>2</sub>C<sub>6</sub>H<sub>4</sub>NC<sub>2</sub>H<sub>6</sub>)OH] (C).** The compound **C** was prepared in accordance with the method used for **A** using 30 mg of 3-(dimethylamino)benzoic anhydride. Yield: 4 mg (9%). <sup>1</sup>H NMR (500 MHz, DMSO-*d*<sub>6</sub>): δ 7.20 (m, 3 H, Ar-H), 6.83 (d, 1 H, Ar-H), 6.08 (m, 6 H, NH<sub>3</sub>, <sup>1</sup>J<sub>HN</sub> = 51.7 Hz, <sup>2</sup>J<sub>HPt</sub> = 52.3 Hz), 2.90 (s, 6 H, Ar-NCH<sub>3</sub>) ppm. <sup>195</sup>Pt NMR (107.6 MHz, DMSO-*d*<sub>6</sub>): 1024.9 ppm. ESI-MS (neg. ion mode):  $m/z$  = 479.9 [M-H]<sup>-</sup>. Purity (HPLC): 95.7% at 254 nm and 95.7% at 280 nm;  $t_r$  = 9.0 min.

**Synthesis of *cis,cis,trans*-[Pt(NH<sub>3</sub>)<sub>2</sub>Cl<sub>2</sub>(CO<sub>2</sub>C<sub>10</sub>H<sub>6</sub>COOH)OH] (D).** Naphthalic anhydride (95 mg, 480 μmol) was added to *cis,cis,trans*-[Pt(NH<sub>3</sub>)<sub>2</sub>Cl<sub>2</sub>(OH)<sub>2</sub>] (60

mg, 180  $\mu\text{mol}$ ) in DMF (5 mL). The reaction was stirred at 80°C for 6 h, treated with deionized water (20 mL) and cooled at 4°C for 12 h. The reaction mixture was filtered through celite to remove unreacted starting material and the solvent removed in vacuo. The residue was extracted with water (3 x 20 mL) and the aqueous extract lyophilized to yield an off-white product. Yield: 38 mg (40%).  $^1\text{H}$  NMR (300 MHz, DMSO- $d_6$ ):  $\delta$  7.85 (d, 1 H, *o*-Ar-H), 7.78 (d, 1 H, *o*-Ar-H), 7.59 (d, 1 H, Ar-H), 7.45-7.38 (m, 3 H, Ar-H), 6.31 (m, 6 H, NH<sub>3</sub>).  $^{195}\text{Pt}$ -NMR (107.6 MHz, DMSO- $d_6$ ): 1015.8 ppm. ESI-MS (neg. ion mode):  $m/z$  = 530.9 [M-H]<sup>-</sup>. Purity (HPLC): 95.0% at 254 nm and 95.2% at 280 nm;  $t_r$  = 7.5 min.

**Synthesis of *cis,cis,trans*-[Pt(NH<sub>3</sub>)<sub>2</sub>Cl<sub>2</sub>(CO<sub>2</sub>CH<sub>2</sub>C<sub>6</sub>H<sub>5</sub>)OH] (E).** Benzeneacetic acid, 2, 5-dioxo-1-pyrrolidinyl ester (42 mg, 180  $\mu\text{mol}$ ) was added to oxoplatin (40 mg, 120  $\mu\text{mol}$ ) in DMSO (12 mL) and stirred overnight (12 h) at 50°C. The reaction mixture was filtered through celite. The filtrate was lyophilized, washed with acetone (1 x 2 mL), diethyl ether (1 x 40 mL) and water (1 x 2 mL) before drying in vacuo to yield the product in white precipitate. Yield: 43.8 mg (81%).  $^1\text{H}$  NMR (300 MHz, DMSO- $d_6$ ):  $\delta$  7.20 (m, 5 H, Ar-H), 6.54 (m, 6 H, NH<sub>3</sub>), 3.52 (s, 2 H, -COOCH<sub>2</sub>-).  $^{195}\text{Pt}$  NMR (107.6 MHz, DMSO- $d_6$ ):  $\delta$  1039.7 ppm. ESI-MS (negative ion mode):  $m/z$  = 451.0 [M-H]<sup>-</sup>.

**Synthesis of *cis,cis,trans*-[Pt(NH<sub>3</sub>)<sub>2</sub>Cl<sub>2</sub>(CO<sub>2</sub>CH<sub>2</sub>C<sub>6</sub>H<sub>4</sub>F)OH] (F).** The compound **F** was prepared in accordance with the method used for **E** using 45 mg of benzeneacetic acid, 4-fluoro-, 2, 5-dioxo-1-pyrrolidinyl ester (179  $\mu\text{mol}$ ). Yield:

45.1 mg (80.1%).  $^1\text{H}$  NMR (300 MHz,  $\text{DMSO-}d_6$ ):  $\delta$  7.29 (t, 2 H, Ar-H), 7.06 (t, 2 H, Ar-H), 5.96 (m, 6 H,  $\text{NH}_3$ ), 3.14 (s, 2 H,  $-\text{COOCH}_2-$ ).  $^{195}\text{Pt}$  NMR (107.6 MHz,  $\text{DMSO-}d_6$ ):  $\delta$  1080.6 ppm ESI-MS (negative ion mode):  $m/z = 469.0$   $[\text{M-H}]^-$ .

**Synthesis of *cis,cis,trans*-[Pt(NH<sub>3</sub>)<sub>2</sub>Cl<sub>2</sub>(CO<sub>2</sub>CH<sub>2</sub>CH<sub>2</sub>CH<sub>2</sub>C<sub>6</sub>H<sub>5</sub>)OH] (G).** The compound **G** was prepared in accordance with the method used for **E** using 48 mg benzenebutanoic acid, 2, 5-dioxo-1-pyrrolidinyl ester (191  $\mu\text{mol}$ ). Yield: 12.6 mg (20.1%).  $^1\text{H}$  NMR (300 MHz,  $\text{DMSO-}d_6$ ):  $\delta$  7.22 (m, 5 H, Ar-H), 5.97 (m, 6 H,  $\text{NH}_3$ ), 2.16 (t, 2 H,  $-\text{COOCH}_2-$ ), 1.74 (m, 2 H,  $-\text{CH}_2-$ ).  $^{195}\text{Pt}$  NMR (107.6 MHz,  $\text{DMSO-}d_6$ ):  $\delta$  1039.4 ppm. ESI-MS (negative ion mode):  $m/z = 479.0$   $[\text{M-H}]^-$ .

**Synthesis of *cis,cis,trans*-[Pt(NH<sub>3</sub>)<sub>2</sub>Cl<sub>2</sub>(CO<sub>2</sub>C<sub>6</sub>H<sub>4</sub>CN)OH] (H).** The compound **H** was prepared in accordance with the method used for **E** using 44 mg of benzoic acid, 4-cyano-, 2, 5-dioxo-1-pyrrolidinyl ester (180  $\mu\text{mol}$ ). Yield: 50.0 mg (83.5 %).  $^1\text{H}$  NMR (300 MHz,  $\text{DMSO-}d_6$ ):  $\delta$  8.00 (d, 2 H, Ar-H), 7.90 (d, 2 H, Ar-H), 6.04 (m, 6 H,  $\text{NH}_3$ ).  $^{195}\text{Pt}$  NMR (107.6 MHz,  $\text{DMSO-}d_6$ ):  $\delta$  1030.8 ppm. ESI-MS (negative ion mode):  $m/z = 462.0$   $[\text{M-H}]^-$ .

**Synthesis of *cis,cis,trans*-[Pt(NH<sub>3</sub>)<sub>2</sub>Cl<sub>2</sub>(CO<sub>2</sub>CH<sub>2</sub>CH<sub>2</sub>CH<sub>2</sub>C<sub>15</sub>H<sub>9</sub>)OH] (I).** The compound **I** was prepared in accordance with the method used for **E** using 30 mg of 1-Pyrenebutyric acid *N*-hydroxysuccinimide ester (78  $\mu\text{mol}$ ). Yield: 27 mg (59%).  $^1\text{H}$  NMR (300 MHz,  $\text{DMSO-}d_6$ ):  $\delta$  8.47 (d, 1 H, Ar-H), 8.26 (m, 2 H, Ar-



H), 8.21 (d, 2 H, Ar-H), 8.12 (d, 2 H, Ar-H), 8.02 (m, 2 H, Ar-H), 6.00 (m, 6 H, NH<sub>3</sub>), 2.34 (t, 2 H, CH<sub>2</sub>), 1.96 (q, 2 H, CH<sub>2</sub>) ppm. <sup>195</sup>Pt NMR (107.6 MHz, DMSO-d<sub>6</sub>): δ 1050.0 ppm. ESI-MS (-ve ion mode): *m/z* = 603.0 [M-H]<sup>-</sup>.

**Synthesis of *cis,cis,trans*-[Pt(NH<sub>3</sub>)<sub>2</sub>Cl<sub>2</sub>(CO<sub>2</sub>C<sub>6</sub>H<sub>5</sub>)(CO<sub>2</sub>CH<sub>3</sub>)] (3).** Compound A (50 mg, 114 μmol) was stirred at r.t. in acetic anhydride (5 mL) for 24 h. The reaction mixture was lyophilized and washed with diethyl ether (2 x 5 mL) to yield **1** as an off-white product after drying in vacuo. Yield: 52 mg (95%). Single crystals suitable for x-ray diffraction were grown from vapor diffusion of diethyl ether into a solution of **1** in acetone. <sup>1</sup>H NMR (300 MHz, acetone-*d*<sub>6</sub>): δ 7.95 (d, 2 H, Ar-H), 7.51 (t, 1 H, Ar-H), 7.40 (t, 2 H, Ar-H), 6.57 (m, 6 H, NH<sub>3</sub>, <sup>1</sup>*J*<sub>HN</sub> = 53.9 Hz, <sup>2</sup>*J*<sub>HPt</sub> = 53.3 Hz), 1.96 (s, 3 H, -COOCH<sub>3</sub>) ppm. <sup>195</sup>Pt-NMR (107.6 MHz, acetone-*d*<sub>6</sub>): 1123.0 ppm. ESI-MS (neg. ion mode): *m/z* = 478.92 [M-H]<sup>-</sup>. Purity (HPLC): 97.3% at 254 nm and 100% at 280 nm; *t<sub>r</sub>* = 9.1 min. Anal. Calcd. for **3**, C<sub>9</sub>H<sub>14</sub>C<sub>12</sub>N<sub>2</sub>O<sub>4</sub>Pt: C, 22.51; H, 2.94; N, 5.83. Found: C, 22.33; H, 2.95; N, 5.79.

**Synthesis of *cis,cis,trans*-[Pt(NH<sub>3</sub>)<sub>2</sub>Cl<sub>2</sub>(CO<sub>2</sub>C<sub>6</sub>H<sub>5</sub>)(CO<sub>2</sub>C<sub>3</sub>H<sub>6</sub>COOH)] (4)** Compound A (38 mg, 86.7 μmol) was stirred with glutaric anhydride (12 mg, 105 μmol) in DMF (10 mL) at 60°C for 12 h. The reaction mixture was cooled to r.t. and added diethyl ether (40 mL) which yielded a white precipitate. The precipitate was collected by centrifugation and washed with diethyl ether (3 x 10 mL) and dichloromethane (10 mL). The product was dried *in vacuo* to yield a white solid. Yield: 13.8 mg (29%). <sup>1</sup>H NMR (500 MHz, DMSO-*d*<sub>6</sub>): δ 7.88 (d, 2 H, Ar-H),

7.52 (t, 1 H, Ar-H), 7.42 (t, 2 H, Ar-H), 6.64 (m, 6 H, NH<sub>3</sub>), 2.28 (m, 4 H, -COOCH<sub>3</sub>), 1.70 (m, 2 H, -CH<sub>2</sub>CH<sub>2</sub>CH<sub>2</sub>-) ppm. <sup>195</sup>Pt-NMR (DMSO-*d*<sub>6</sub>, 107.6 MHz): 1195.7 ppm. ESI-MS (neg. ion mode): *m/z* = 550.9 [M-H]<sup>-</sup>. Purity (HPLC): 95.4% at 254 nm and 95.9% at 280 nm; *t<sub>r</sub>* = 9.7 min.

**Synthesis of *cis,cis,trans*-[Pt(NH<sub>3</sub>)<sub>2</sub>Cl<sub>2</sub>(CO<sub>2</sub>C<sub>6</sub>H<sub>5</sub>)(CO<sub>2</sub>C<sub>6</sub>H<sub>4</sub>COOH)] (5).** The compound was prepared in accordance with the method used for **4** using 30 mg of compound **A** as starting material. Yield: 15.7 mg (39%). <sup>1</sup>H NMR (500 MHz, DMSO-*d*<sub>6</sub>): δ 7.91 (d, 1 H, Ar-H), 7.44- 7.54 (m, 8 H, Ar-H), 6.69 (br, 6 H, NH<sub>3</sub>) ppm. <sup>195</sup>Pt NMR (107.6 MHz, DMSO-*d*<sub>6</sub>): 1175.7 ppm. ESI-MS (neg. ion mode, MeOH): *m/z* = 584.9 [M-H]<sup>-</sup>. Purity (HPLC): 97.1% at 254 nm and 97.7% at 280 nm respectively; *t<sub>r</sub>* = 10.8 min.

**Synthesis of *cis,cis,trans*-[Pt(NH<sub>3</sub>)<sub>2</sub>Cl<sub>2</sub>(CO<sub>2</sub>C<sub>6</sub>H<sub>5</sub>)(CO<sub>2</sub>CH<sub>2</sub>CH<sub>3</sub>)] (6).** Compound **A** (50 mg, 114 μmol) was stirred with propionic anhydride (5 mL) in DMF (5 mL). The reaction mixture was stirred for 5 h at 40°C and filtered through celite. The filtrate was lyophilized and washed with DCM (1 x 2 mL) and diethyl ether (1 x 40 mL) and dried in vacuo to yield the product as white precipitate. Yield: 29.9 mg (53%). <sup>1</sup>H NMR (500 MHz, DMSO-*d*<sub>6</sub>): δ 7.88 (d, 2 H, Ar-H), 7.51 (t, 1 H, Ar-H), 7.42 (t, 2 H, Ar-H), 6.65 (m, 6 H, NH<sub>3</sub>), 2.28 (q, 2 H, -COOCH<sub>2</sub>-), 0.97 (t, 3 H, -CH<sub>3</sub>) ppm. <sup>195</sup>Pt NMR (107.6 MHz, DMSO-*d*<sub>6</sub>): δ 1210.1 ppm. ESI-MS (negative ion mode): *m/z* = 493.0 [M-H]<sup>-</sup>. Anal. Calcd. for **6**, C<sub>10</sub>H<sub>16</sub>C<sub>12</sub>N<sub>2</sub>O<sub>4</sub>Pt: C 24.30, H 3.26, N 5.67. Found: C 24.73, H 3.39, N 5.66.

**Synthesis of *cis,cis,trans*-[Pt(NH<sub>3</sub>)<sub>2</sub>Cl<sub>2</sub>(CO<sub>2</sub>C<sub>6</sub>H<sub>5</sub>)(CO<sub>2</sub>CH(CH<sub>3</sub>)<sub>2</sub>)] (7).** The synthesis was based on the procedure for **6** except isobutyric anhydride (5 mL) and reaction was heated for 5 h at 60°C. Yield: 30.5 mg (53%). <sup>1</sup>H NMR (300 MHz, DMSO-*d*<sub>6</sub>): δ 7.87 (d, 2 H, Ar-H), 7.52 (t, 1 H, Ar-H), 7.42 (t, 2 H, Ar-H), 6.65 (m, 6 H, NH<sub>3</sub>), 1.02 (m, 7 H, -CH(CH<sub>3</sub>)<sub>2</sub>) ppm. <sup>195</sup>Pt NMR (107.6 MHz, DMSO-*d*<sub>6</sub>): δ 1200.4 ppm. ESI-MS (negative ion mode): *m/z* = 507.1 [M-H]<sup>-</sup>. Anal. Calcd. for **7**, C<sub>10</sub>H<sub>16</sub>Cl<sub>2</sub>N<sub>2</sub>O<sub>4</sub>Pt: C 25.99, H 3.57, N 5.51. Found: C 25.44, H 3.77, N 5.85.

**Synthesis of *cis,cis,trans*-[Pt(NH<sub>3</sub>)<sub>2</sub>Cl<sub>2</sub>(CO<sub>2</sub>C<sub>6</sub>H<sub>5</sub>)(CO<sub>2</sub>C(CH<sub>3</sub>)<sub>3</sub>)] (8).** The synthesis was based on the procedure for **6** except trimethylacetic anhydride (5 mL) and reaction was heated for 5 h at 80°C. Yield: 24.7 mg (41%). <sup>1</sup>H NMR (300 MHz, DMSO-*d*<sub>6</sub>): δ 7.88 (d, 2 H, Ar-H), 7.52 (t, 1 H, Ar-H), 7.42 (t, 2 H, Ar-H), 6.60 (m, 6 H, NH<sub>3</sub>), 1.08 (s, 9 H, -C(CH<sub>3</sub>)<sub>3</sub>) ppm. <sup>195</sup>Pt NMR (107.6 MHz, DMSO-*d*<sub>6</sub>): δ 1189.8 ppm. ESI-MS (negative ion mode): *m/z* = 521.0 [M-H]<sup>-</sup>. Anal. Calcd. for **8**, C<sub>12</sub>H<sub>20</sub>Cl<sub>2</sub>N<sub>2</sub>O<sub>4</sub>Pt: C 27.60, H 3.86, N 5.36. Found: C 27.60, H 3.74, N 5.40.

**Synthesis of *cis,cis,trans*-[Pt(NH<sub>3</sub>)<sub>2</sub>Cl<sub>2</sub>(CO<sub>2</sub>C<sub>6</sub>H<sub>5</sub>)(CO<sub>2</sub>CH<sub>2</sub>Cl)] (9).** The synthesis was based on the procedure for **6** except chloroacetic anhydride (40 mg, 236 μmol) and reaction was stirred overnight at r.t. Yield: 25.6 mg (44%). <sup>1</sup>H NMR (300 MHz, DMSO-*d*<sub>6</sub>): δ 7.88 (d, 2 H, Ar-H), 7.53 (t, 1 H, Ar-H), 7.42 (t, 2 H, Ar-H), 6.65 (m, 6 H, NH<sub>3</sub>), 4.24 (s, 2 H, -CH<sub>2</sub>Cl) ppm. <sup>195</sup>Pt NMR (107.6

MHz, DMSO- $d_6$ ):  $\delta$  1212.7 ppm. ESI-MS (negative ion mode):  $m/z = 513.0$  [M-H]<sup>-</sup>. Anal. Calcd. for **9**, C<sub>9</sub>H<sub>13</sub>Cl<sub>3</sub>N<sub>2</sub>O<sub>4</sub>Pt: C 21.00, H 2.55, N 5.44. Found: C 20.61, H 2.82, N 5.64.

**Synthesis of *cis,cis,trans*-[Pt(NH<sub>3</sub>)<sub>2</sub>Cl<sub>2</sub>(CO<sub>2</sub>C<sub>6</sub>H<sub>5</sub>)(CO<sub>2</sub>CHCl<sub>2</sub>)] (10).**

Compound **A** (50 mg, 114  $\mu$ mol) was stirred with dichloroacetic anhydride (174  $\mu$ L, 571  $\mu$ mol) in DCM (5 mL). The reaction mixture was stirred overnight (12 h) at room temperature and centrifuged. The residue was collected and washed with diethyl ether (3 x 15 mL) and dried in vacuo to yield the product as white precipitate. Yield: 48.2 mg (77%). <sup>1</sup>H NMR (300 MHz, DMSO- $d_6$ ):  $\delta$  7.8 (d, 2 H, Ar-H), 7.55 (t, 1 H, Ar-H), 7.43 (t, 2 H, Ar-H), 6.63 (m, 6 H, NH<sub>3</sub>), 6.51 (s, 1 H, -CHCl<sub>2</sub>) ppm. <sup>195</sup>Pt NMR (107.6 MHz, DMSO- $d_6$ ):  $\delta$  1203.1 ppm. ESI-MS (negative ion mode):  $m/z = 546.9$  [M-H]<sup>-</sup>. Anal. Calcd. for **10**, C<sub>9</sub>H<sub>12</sub>Cl<sub>4</sub>N<sub>2</sub>O<sub>4</sub>Pt: C 19.69, H 2.20, N 5.10. Found: C 19.32, H 2.19, N 4.96.

**Synthesis of *cis,cis,trans*-[Pt(NH<sub>3</sub>)<sub>2</sub>Cl<sub>2</sub>(CO<sub>2</sub>C<sub>6</sub>H<sub>5</sub>)(CO<sub>2</sub>CHCl<sub>3</sub>)] (11).** The synthesis was based on the procedure for **10** except trichloroacetic anhydride (100  $\mu$ L) was used. Yield: 47.9 mg (72%). <sup>1</sup>H NMR (300 MHz, DMSO- $d_6$ ):  $\delta$  7.89 (d, 2 H, Ar-H), 7.52 (t, 1 H, Ar-H), 7.44 (t, 2 H, Ar-H), 6.58 (m, 6 H, NH<sub>3</sub>) ppm. <sup>195</sup>Pt NMR (107.6 MHz, DMSO- $d_6$ ):  $\delta$  1205.0 ppm. ESI-MS (negative ion mode):  $m/z = 580.9$  [M-H]<sup>-</sup>. Anal. Calcd. for **11**, C<sub>9</sub>H<sub>11</sub>Cl<sub>5</sub>N<sub>2</sub>O<sub>4</sub>Pt: C 18.52, H 1.90, N 4.80. Found: C 18.25, H 1.98, N 4.84.

**Synthesis of *cis,cis,trans*-[Pt(NH<sub>3</sub>)<sub>2</sub>Cl<sub>2</sub>(CO<sub>2</sub>C<sub>6</sub>H<sub>5</sub>)(CO<sub>2</sub>CH<sub>2</sub>Br)] (12).** The synthesis was based on the procedure for **6** except bromoacetic anhydride (5 mL) and reaction was stirred overnight at r.t. Yield: 41.6 mg (66%). <sup>1</sup>H NMR (300 MHz, DMSO-*d*<sub>6</sub>): δ 7.87 (d, 2 H, Ar-H), 7.53 (t, 1 H, Ar-H), 7.42 (t, 2 H, Ar-H), 6.65 (m, 6 H, NH<sub>3</sub>), 4.08 (s, 2 H, -CH<sub>2</sub>Br) ppm. <sup>195</sup>Pt NMR (107.6 MHz, DMSO-*d*<sub>6</sub>): δ 1211.6 ppm. ESI-MS (negative ion mode): *m/z* = 558.9 [M-H]<sup>-</sup>. Anal. Calcd. for **12**, C<sub>9</sub>H<sub>13</sub>BrCl<sub>2</sub>N<sub>2</sub>O<sub>4</sub>Pt: C 19.33, H 2.43, N 5.01. Found: C 19.55, H 2.27, N 5.08.

**Synthesis of *cis,cis,trans*-[Pt(NH<sub>3</sub>)<sub>2</sub>Cl<sub>2</sub>(CO<sub>2</sub>C<sub>6</sub>H<sub>5</sub>)(CO<sub>2</sub>CH<sub>2</sub>I)] (13).** The synthesis was based on the procedure for **6** except iodoacetic anhydride (2 mL) and reaction was heated at 40°C for 5 h. Yield: 50.6 mg (83%). <sup>1</sup>H NMR (300 MHz, DMSO-*d*<sub>6</sub>): δ 7.88 (d, 2 H, Ar-H), 7.53 (t, 1 H, Ar-H), 7.42 (t, 2 H, Ar-H), 6.63 (m, 6 H, NH<sub>3</sub>), 3.82 (s, 2 H, -CH<sub>2</sub>I) ppm. <sup>195</sup>Pt NMR (107.6 MHz, DMSO-*d*<sub>6</sub>): δ 1211.6 ppm. ESI-MS (negative ion mode): *m/z* = 558.9 [M-H]<sup>-</sup>. Anal. Calcd. for **13**, C<sub>9</sub>H<sub>13</sub>ICl<sub>2</sub>N<sub>2</sub>O<sub>4</sub>Pt: C 17.84, H 2.16, N 4.62. Found: C 17.39, H 2.22, N 4.40.

**Synthesis of *cis,cis,trans*-[Pt(NH<sub>3</sub>)<sub>2</sub>Cl<sub>2</sub>(CO<sub>2</sub>C<sub>6</sub>H<sub>5</sub>)(CO<sub>2</sub>CHF<sub>3</sub>)] (14).** The synthesis was based on the procedure for **10** except trifluoroacetic anhydride (100 μL) was used. Yield: 61.0 mg (84%). <sup>1</sup>H NMR (300 MHz, DMSO-*d*<sub>6</sub>): δ 7.89 (d, 2 H, Ar-H), 7.55 (t, 1 H, Ar-H), 7.44 (t, 2 H, Ar-H), 6.69 (m, 6 H, NH<sub>3</sub>) ppm. <sup>195</sup>Pt NMR (107.6 MHz, DMSO-*d*<sub>6</sub>): δ 1194.9 ppm. ESI-MS (negative ion mode):

$m/z = 533.0$  [M-H]<sup>-</sup>. Anal. Calcd. for **14**, C<sub>9</sub>H<sub>11</sub>Cl<sub>2</sub>F<sub>3</sub>N<sub>2</sub>O<sub>4</sub>Pt: C 20.24; H 2.08, N 5.24. Found: C 20.13, H 2.18, N 5.01.

**Synthesis of *cis,cis,trans*-[Pt(NH<sub>3</sub>)<sub>2</sub>Cl<sub>2</sub>(CO<sub>2</sub>CH<sub>2</sub>C<sub>6</sub>H<sub>5</sub>)(CO<sub>2</sub>CH<sub>3</sub>)] (15).**

Complex **E** (20 mg, 44.2 μmol) was stirred with acetic anhydride (2 mL) in DMF (4 mL). The reaction mixture was stirred for 5 h at 40°C and filtered through celite. The filtrate was lyophilized, washed with acetone (1 x 2 mL) and diethyl ether (1 x 40 mL) and dried in vacuo to yield the product as white precipitate. Yield: 16.8 mg (77%). <sup>1</sup>H NMR (300 MHz, DMSO-*d*<sub>6</sub>): δ 7.29 (m, 5 H, Ar-H), 6.63 (m, 6 H, NH<sub>3</sub>), 3.59 (s, 2 H, -COOCH<sub>2</sub>-), 1.92 (s, 3 H, -CH<sub>3</sub>) ppm. <sup>195</sup>Pt NMR (107.6 MHz, DMSO-*d*<sub>6</sub>): δ 1224.7 ppm. ESI-MS (negative ion mode):  $m/z = 493.0$  [M-H]<sup>-</sup>. Anal. Calcd. for **15**, C<sub>10</sub>H<sub>16</sub>Cl<sub>2</sub>N<sub>2</sub>O<sub>4</sub>Pt: C 24.30; H 3.26, N 5.67. Found: C 24.81, H 3.43, N 5.45.

**Synthesis of *cis,cis,trans*-[Pt(NH<sub>3</sub>)<sub>2</sub>Cl<sub>2</sub>(CO<sub>2</sub>CH<sub>2</sub>C<sub>6</sub>H<sub>4</sub>F)(CO<sub>2</sub>CH<sub>3</sub>)] (16).** The synthesis was based on the procedure for **15** except complex **F** (20 mg, 42.5 μmol) was used. Yield: 15.1 mg (69%). <sup>1</sup>H NMR (300 MHz, DMSO-*d*<sub>6</sub>): δ 7.30 (t, 2 H, Ar-H), 7.09 (t, 2 H, Ar-H), 6.52 (m, 6 H, NH<sub>3</sub>), 3.58 (s, 2 H, -COOCH<sub>2</sub>-), 1.91 (s, 3 H, -CH<sub>3</sub>) ppm. <sup>195</sup>Pt NMR (107.6 MHz, DMSO-*d*<sub>6</sub>): δ 1228.0 ppm. ESI-MS (negative ion mode):  $m/z = 511.0$  [M-H]<sup>-</sup>. Purity (HPLC): 97.1% at 254 nm and 92.6% at 280 nm respectively;  $t_r = 3.51$  min.

**Synthesis of *cis,cis,trans*-[Pt(NH<sub>3</sub>)<sub>2</sub>Cl<sub>2</sub>(CO<sub>2</sub>CH<sub>2</sub>CH<sub>2</sub>CH<sub>2</sub>C<sub>6</sub>H<sub>5</sub>)(CO<sub>2</sub>CH<sub>3</sub>)] (17).**

The synthesis was based on the procedure for **15** except complex **G** (20 mg, 41.6  $\mu$ mol) was used. Yield: 10.5 mg (48%). <sup>1</sup>H NMR (300 MHz, DMSO-*d*<sub>6</sub>):  $\delta$  7.21 (m, 5 H, Ar-H), 6.53 (m, 6 H, NH<sub>3</sub>), 3.58 (s, 2 H, -COOCH<sub>2</sub>-), 1.91 (s, 3 H, -CH<sub>3</sub>) ppm. <sup>195</sup>Pt NMR (107.6 MHz, DMSO-*d*<sub>6</sub>):  $\delta$  1221.2 ppm. ESI-MS (negative ion mode):  $m/z$  = 521.0 [M-H]<sup>-</sup>. Anal. Calcd. for **17**, C<sub>12</sub>H<sub>20</sub>C<sub>12</sub>N<sub>2</sub>O<sub>4</sub>Pt: C 27.60; H 3.86, N 5.36. Found: C 27.73, H 3.74, N 5.40.

**Synthesis of *cis,cis,trans*-[Pt(NH<sub>3</sub>)<sub>2</sub>Cl<sub>2</sub>(CO<sub>2</sub>C<sub>6</sub>H<sub>4</sub>OCH<sub>3</sub>)(CO<sub>2</sub>CH<sub>3</sub>)] (18).**

The synthesis was based on the procedure for **15** except complex **B** (20 mg, 42.7  $\mu$ mol) was used. Yield: 12.9 mg (57 %). <sup>1</sup>H NMR (300 MHz, DMSO-*d*<sub>6</sub>):  $\delta$  7.82 (d, 2 H, Ar-H), 6.95 (d, 2 H, Ar-H), 6.64 (m, 6 H, NH<sub>3</sub>), 3.80 (s, 3 H, -OCH<sub>3</sub>), 1.94 (s, 3 H, -CH<sub>3</sub>) ppm. <sup>195</sup>Pt NMR (107.6 MHz, DMSO-*d*<sub>6</sub>):  $\delta$  1212.5 ppm. ESI-MS (negative ion mode):  $m/z$  = 509.1 [M-H]<sup>-</sup>. Purity (HPLC): 99.9% at 254nm and 99.8% at 280nm respectively;  $t_r$  = 3.38 min.

**Synthesis of *cis,cis,trans*-[Pt(NH<sub>3</sub>)<sub>2</sub>Cl<sub>2</sub>(CO<sub>2</sub>C<sub>6</sub>H<sub>4</sub>CN)(CO<sub>2</sub>CH<sub>3</sub>)] (19).**

The synthesis was based on the procedure for **15** except complex **H** (20 mg, 39.6  $\mu$ mol) was used. Yield: 11.5 mg (22 %). <sup>1</sup>H NMR (300 MHz, DMSO-*d*<sub>6</sub>):  $\delta$  7.95 (m, 5 H, Ar-H), 6.64 (m, 6 H, NH<sub>3</sub>), 1.85 (s, 3 H, -CH<sub>3</sub>) ppm. <sup>195</sup>Pt NMR (107.6 MHz, DMSO-*d*<sub>6</sub>):  $\delta$  1240.5 ppm. ESI-MS (negative ion mode):  $m/z$  = 504.0 [M-H]<sup>-</sup>. Purity (HPLC): 98.4% at 254nm and 98.7% at 280nm respectively;  $t_r$  = 3.21 min.

**Synthesis of *cis,cis,trans*-[Pt(NH<sub>3</sub>)<sub>2</sub>Cl<sub>2</sub>(CO<sub>2</sub>CH<sub>2</sub>CH<sub>2</sub>CH<sub>2</sub>C<sub>15</sub>H<sub>9</sub>)(CO<sub>2</sub>CH<sub>3</sub>] (20).**

The synthesis was based on the procedure for **15** except complex **I** (70mg, 116μmol) was used. Yield: 62 mg (83%). <sup>1</sup>H NMR (300 MHz, DMSO-*d*<sub>6</sub>): δ 8.47 (d, 1 H, Ar-H), 8.27 (m, 2 H, Ar-H), 8.22 (d, 2 H, Ar-H), 8.13 (d, 2 H, Ar-H), 8.03 (m, 2 H, Ar-H), 6.56 (m, 6 H, NH<sub>3</sub>), 2.38 (t, 2 H, CH<sub>2</sub>), 1.97 (q, 2 H, CH<sub>2</sub>), 1.92 (s, 3 H, CH<sub>3</sub>) ppm. <sup>195</sup>Pt NMR (107.6 MHz, DMSO-*d*<sub>6</sub>): δ 1228.2 ppm. ESI-MS (-ve ion mode): *m/z* = 645.0 [M-H]<sup>-</sup>.

**Synthesis of *cis,cis,trans*-[Pt(NH<sub>3</sub>)<sub>2</sub>Cl<sub>2</sub>(CO<sub>2</sub>CH<sub>2</sub>CH<sub>2</sub>CH<sub>2</sub>C<sub>15</sub>H<sub>9</sub>)(CO<sub>2</sub>C<sub>6</sub>H<sub>5</sub>]**

**(21)**. Compound **I** (57mg, 94μmol) was stirred with benzoic anhydride (23mg, 99μmol) in DMF (5mL) at 70°C for 12 h. The reaction mixture was lyophilized and washed with diethyl ether (3 x 5mL) to yield **21** as a brown precipitate. Yield: 30 mg (45%). <sup>1</sup>H NMR (300 MHz, DMSO-*d*<sub>6</sub>): δ 8.47 (d, 1 H, Ar-H), 8.27 (m, 2 H, Ar-H), 8.22 (d, 2 H, Ar-H), 8.16 (d, 2 H, Ar-H), 8.03 (m, 2 H, Ar-H), 7.89 (d, 2 H, Ar-H), 7.53 (t, 1 H, Ar-H), 7.42 (t, 2 H, Ar-H), 6.69 (m, 6 H, NH<sub>3</sub>), 2.43 (t, 2 H, CH<sub>2</sub>), 2.00 (q, 2 H, CH<sub>2</sub>) ppm. <sup>195</sup>Pt NMR (107.6 MHz, DMSO-*d*<sub>6</sub>): δ 1212.3 ppm. ESI-MS (-ve ion mode): *m/z* = 707.0 [M-H]<sup>-</sup>.

**Synthesis of *cis,cis,trans*-[Pt(NH<sub>3</sub>)<sub>2</sub>Cl<sub>2</sub>(CO<sub>2</sub>C<sub>6</sub>H<sub>5</sub>)(CO<sub>2</sub>C<sub>2</sub>H<sub>4</sub>COOH)] (22)**

Compound **A** (50 mg, 114 μmol) was stirred with succinic anhydride (70 mg, 700 μmol) in DMF (10 mL) at 50°C for 24 h. The reaction mixture was lyophilized and washed with DCM (5 x 5 mL) to yield **22** as an off-white product after drying *in vacuo*. Yield: 44 mg (72%). <sup>1</sup>H NMR (500 MHz, DMSO-*d*<sub>6</sub>): δ 12.00 (br, s, 1



H, -COOH), 7.88 (d, 2 H, Ar-H), 7.51 (t, 1 H, Ar-H), 7.42 (t, 2 H, Ar-H), 6.62 (br, 6 H, NH<sub>3</sub>), 2.53 (t, 2 H, -CH<sub>2</sub>), 2.40 (t, 2 H, -CH<sub>2</sub>) ppm. ESI-MS (-ve mode):  $m/z$  = 537.0 [M-H]<sup>-</sup>.

## Chapter 4

# Tuning the Pharmacological Properties of Asymmetric Platinum(IV) Bis-Carboxylates

### 4.1 Introduction

From a drug design perspective, the platinum(IV) scaffold provides an excellent platform upon which functionalities can be attached while maintaining the integrity of the platinum(II) pharmacophore [*cis*-Pt(NH<sub>3</sub>)<sub>2</sub>Cl<sub>2</sub>] associated with cisplatin. The development of asymmetric platinum(IV) bis-carboxylates allows different ligands with contrasting properties to be placed in the axial positions. In this chapter, the tunable pharmacological properties of asymmetric platinum(IV) prodrugs of cisplatin, particularly their aqueous solubility, stability and lipophilicity leading to viable anticancer complexes with enhanced cytotoxic profiles are investigated. Structure activity relationship studies have shown that the redox potential, rate of reduction, lipophilicity, and cytotoxicity of platinum(IV) prodrugs can be altered by varying the axial ligands.<sup>93, 94, 95, 96</sup> For example, symmetric platinum(IV) prodrugs bearing hydrophobic aromatic carboxylate ligands exhibit more than 10-fold increase in cytotoxicity against a panel of lung, colon and breast carcinoma cell lines compared to cisplatin due to improved lipophilicity. Platinum(IV) prodrugs containing alkyl carboxylate axial ligands, on the other hand, are generally less efficacious.<sup>140</sup>

Henceforth, we postulate that asymmetric platinum(IV) prodrugs bearing both hydrophobic aromatic and hydrophilic alkyl carboxylate ligands on the same scaffolds will exhibit good lipophilicity and solubility, and ultimately enhance their anti-proliferative efficacies against cancer cells.

## 4.2 Evaluating the Tunable Pharmacological Properties of Asymmetric Platinum(IV) Bis-Carboxylates

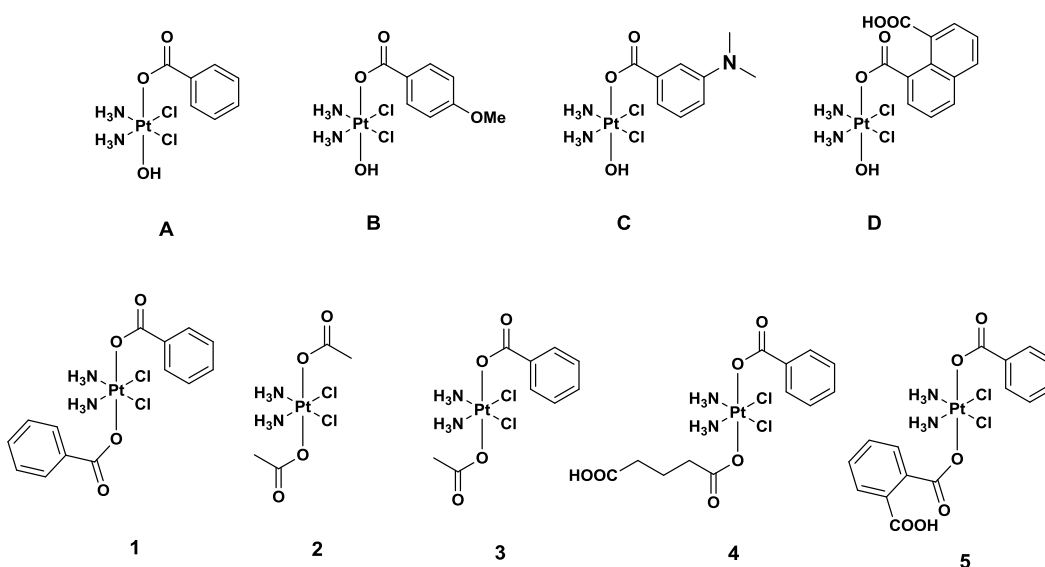


**Figure 16.** Chemical structure of platinum(IV) complexes evaluated for tunable pharmacological properties

As a proof of concept, platinum(IV) complexes **A-D** and **1-5** were synthesized (Chapter 3) and their lipophilicities, solubilities, and cytotoxicities studied to evaluate the tunable properties of asymmetric scaffolds. Other than cisplatin and oxoplatin, symmetric platinum(IV) bis-benzoates **1** and bis-acetates **2** were also used as controls since they consist of axial ligands with contrasting properties and would be expected to exhibit distinctive results in the studies, while the

asymmetric platinum(IV) bis-carboxylates were expected to exhibit parameters intermediate of **1** and **2**.

#### **4.2.1 Evaluating the Tunable Lipophilicity and Aqueous Solubility of Asymmetric Platinum(IV) Bis-Carboxylates**

Lipophilicity, expressed as the logarithms of *n*-octanol/water partition coefficient  $\text{Log}P_{\text{ow}}$ , is a good estimate for the drugs' ability to penetrate cancer cells. It describes the distribution of the drug between the polar water phase and non-polar *n*-octanol phases, and an important tool in predicting the transport and activity of the drugs.<sup>152</sup> Recently, Hall and co-workers developed a method to computationally derive  $\text{Log}P_{\text{ow}}$  values of platinum(IV) complexes using quantum mechanical calculations in order to predict their whole-molecule lipophilicity and concluded that there is a strong correlation between lipophilicity and drug accumulation.<sup>153, 154</sup> Notably, complexes that are too lipophilic or hydrophilic show little or poor bioavailability.<sup>155</sup> Platinum(IV) complexes that are highly lipophilic will get embedded in the membrane due to favorable hydrophobic interaction or be too insoluble in aqueous media, an important pharmacological property. Platinum(IV) complexes that are highly hydrophilic will not be able to pass through the cell membrane and exert its activity.

$\text{Log}P_{\text{ow}}$  values of the synthesized platinum(IV) complexes were determined using the shake-flask method (Table 2). The concentrations of the platinum(IV) complexes in aqueous and *n*-octanol media were determined by ICP-OES. In addition, the tested compounds exhibited stability up to 72 hours when studied

with RP-HPLC, providing a good validation of the shake-flask method in ascertaining the lipophilicity of the platinum(IV) complexes. Besides shake-flask,  $\text{Log}P_{\text{ow}}$  values of other anticancer drugs had also been determined using RP-HPLC and group-additive methods.<sup>156</sup> The synthesized complexes, each containing at least an aromatic carboxylate axial ligand, were significantly more hydrophilic than symmetric platinum(IV) bis-benzoate **1** as evidenced by their lower  $\text{Log}P_{\text{ow}}$  values. Mono-carboxylated complexes **A-D** were evidently more hydrophilic than the bis-carboxylates, presumably due to the presence of uncarboxylated hydroxyl ligand. Functionalization of the benzoate ligands with H-bonding groups such as carboxylic group increased hydrophilicity, with **D** displaying the lowest  $\text{Log}P_{\text{ow}}$  amongst its class despite the bulkier naphthalate ligand. Comparing **1** with the series of asymmetric platinum(IV) bis-carboxylates **3-5**, replacement of one benzoate with a less lipophilic ligand, namely acetate, glutarate or phthalate, improved hydrophilicity significantly. For example, **5** differed structurally from **1** by the addition of an *ortho*-carboxylic group and exhibited a 0.75 units reduction in  $\text{Log}P_{\text{ow}}$ . Notably, **A** and **3** exhibited a  $\text{Log}P_{\text{ow}}$  reduction of -1.6 and -1.2 unit compared to **1** and differing only in the nature of the one of the axial ligand. In comparison, cisplatin, oxoplatin and platinum(IV) bis-acetate **2** were highly hydrophilic with  $\text{Log}P_{\text{ow}}$  values determined to be -2.03, -2.12 and -2.00, respectively. Under normal room conditions, the solubility of **A** and **3** in water were observed to be higher than 300  $\mu\text{g/mL}$  whereas **1** was observed to be too poorly soluble to be determined. Cisplatin and **2** both exceeded 1  $\text{mg/mL}$  solubility under these conditions. For a more quantitative measurement,

saturated solutions of **A**, **1** and **3** were prepared at 80°C under agitation, filtered and their platinum levels determined by ICP-OES. The results indicated that mono-carboxylate **A** was twice as soluble as asymmetric bis-carboxylate **3** and four times more soluble than symmetric bis-benzoate **1**. This provided a validation on the proposed approach of tuning the lipophilicity of platinum(IV) carboxylate complexes through asymmetric ligands with contrasting attributes. The lipophilicity of the platinum(IV) complexes was also determined by reversed-phase liquid chromatography where a standard curve was first obtained by determining the retention time of compounds with known  $\log P_{\text{oct}}$  values.<sup>157</sup> However, this method is more suitable for comparison of lipophilic compounds as it is only able to generate positive  $\log P_{\text{oct}}$  values. The group additive method, on the other hand, is generally used for organic compounds and not applicable for the platinum(IV) complexes studied.

**Table 2.** Properties of platinum(IV) complexes

| Complex  | $\text{Log}P_{\text{ow}}^a$ | $\text{Log}P_{\text{ow}}^b$ | Solubility at   | $\text{IC}_{50}$ [ $\mu\text{M}$ ] <sup>c</sup> |                  | resistance          |
|----------|-----------------------------|-----------------------------|-----------------|---|------------------|---------------------|
|          |                             |                             | 80°C<br>(mg/mL) | A2780   | A2780/Cis        | factor <sup>d</sup> |
| <b>A</b> | $-0.59 \pm 0.12$            | 0.79                        | $1.22 \pm 0.03$ | $2.41 \pm 0.27$                                 | $7.30 \pm 2.31$  | 3.0                 |
| <b>B</b> | $-0.50 \pm 0.09$            | 0.92                        | -               | $5.11 \pm 0.61$                                 | $16.97 \pm 4.01$ | 3.3                 |
| <b>C</b> | $-0.87 \pm 0.16$            | 1.17                        | -               | $5.80 \pm 0.73$                                 | $20.21 \pm 5.26$ | 3.5                 |
| <b>D</b> | $-1.14 \pm 0.18$            | 0.93                        | -               | $19.03 \pm 0.91$                                | > 50             | -                   |
| <b>1</b> | $1.01 \pm 0.01$             | 1.19                        | $0.27 \pm 0.01$ | $0.048 \pm 0.004$                               | $0.23 \pm 0.07$  | 4.8                 |
| <b>2</b> | $-2.00 \pm 0.18$            | 1.34                        | -               | > 20  | > 20             | -                   |
| <b>3</b> | $-0.19 \pm 0.04$            | 1.54                        | $0.62 \pm 0.04$ | $0.83 \pm 0.14$                                 | $6.24 \pm 0.94$  | 7.5                 |

|           |                  |      |                 |                 |                  |      |
|-----------|------------------|------|-----------------|-----------------|------------------|------|
| <b>4</b>  | $-0.46 \pm 0.04$ | 2.19 | -               | $1.95 \pm 0.30$ | $26.41 \pm 1.72$ | 13.5 |
| <b>5</b>  | $0.25 \pm 0.02$  | -    | -               | $4.95 \pm 0.77$ | $24.90 \pm 1.81$ | 5.0  |
| cisplatin | $-2.03 \pm 0.47$ | -    | $3.37 \pm 0.05$ | $1.63 \pm 0.17$ | $13.91 \pm 2.04$ | 8.5  |
| oxoplatin | $-2.12 \pm 0.24$ | -    | -               | > 50            | > 50             | -    |

<sup>a</sup>  $\text{Log}P_{ow}$  values determined via the shake-flask method against 1:1 *n*-octanol:0.9% v/w NaCl partition.

<sup>b</sup>  $\text{Log}P_{ow}$  values determined via RP-HPLC method.

<sup>c</sup>  $\text{IC}_{50}$  values is the concentration of platinum complexes required to inhibit 50% of the cell growth with respect to control groups, measured by MTT assay after 72 h exposure. Data obtained are based on the average of at least three independent trials and the reported errors are the corresponding standard deviations. The  $\text{IC}_{50}$  were corrected using actual [Pt] determined using ICP-OES.

<sup>d</sup> Based on the ratio of  $\text{IC}_{50}[\text{A2780/Cis}]$  to  $\text{IC}_{50}[\text{A2780}]$ .

#### 4.2.2 Evaluating the Tunable Anti-Proliferative Properties of Asymmetric Platinum(IV) Bis-Carboxylates

The efficacy of cisplatin and platinum(IV) prodrugs on the cell-growth inhibition of A2780 and A2780/Cis human ovarian carcinoma was evaluated to determine the cytotoxicity of the complexes (Table 2). Briefly, after the cells were adhered to the multiwell plate surface, they were exposed to varying concentrations of the platinum complexes in serum-free medium for 6 hours. The media was replaced with complete media and left to incubate for a further 66 hours before the viability of the remaining cells was determined. The data was presented as % survival against non-treated controls and the concentrations required to inhibit cell viability by 50% ( $\text{IC}_{50}$ ) were interpolated from the graph (Figure 17). All experiments were carried out in triplicates and repeated. The purity of the compounds was established using elemental analysis and RP-HPLC and found to exceed 95%. To further mitigate the effects of contamination, platinum concentration of the platinum complex stock solutions were determined using

---

ICP-OES and the IC<sub>50</sub> values were adjusted to actual platinum concentration values.

The archetypal complex **1** was 30-fold more cytotoxic than cisplatin in both cell lines. The enhanced activity was earlier attributed to its high lipophilicity and increased drug uptake. On the other hand, **2**, despite sharing the same [*cis*-Pt(NH<sub>3</sub>)<sub>2</sub>]-pharmacophore as **1**, was poorly cytotoxic despite its good aqueous solubility. The poor aqueous solubility of **1** undermined its usefulness as a potential drug that can be administered intravenously.<sup>95, 140</sup> With the exception of mono-carboxylate **D**, the newly synthesized platinum(IV) complexes exhibited the same order of magnitude of cytotoxicity as cisplatin (Table 2). Complex **A** was the most efficacious amongst the mono-carboxylate complexes tested while **3** was the most effective among the panel of asymmetric platinum(IV) bis-carboxylate prepared. The IC<sub>50</sub> values of these complexes against both cell lines were in the same order of magnitude range comparable to cisplatin. Notably, all platinum(IV) prodrug complexes exhibited cross-resistance to the cisplatin-resistant A2780 variant (A2780/Cis) with resistance factors between 3.3 to 13.5. Resistance to cisplatin in A2780/Cis cells had been attributed to enhanced cellular repair via mismatch repair mechanisms.<sup>158</sup> This was reasonable since these complexes are expected to exert their activity via DNA-binding after intracellular reduction to cisplatin, they would be affected by the same resistance mechanisms resulting in lower efficacies.



Taken together, the data obtained suggested a direct link between lipophilicities and efficacies in inhibiting cancer cell viability within this class of platinum(IV) complexes (Table 2). Highly hydrophilic platinum(IV) complexes oxoplatin and **2** are poorly efficacious when compared to the lipophilic mono- and bis-platinum(IV) carboxylates. Furthermore, lipophilic platinum(IV) bis-carboxylates were generally more efficacious than platinum(IV) mono-carboxylates despite only minor structural changes. Complexes **A** and **3**, for example, differed only by one axial ligand group (hydroxyl vs acetate). It was previously noted that these axial ligands affected reduction potential of platinum(IV) complexes, particularly hydroxyl ligands, which accounted in part for the poor efficacy of oxoplatin.<sup>159</sup> In addition, asymmetric platinum(IV) complex **3** benefitted directly from higher lipophilicity than **A**. It should also be highlighted that both complex **A** and **3** were less efficacious compared to **1**. Their lower efficacies may be directly due to their significantly lowered lipophilicities and hence poorer uptake. However, complex **1** was not directly soluble in water, unlike **A** and **3**, and would be problematic for intravenous administration and further pharmaceutical development. The poorer efficacy of **D**, ca. 12-fold less than cisplatin, could be attributed to the formation of charged species in the culture media upon dissociation of the acidic carboxylic proton which would be repelled from the hydrophobic cellular membrane resulting in lower cellular uptake, and could also explain the slightly higher IC<sub>50</sub> values for **4** and **5** compared to **3**.<sup>140</sup> In addition, complex **3**, consisting of both benzoate and acetate ligands in the axial positions, exhibited IC<sub>50</sub> between **1** and **2**

while being comparable to cisplatin. This validated our hypothesis of tuning the cytotoxicities of platinum(IV) prodrugs through asymmetric acylation.

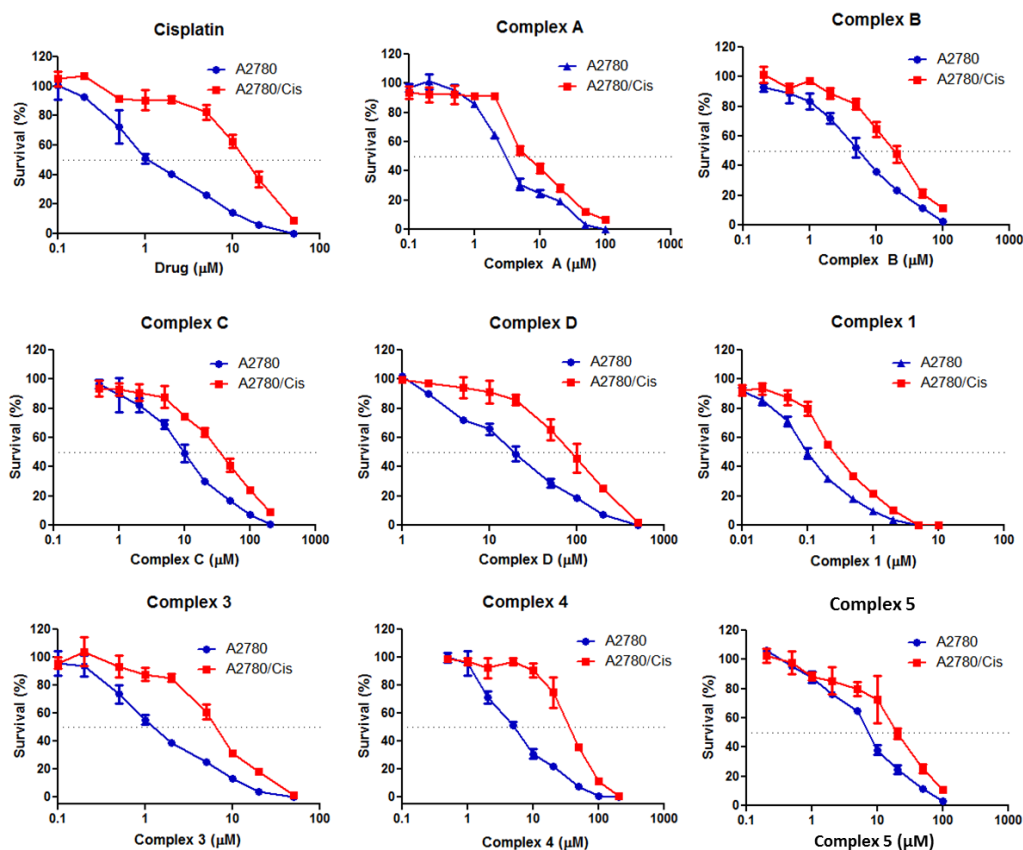


**Figure 17.** Dose-dependent drug efficacy studies for cisplatin, complexes A-D, 1 and 3-5 on A2780 and A2780/Cis tumor cells

### 4.3 Evaluation of the Mechanism of Asymmetric Platinum(IV) Bis-Carboxylates

The putative mechanism of action of inert platinum(IV) prodrugs involved their conversion to cytotoxic platinum(II) species via chemical reduction. Earlier reports suggested a strong relationship between the ease of reduction with

anticancer activity of these complexes. For example, platinum(IV) complexes with axial chloro ligands were easily reduced and exhibited high cytotoxicity while those with axial hydroxyl ligands were poorly cytotoxic by virtue of their unfavorable reduction potential.<sup>159</sup> We therefore sought to establish whether these newly synthesized water-stable asymmetric platinum(IV) carboxylates require reduction to their platinum(II) congeners for activity, therefore fulfilling their role of prodrugs. This was corroborated in part by previous experimental evidence showing that **1** reacted with sodium diethyldithiocarbamate (DDTC) only after treatment with a bio-reductant such as ascorbic acid or glutathione to form yellow Pt(DDTC)<sub>2</sub> in the same manner as cisplatin.<sup>160</sup> Without reduction, platinum(IV) complex **1** remained unreactive towards DDTC.<sup>122</sup> To establish the prodrug mechanism from the inert platinum(IV) carboxylates to reactive platinum(II) species, we investigated their ability to bind DNA, the putative biological target, after activation by chemical reduction. In its active platinum(II) state, cisplatin exerts its bioactivity by forming genomic Pt-DNA adducts that interfered with replication and transcription processes.<sup>161</sup> The high reactivity of platinum drugs towards guanosine arose from the nucleophilic nature of the N7-position on the guanosine base and cooperative H-bonding interaction between the ammine ligand and exocyclic O6-position. 5'-Guanosine-2'-deoxymonophosphate (5'-dGMP) was used as a model for DNA so that analysis could be carried out using RP-HPLC.

Treatment with cisplatin readily yielded mono-functional  $[\text{Pt}(\text{NH}_3)_2\text{Cl}(5'\text{dGMP})]$  and bis-functional  $[\text{Pt}(\text{NH}_3)_2(5'\text{dGMP})_2]$  adducts, consistent with literature reports,<sup>162, 163</sup> which could be isolated from RP-HPLC and identified using ESI-MS. Treatment of platinum(IV) complexes oxoplatin, **A**, **1**, and **3** with 5'dGMP however, did not elicit the same response and the complexes remained unreactive towards 5'dGMP over a period of 72 hours. However, after these complexes were incubated with 3 mM ascorbic acid, they reacted readily with 5'dGMP to form monofunctional  $[\text{Pt}(\text{NH}_3)_2\text{Cl}(5'\text{dGMP})]$  and bifunctional  $[\text{Pt}(\text{NH}_3)_2(5'\text{dGMP})_2]$  adducts akin to those formed by cisplatin (Figure 18). Based on the results, we concluded that the platinum(IV) carboxylates were themselves inert to ligand substitution reactions. The RP-HPLC studies reaffirmed their aqueous stability in the presence of 5'dGMP after 72 hours. However, upon reduction by ascorbic acid, reactive platinum(II) species were formed which bind readily with 5'dGMP to form platinated adducts. These adducts were consistent with those formed by cisplatin under ambient conditions. Previous studies done by our group also showed that asymmetric platinum(IV) complexes bearing the cisplatin template were reduced to cisplatin conclusively.<sup>84</sup> Taken together, these results suggested that the inert and stable platinum(IV) carboxylates, including the newly synthesized mono-carboxylates and asymmetric bis-carboxylates, functioned as prodrugs of cisplatin that were activated upon chemical reduction.

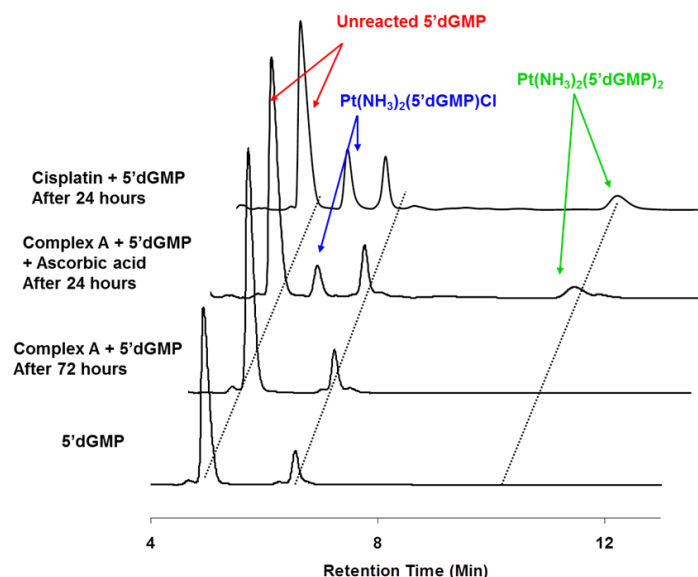


**Figure 18.** HPLC chromatograms showing 5'-dGMP; reaction of complex **A** with 5'-dGMP; reaction of complex **A** with 5'-dGMP in the presence of 3 mM ascorbic acid; and reaction of cisplatin with 5'-dGMP

#### 4.4 Expanding the Scope of Investigation on Asymmetric Platinum(IV) Bis-Carboxylates

Having proved platinum(IV) prodrugs could be fine-tuned to achieve desired pharmacological properties using asymmetric carboxylation and successfully developed a lead compound **3**,<sup>79</sup> we expanded our scope of investigation to a library of asymmetric platinum(IV) bis-carboxylates. Through minor structural variation of the axial ligands whilst keeping the cisplatin pharmacophore intact, we rationally designed 3 series of asymmetric platinum(IV) bis-carboxylates **6-19** (Figure 19) to establish how the structural parameters would affect the pharmacological attributes. This expanded class of asymmetric platinum(IV) complexes were synthesized using the strategy detailed in Chapter 3 involving

sequential acylation of oxoplatin to yield the platinum(IV) mono-carboxylates

**A-B** and **E-H** (Figure 19) before reacting with acid anhydrides to yield **6-19**.

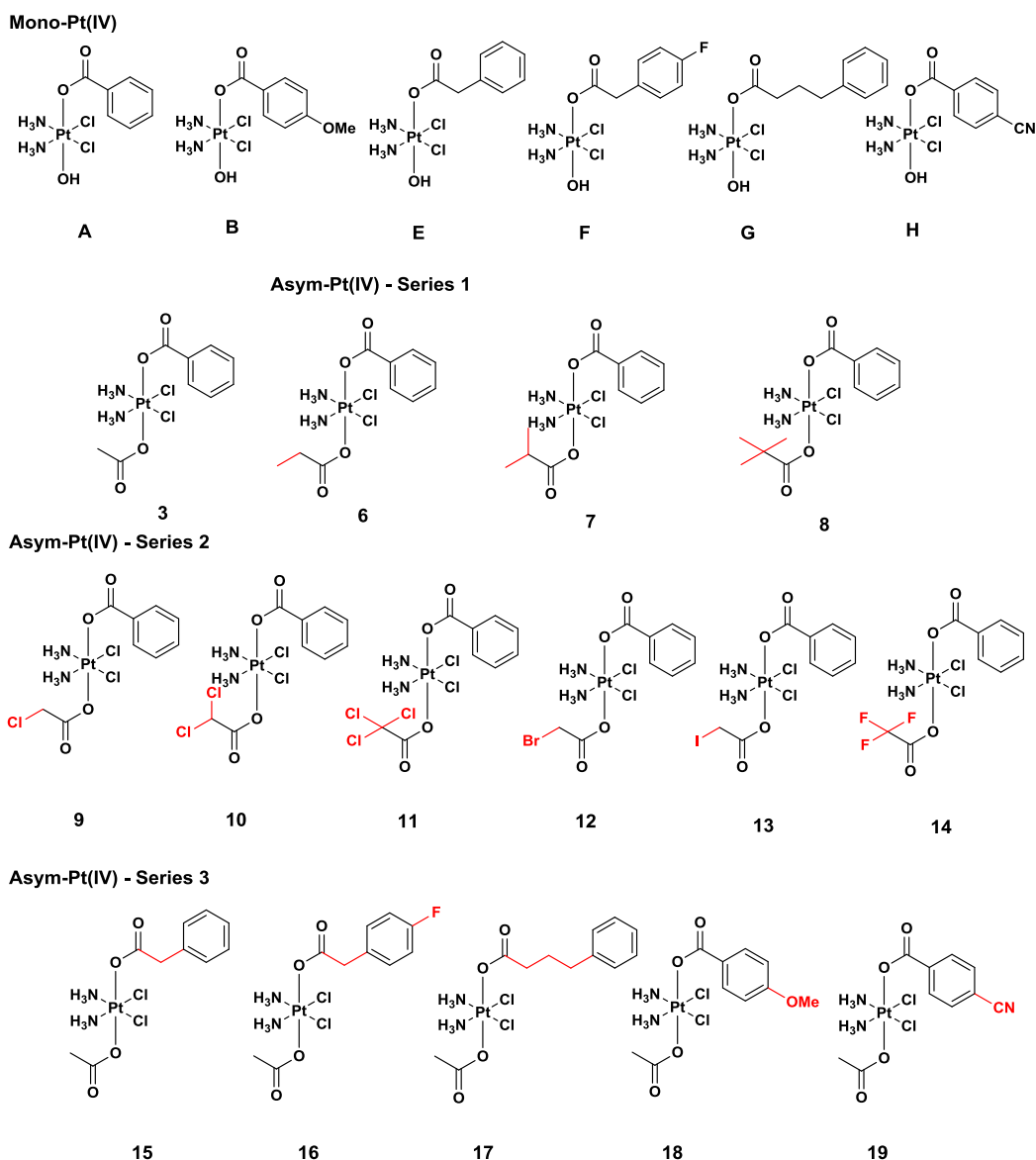


**Figure 19.** Chemical structure of asymmetric platinum(IV) complexes investigated for their structure activity relationships

In series 1 (**6-8**), the acetate ligand was replaced with alkyl carboxylates with increasing steric encumbrance. In series 2 (**9-14**), the acetate ligand was replaced

with haloacetate ligands with vary electron-withdrawing properties. In series 3 (15–19), the benzoate ligand was altered either by adding electron-donating/withdrawing groups directly to the phenyl moiety or increasing the distance between the phenyl and carboxylate groups. This systematic exploration of their structural space was geared towards the discovery and pharmacological optimization of a cisplatin prodrug suitable for eventual drug development.

#### 4.4.1 Evaluating the Stability of the Expanded Asymmetric Platinum(IV) Bis-Carboxylates Series

One of the main considerations in developing stable platinum(IV) prodrugs was to ensure the low spin octahedral  $d^6$  platinum(IV) would remain inert and get activated only via cellular reduction at the tumor sites to release the high spin square-planar  $d^8$  platinum(II) drugs. To determine the stability of this class of compounds, asymmetric platinum(IV) bis-carboxylates **6-19** were dissolved in 40 mM of HEPES buffer at pH 7.4 for 72 hours. The stability of the complexes was monitored by RP-HPLC (Figure 20) and the results depicted in Table 3. The stability of **3** was also studied as a reference control. Other than complex **10**, **11** and **14**, all asymmetric platinum(IV) bis-carboxylates exhibited good aqueous stability for at least 72 hours. From the RP-HPLC spectra, the intensity of the peaks signaling **10**, **11** and **14** decreased significantly within 24 hours, which was likely due to rapid hydrolysis of the strong electron-withdrawing halogenoacetato axial ligands.<sup>113</sup>

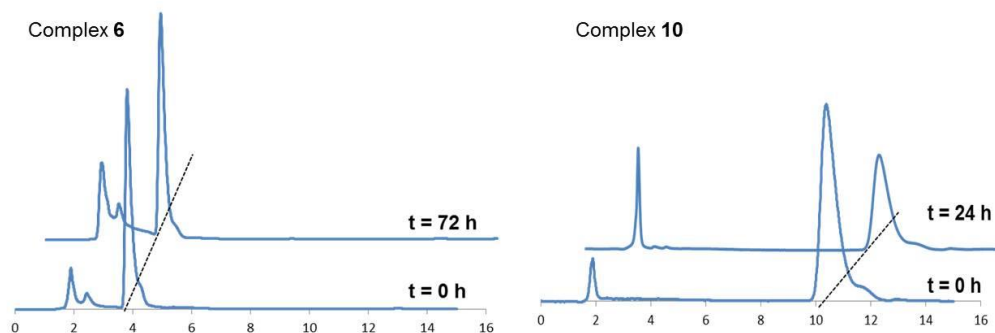


**Figure 20.** HPLC chromatograms depicting the stability of complex **6** after 72 h and instability of complex **10** after 24 h

Previously, it was shown that platinum(IV) prodrugs bearing strong electron withdrawing bis-haloacetato ligands such as dichloroacetate and trifluoroacetate in the axial positions were unstable.<sup>112, 113</sup> We attempted to circumvent this limitation through mono acylation of these ligands in our asymmetric platinum(IV) scaffolds with limited success. The poor stability of **10**, **11** and **14** rendered them unsuitable for further studies.

#### 4.4.2 Evaluating the Reduction Rate of the Expanded Asymmetric Platinum(IV) Bis-Carboxylates Series

The reduction rate of platinum(IV) complexes played an important role in determining the cytotoxicity of the prodrugs, as platinum(IV) complexes that reduced readily would result in unfavorable side effects associated with platinum(II) species, while those that reduced too slowly might pass through the body without exerting anticancer activity.<sup>37, 38, 39, 40</sup> The reduction rate of the platinum (IV) complexes were studied in the presence of 30 mM ascorbic acid as a model of outer space reductant in 40 mM HEPES buffer and monitored at



regular time intervals using RP-HPLC. A significantly higher concentration of ascorbic acid was used to minimize experimental error due to oxidation of ascorbic acid by dissolved  $O_2$  and to stimulate psychological reductive environment. The area of the signal corresponding to each platinum(IV) complex in the RP-HPLC spectra were monitored and measured at regular time intervals upon addition of ascorbic acid. The reduction of the platinum(IV) complexes with respect to time were plotted in Figure 21 and the time taken for platinum(IV) complexes to be reduced to 50% of its initial concentration ( $t_{1/2}$ ) were tabulated in Table 3. Platinum(IV) mono-carboxylate **A** registered a  $t_{1/2}$  of 13 min, which was significantly lower than asymmetric platinum(IV) bis-carboxylate **3** ( $t_{1/2} = 124$  min). The reduction rates of all asymmetric platinum(IV) bis-carboxylates were significantly lower than platinum(IV) mono-carboxylate despite being endowed with an additional electron withdrawing carboxylate ligand. This indicated that the rate of reduction is dependent on the ability of the platinum(IV) complex to bridge with reducing agents and facilitate electron transfer resulting in reduction of platinum(IV) to platinum(II) complexes.<sup>164</sup>

Across series 1, increased steric encumbrance and presence of more electron donating methyl groups reduced the rate of reductions, suggesting stabilization of the platinum(IV) complexes. Complexes **6-8** had  $t_{1/2}$  of 148, 164 and 197 min respectively. The presence of electron donating methyl groups would increase the electron density around the platinum(IV) metal center and strengthen the Pt- $O_{alkyl}$  bond, making the compounds less susceptible to reduction. Across series 2, the

reduction of the platinum(IV) complexes did not proceed faster than anticipated when the methyl groups were replaced with electron withdrawing halogen groups. Instead, the reduction rate of complex **9** and **12** was comparable to **3** with  $t_{1/2}$  of 129 and 128 min respectively. Complex **13** reduced the slowest in series 2, with a  $t_{1/2}$  of 209 min, presumably due to steric hindrance of bulky iodoacetate group that blocked ascorbic acid from accessing the platinum(IV) metal center.

Across series 3, the asymmetric platinum(IV) bis-carboxylates were more stable towards reduction compared to **3**, particularly **15-17** which were platinum(IV) bis-alkyl carboxylates with distal aryl groups. Complex **15** had a  $t_{1/2}$  of 333 min while **17** had  $t_{1/2}$  of >400 min, indicating a longer alkyl chain could nullify the electron withdrawing effect of the benzoate moiety and stabilize the platinum(IV) complex. Interestingly, Complex **16** also had a  $t_{1/2}$  of >400 min, indicating that the addition of electron-withdrawing fluoro group at the benzyl moiety in **16** did not significantly perturb the reduction rates of **15**. This was in contrast to platinum(IV)-bis-aryl carboxylates **18** and **19**, where the presence of electron donating methoxy substituent helped to stabilize **18** ( $t_{1/2}$  >400 min), while electron withdrawing cyano substituent destabilized **19** ( $t_{1/2}$  = 205 min). This could mean that increasing the bond distance between the benzoate moiety and platinum(IV) metal center could neutralize the electron withdrawing effect by the substituents on the aromatic ring. Henceforth, This result validated our approach of achieving fine-tuning into the intrinsic properties of asymmetric platinum(IV) bis-carboxylates through minor structural variations of the axial ligands.

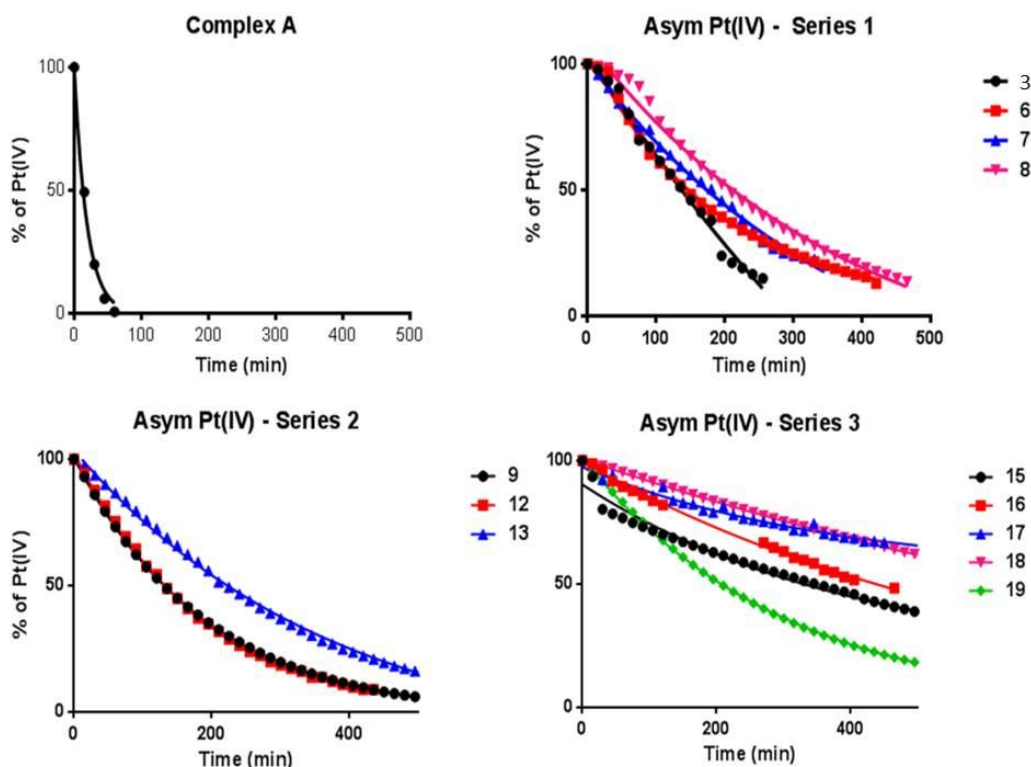


**Figure 21.** Graphs depicting the reduction asymmetric platinum(IV) complexes

**Table 3.** Stability and reduction rates of asymmetric platinum(IV) complexes

| Complex | -CO <sub>2</sub> R | -CO <sub>2</sub> R'                | Stability | Pseudo 1 <sup>st</sup> Order                       | Half -life<br>(min) |
|---------|--------------------|------------------------------------|-----------|--|---------------------|
|         |                    |                                    |           | Rate constant<br>(min <sup>-1</sup> ) <sup>a</sup> |                     |
| A       | Ph                 | (OH)                               | > 3days   | $(5.3 \pm .3) \times 10^{-2}$                      | 13                  |
| 3       | Ph                 | CH <sub>3</sub>                    | > 3days   | $(5.6 \pm 0.3) \times 10^{-3}$                     | 124                 |
| 6       | Ph                 | CH <sub>2</sub> (CH <sub>3</sub> ) | > 3days   | $(4.7 \pm 0.1) \times 10^{-3}$                     | 148                 |
| 7       | Ph                 | CH(CH <sub>3</sub> ) <sub>2</sub>  | > 3days   | $(4.2 \pm 0.1) \times 10^{-3}$                     | 164                 |
| 8       | Ph                 | C(CH <sub>3</sub> ) <sub>3</sub>   | > 3days   | $(3.5 \pm 0.0) \times 10^{-3}$                     | 197                 |
| 9       | Ph                 | CH <sub>2</sub> Cl                 | > 3days   | $(5.4 \pm 0.0) \times 10^{-3}$                     | 129                 |
| 10      | Ph                 | CHCl <sub>2</sub>                  | < 1 day   | -  | -                   |
| 11      | Ph                 | CCl <sub>3</sub>                   | < 1 day   | -  | -                   |
| 12      | Ph                 | CH <sub>2</sub> Br                 | > 3days   | $(5.4 \pm 0.1) \times 10^{-3}$                     | 128                 |
| 13      | Ph                 | CH <sub>2</sub> I                  | > 3days   | $(3.3 \pm 0.1) \times 10^{-3}$                     | 209                 |
| 14      | Ph                 | CF <sub>3</sub>                    | < 1 day   | -  | -                   |
| 15      | CH <sub>2</sub> Ph | CH <sub>3</sub>                    | > 3days   | $(2.1 \pm 0.1) \times 10^{-3}$                     | 333                 |

|           |                                  |                 |         |                                |       |
|-----------|----------------------------------|-----------------|---------|--------------------------------|-------|
| <b>16</b> | CH <sub>2</sub> PhF              | CH <sub>3</sub> | > 3days | (1.5 ± 0.0) x 10 <sup>-3</sup> | > 400 |
| <b>17</b> | C <sub>3</sub> H <sub>6</sub> Ph | CH <sub>3</sub> | > 3days | (9.2 ± 0.3) x 10 <sup>-4</sup> | > 400 |
| <b>18</b> | PhOMe                            | CH <sub>3</sub> | > 3days | (9.5 ± 0.4) x 10 <sup>-4</sup> | > 400 |
| <b>19</b> | PhCN                             | CH <sub>3</sub> | > 3days | (3.4 ± 0.0) x 10 <sup>-3</sup> | 205   |

<sup>a</sup> The rate equations were taken to be pseudo 1st order reaction as large excess of ascorbic acid were used with respect to the concentration of platinum(IV) complexes

#### 4.4.3 Evaluating the Lipophilicities and Aqueous Solubilities of the Expanded Asymmetric Platinum(IV) Bis-Carboxylates Series

Log $P_{ow}$  values of the platinum(IV) complexes were determined using the shake-flask method, where the relative solubility of the compounds in *n*-octanol and water were measured.<sup>165</sup> The platinum (IV) mono-carboxylate **A** was more hydrophilic than the asymmetric platinum(IV) bis-carboxylates with a Log $P_{ow}$  of -0.70 (Table 4) due to the presence of the uncarboxylated hydroxyl ligand capable of forming hydrogen bonds with water molecules. Complex **3** exhibited Log $P_{ow}$  of -0.28, which was slightly more hydrophilic than previously measured Log $P_{ow}$  of -0.19 (Table 2). This is likely to be due to difference in experimental setups and errors. Nonetheless, each set of experiment was repeated in triplicates to ensure consistency in the results.

In series 1, the Log $P_{ow}$  values of the complexes lie between -0.08 and 0.46, where bis-carboxylated platinum(IV) complexes become increasingly more lipophilic with additional methyl groups. In series 2, the Log $P_{ow}$  values lie between 0.13 and 0.56. Complex **13** was the most lipophilic with a Log $P_{ow}$  of 0.56 in the series and this was attributed to the presence of sterically bulky iodomethyl ligand.<sup>88</sup> In series 3, the Log $P_{ow}$  values lie between -0.47 and 0.24. Complex **17** was the most

lipophilic in the series with a  $\text{Log}P_{\text{ow}}$  value of 0.24, which was attributed to the presence of increased alkyl chains.

Among the synthesized asymmetric platinum(IV) complexes, Complex **8** and **13** exhibited the highest lipophilicity and were due to the increased size of the overall complex which outweighed the effect of other factors such as polarity and hydrogen bonding capacity. On the other hand, complex **15** and **18** were the most hydrophilic. The  $-\text{CH}_2$  linker between benzoate moiety and carboxylate could decrease the rigidity of complex **15** and promote hydrogen bonding. Similarly, the presence of lone pairs in the methoxy group of **18** would favor the formation of hydrogen bond in the aqueous partition leading to lowered lipophilicity.

With increased lipophilicity, hydrophilicity will be compromised and thus poor aqueous solubility would be expected. Generally, the aqueous solubility of the asymmetric platinum(IV) complexes followed an inverse relationship with lipophilicity. Complex **8** and **13** were the most lipophilic and hence the least soluble in aqueous media, with solubility of 0.12 and 0.30 mg/mL respectively. Complex **15** and **18** were the most hydrophilic and exhibited the highest aqueous solubility of 1.52 and 1.97 mg/mL respectively.

**Table 4.** Properties of asymmetric platinum(IV) complexes

| Complex          | Log P <sub>ow</sub> <sup>b</sup> | Aqueous Solubility (mg/mL) <sup>a</sup> | IC <sub>50</sub> [μM] <sup>c</sup> |               | Resistance factor <sup>d</sup> |
|------------------|----------------------------------|---|------------------------------------|---------------|--------------------------------|
|                  |                                  |   | A2780                              | A2780/cis     |                                |
| <b>Cisplatin</b> | -2.03 ± 0.47                     | 3.37 ± 0.05                             | 2.56 ± 1.97                        | 27.09 ± 6.35  | 10.6                           |
| <b>A</b>         | -0.70 ± 0.02                     | 1.31 ± 0.02                             | 4.50 ± 1.97                        | 19.94 ± 8.27  | 4.4                            |
| <b>3</b>         | -0.28 ± 0.13                     | 0.52 ± 0.04                             | 4.25 ± 0.66                        | 16.26 ± 4.18  | 3.8                            |
| <b>6</b>         | -0.08 ± 0.08                     | 0.44 ± 0.00                             | 3.10 ± 0.66                        | 18.40 ± 1.53  | 5.9                            |
| <b>7</b>         | 0.28 ± 0.05                      | 0.26 ± 0.06                             | 1.01 ± 0.45                        | 3.75 ± 1.32   | 3.7                            |
| <b>8</b>         | 0.46 ± 0.01                      | 0.12 ± 0.01                             | 1.14 ± 0.46                        | 6.52 ± 2.98   | 5.7                            |
| <b>9</b>         | 0.19 ± 0.06                      | 0.96 ± 0.02                             | 3.13 ± 0.63                        | 23.02 ± 4.33  | 7.4                            |
| <b>10</b>        | -                                | -                                       | -                                  | -             | -                              |
| <b>11</b>        | -                                | -                                       | -                                  | -             | -                              |
| <b>12</b>        | 0.13 ± 0.02                      | 0.28 ± 0.01                             | 2.81 ± 1.34                        | 14.72 ± 2.73  | 5.2                            |
| <b>13</b>        | 0.56 ± 0.01                      | 0.30 ± 0.01                             | 0.85 ± 0.56                        | 2.30 ± 0.49   | 2.7                            |
| <b>14</b>        | -                                | -                                       | -                                  | -             | -                              |
| <b>15</b>        | -0.47 ± 0.11                     | 1.52 ± 0.03                             | 9.94 ± 1.89                        | > 50          | -                              |
| <b>16</b>        | -0.20 ± 0.01                     | 0.69 ± 0.01                             | 7.32 ± 2.02                        | 30.99 ± 14.39 | 4.2                            |
| <b>17</b>        | 0.24 ± 0.02                      | 0.98 ± 0.02                             | 3.83 ± 1.44                        | 13.15 ± 6.48  | 3.4                            |
| <b>18</b>        | -0.41 ± 0.02                     | 1.97 ± 0.02                             | 4.14 ± 0.23                        | 19.09 ± 5.62  | 4.6                            |
| <b>19</b>        | -0.31 ± 0.02                     | 0.18 ± 0.00                             | 6.93 ± 1.25                        | > 50          | -                              |

<sup>a</sup>Complexes were dissolved in 8mL of water to saturation and filtered, [Pt] were determined through ICP-OES. <sup>b</sup>Log P<sub>ow</sub> values were determined through shake flask method using n-octanol and ultrapure water. <sup>c</sup>IC<sub>50</sub> is the concentration required to inhibit 50% of cell growth. <sup>d</sup>Resistance factor is the ratio between the IC<sub>50</sub> values of A2780/cis and A2780.

#### 4.4.4 Evaluating the Anti-Proliferative Properties of the Expanded Asymmetric Platinum(IV) Bis-Carboxylates Series

Efficacies of the various platinum (IV) carboxylates were tested on A2780 and A2780/cis human ovarian carcinoma cells and compared against cisplatin. IC<sub>50</sub>, the concentration required to inhibit 50% of the cell growth, was interpolated

from the mid-point of each graphs plotted in Figure 22, and tabulated in Table 4. Asymmetric platinum(IV) bis-carboxylates **7**, **8** and **13** exhibited the greatest cytotoxicity and were more than 2-folds more cytotoxic than cisplatin against A2780 ovarian carcinoma cell line. Complex **7** and **13** exhibited 7 and 9-folds increased potency against cisplatin in (A2780/cis) cisplatin-resistance A2780 variant respectively. These observations were attributed to the increased lipophilicity of the platinum(IV) complexes. With improved lipophilicity, the complexes can penetrate through the biological membrane more favorably and hence improve cellular accumulation leading to enhanced cytotoxicity. Notably, complex **7**, **8** and **13** were the most lipophilic complexes in the library of synthesized compounds. All the synthesized asymmetric platinum(IV) complexes exhibited higher lipophilicity than cisplatin, but some of them were less efficacious against the tested carcinoma cell lines. This could be attributed to slower rates of reduction to yield the active platinum(II) species, resulting in poor drug activities. All platinum(IV) prodrugs exhibited cross-resistance to A2780/Cis with resistance factors between 2.7 and 7.4, which was significantly lower than cisplatin's resistance factor of 10.6. This cross-resistance phenomena was anticipated since both platinum(IV) complexes and cisplatin shared the same pharmacophore. However, the structural modifications applied to the platinum(IV) scaffolds could have improved uptake of the newly synthesized complexes rendering them more bioavailable *in vitro*.

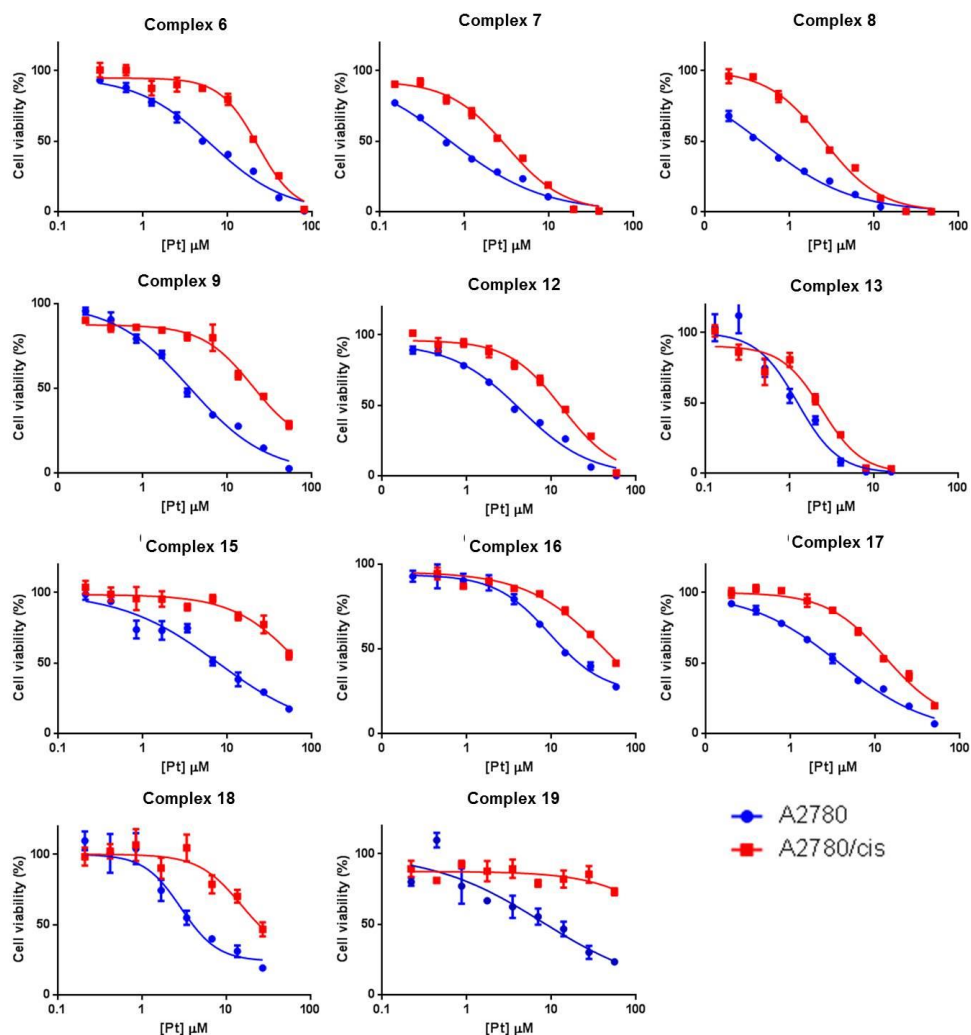


**Figure 22.** Dose-dependent drug efficacy studies for asymmetric platinum(IV) complexes **6-9**, **12-13** and **15-19**

#### 4.4.5 Investigation for Inter-Dependency Properties within the Expanded Asymmetric Platinum(IV) Bis-Carboxylates Series

The anti-proliferative data were taken together with the reduction rates and lipophilicities studies to analyze for any discernable inter-dependency properties relationship within this library of asymmetric platinum(IV) bis-carboxylates. Complex **3**, which exhibited  $t_{1/2}$  of 124 min and  $\text{Log}P_{\text{ow}}$  of -0.28, was found to be comparable to cisplatin in cell inhibition. Although complexes **9** and **12** exhibited



greater  $\text{Log}P_{ow}$  than **3**, they were not more efficacious than cisplatin due to similar reduction rates as **3**. On the other hand, complexes **15-18** which showed relatively similar  $\text{Log}P_{ow}$  values but lower reduction rates than **3** were less efficacious than cisplatin against the tested cancer cell lines. This finding was consistent with earlier reports which showed that an intracellular environment could even effectively reduce poorly cytotoxic oxoplatin, despite exhibiting high reduction potentials.<sup>159, 166</sup> Interestingly, **A** was as efficacious as **3** and **18** despite being less lipophilic and an order magnitude more readily reducible. A plausible explanation could be the rapid reduction of **A** to yield cisplatin resulting in increased efficacy. However, the fast reduction of platinum(IV) mono-carboxylate **A** would result in an increase in toxicity as it would reduce readily in the bloodstream, giving rise to negative side effects.<sup>24</sup>

Only complexes **7**, **8** and **13** were more effective than cisplatin against the ovarian carcinoma. They were generally more lipophilic and reduced to platinum(II) species at a slightly slower rate than **3**. While platinum(IV) prodrugs were known to undergo cellular uptake via passive diffusion which improves with increased lipophilicity and cytotoxicity,<sup>34</sup> our studies showed that the reduction rates of platinum(IV) prodrugs also played an important role in determining the overall potency.

Intriguingly, bis-carboxylate platinum(IV) complexes **17** and **18** resisted reduction under our assay conditions but exhibited anti-proliferative efficacies

that were comparable to cisplatin. The axial phenylbutyrate ligand in **17** is a known histone deacetylase inhibitor and can work synergistically with cisplatin to influence chromatin remodeling.<sup>167</sup> On the other hand, methoxybenzoate ligand in **18** does not have a definitive biological role but its electron-donating substituent can decrease the platinum(IV) complex's susceptibility to reduction while preserving its lipophilic character and potency, thus an alternative lead structure for future investigation.

## 4.5 Summary

Asymmetric platinum(IV) bis-carboxylates allow ligands with different properties to be accommodated within a common scaffold while preserving the platinum(II) pharmacophore. Using axial ligands with contrasting lipophilicity and hydrophilicity attributes, we are able to access novel platinum(IV) prodrug complexes that are not possible with classical symmetric acylation reactions. This strategy can be harnessed to fine-tune the properties of platinum(IV) prodrugs of cisplatin and bridge the gap between highly lipophilic and hydrophilic platinum(IV) complexes. We showed that in the expanded class of asymmetric platinum(IV) bis-carboxylates, lipophilicity and reduction rates are important determinant of prodrugs' anti-proliferative efficacy. This development can pave the way for the discovery of new platinum(IV) prodrugs with highly predictable and tuned properties for eventual clinical development.

## 4.6 Experimental Procedures

Unless otherwise noted, all procedures were carried out without taking precautions to exclude air and moisture. All solvents and chemicals were used as received without further treatment. The platinum(IV) complexes used in the studies were synthesized as described in Chapter 3. RPMI 1640 medium was purchased from Invitrogen (Carlsbad, CA, USA). Penicillin, streptomycin and thiazolyl blue tetrazolium bromide (MTT) were all obtained from Sigma Chemical Co (St. Louis, MO, USA). Fetal bovine serum (FBS) was from Hyclone (Thermo Scientific Inc., Logan, UT, USA). The water used was of Milli-Q grade purified by a Milli-Q UV Purification System (Sartorius Stedim Biotech S.A., Aubagne Cedex, France). All other solvents and chemicals were of analytical grade or HPLC grade obtained from commercial sources.

**Instrumentation.** UV spectra were recorded on a Shimadzu UV-1800 UV spectrophotometer using 1 cm path-length quartz cuvettes. Platinum concentration determination was performed using Inductively-Coupled Plasma Optical Emission Spectroscopy (ICP-OES) by CMMAC, NUS. Elemental analyses of selected platinum compounds were carried out on the Perkin-Elmer PE 2400 elemental analyzer by CMMAC, NUS. Dual-view Optima 5300 DV ICP-OES system was used to determine the platinum content in the aqueous phase. The stability and kinetic studies of platinum(IV) compounds were conducted using analytical HPLC on a Shimadzu Prominence using a Shimpack VP-ODS C18 (5

$\mu\text{M}$ , 120 Å, 250 x 4.60 mm i.d) column at r.t at a flow rate of 1.0 mL/min with 254 nm and 280 nm UV detection.

**Log $P_{ow}$  and aqueous solubility determination.** The Log $P_{ow}$  determination of platinum(IV) compounds were conducted using the shake flask method.<sup>168</sup> Platinum(IV) compounds were dissolved in 0.9% NaCl w/v ultrapure water (pre-saturated with *n*-octanol for 96 h and left to stand overnight). The solutions were sonicated and filtered through celite to remove undissolved platinum(IV) compounds. The initial concentrations of platinum content were determined by ICP-OES to ascertain the maximum solubility of the complexes. Subsequently, the platinum(IV) solutions were added an equal volume of *n*-octanol (pre-saturated with 0.9% NaCl w/v ultrapure water for 96 h and left to stand overnight). The heterogeneous mixtures were shaken vigorously for 2 h before centrifuging at 4200g for 15 min to achieve phase separation. The final concentration of platinum content in the aqueous phase was determined again by ICP-OES and the water-octanol partition coefficient was calculated. All experiments were done in triplicates.

**Cell Culture.** The human ovarian carcinoma cells A2780 and A2780/Cis were provided by Prof. Paul Dyson (EPFL). Both cell lines were cultured in complete RPMI 1640 medium containing 100 units/mL penicillin, 100  $\mu\text{g/mL}$  streptomycin and 10% fetal bovine serum. In order to retain resistance, 1  $\mu\text{M}$  cisplatin need to be added to the media for A2780/Cis every 2-3 passages. The two cell lines were

grown at 37°C in a humidified atmosphere of 95% air and 5% CO<sub>2</sub>. Experiments were performed on cells within 10 passages. Viable cells were counted using the trypan blue exclusion method.

**Inhibition of cell viability assay.** Drug effects on exponentially growing tumor cells were determined using MTT assay as described previously.<sup>169</sup> A2780 and A2780/Cis cells were seeded at a density of 6,000 cells/100 µL per well in 96-well plates and incubated for 24 h. Thereafter, tumor cells were exposed to drugs at different concentrations in RPMI medium without FBS and antibiotics. Compounds were dissolved as DMSO stock solutions and serially diluted with DMSO to a series of decreasing concentrations. The final concentration of DMSO in medium was 1% (v/v) and such concentration showed little cytotoxicity to both strains of cells when incubated for 6 h. The drug-containing medium was removed by aspiration, and fresh drug-free complete medium with FBS and antibiotics was added and the cells were incubated for additional 66 h. At 72 h after drug addition, the medium was aspirated, replaced with 100 µL MTT solution (0.5 mg/mL in PBS) and incubated for a further 4 h at 37°C. The medium was aspirated and the purple formazan precipitate dissolved in 100 µL DMSO. UV-vis absorbance was measured at a 595 nm using a microplate reader (Tecan). Experiments were performed in triplicates for each drug concentration and carried out independently at least three times. Cytotoxicity was evaluated with reference to the IC<sub>50</sub> value which was defined as the concentration needed for a 50% reduction of survival based on the survival curves. IC<sub>50</sub> values were calculated

from dose-response curves (cell survival *vs.* drug concentration) obtained in repeated experiments and adjusted to actual [Pt] administered which was determined using ICP-OES

**DNA-binding studies.** Studies on the reaction of platinum compounds with 5'-dGMP were conducted using analytical HPLC on a Agilent 1200 series DAD using a Phenomenex Luna C18 (5  $\mu$ M, 100 Å, 250 x 4.60 mm i.d) column at r.t at a flow rate of 1.0 mL/min with 254 nm and 280 nm UV detection. The gradient eluent conditions were as follows: 5-7% solvent A for 20 min followed by 80% solvent B for 5 min, where solvent A was NH<sub>4</sub>OAc buffer (10 mM, pH 7.0) and solvent B was MeOH. The purity of platinum(IV) compounds were conducted using analytical HPLC on a Shimadzu Prominence using a Shimpack VP-ODS C18 (5  $\mu$ M, 120 Å, 250 x 4.60 mm i.d) column at r.t at a flow rate of 1.0 mL/min with 254 nm and 280 nm UV detection. The gradient eluent conditions were as follows: 20-80% solvent A for 20 min followed by 80% solvent B for 5 min, where solvent A was NH<sub>4</sub>OAc buffer (10 mM, pH 3.8) and solvent B was MeCN. Eluted fractions, besides peaks arising from 5'-dGMP, were collected and analyzed by ESI/MS.

**Aqueous stability measurement.** The synthesized platinum(IV) complexes were dissolved in 1 mL of 40 mM HEPES buffer under pH 7.4 in 2 mL microtubes, centrifuged and analyzed using analytical HPLC on a Shimadzu Prominence using a Agilent ZORBAX Eclipse Plus column (5  $\mu$ M, 120 Å, 4.60 x 150 mm, 1.0

mL min<sup>-1</sup> flow) with UV detection at 254 nm and 280 nm. The gradient eluent conditions were as follows: 80 % solvent A and 20 % solvent B for first 8 min followed by 60 % solvent A and 40 % solvent B for next 7 min. The solvent A used was NH<sub>4</sub>OAc buffer (10 mM, pH 7.4) and solvent B was MeCN.

**Kinetics Measurement.** The synthesized platinum(IV) complexes were dissolved in 1 mL of 40 mM HEPES buffer in 2 mL microtubes, centrifuged and analyzed. Redox reactions of the various platinum compounds were conducted using analytical HPLC on a Shimadzu Prominence using an Agilent ZORBAX Eclipse Plus column (5 μm, 120 Å, 4.60 x 150 mm, 1.0 mL min<sup>-1</sup> flow) with UV detection at 254 nm and 280 nm. The isocratic eluent conditions were as follows: 60% solvent A and 40% solvent B for 10 mins. The experiment was conducted by mixing ascorbic acid (100 μL, 30 mM), dissolved platinum(IV) complexes (100 μL, 1 mM) and HEPES buffer (800 μL, 40 mM, pH 7.4) in a vial. Aliquots of the reaction mixtures were injected at regular time interval of 15 minutes. The depletion of the platinum(IV) content was monitored up to 500 min. The chromatograms were recorded and integrated. The integrated peak areas with respect to time were plotted and the time taken for 50 % of platinum(IV) complex to be reduced ( $t_{1/2}$ ) were determined from the graphs.

## Chapter 5

# Photoactivatable Properties of Asymmetric Platinum(IV) Bis-Carboxylates

### 5.1 Introduction

Platinum(IV) prodrugs can be used as phototherapeutic agents by being selectively photoreduced using light to release cytotoxic platinum(II) species which can bind to DNA.<sup>133</sup> By irradiating the tumor area with therapeutic dosage of light, physical discrimination between diseased and healthy tissue can be achieved, enabling unprecedented spatial and temporal control over the treatment regimen. Bednarski *et al.* first demonstrated this approach using platinum(IV)-iodo complex containing equatorial iodide ligands (Figure 23) and showed that it can be reduced to platinum(II) species upon UV irradiation resulting in the dissociation of iodide ligands.<sup>134</sup> Later on, Sadler *et al.* showed that the replacement of iodide ligands with azide in platinum(IV)-azido complex can greatly enhance its photoreductive properties since the dissociated azido ligands will irreversibly recombine to nitrogen and will not be able to reoxidise the platinum(II) metal centre.<sup>135, 136</sup> By varying the ammine ligands and their positions in the equatorial region, Sadler *et al.* was able to tune the photoactivation of this class of platinum(IV)-azido compounds from short wavelength (UVA, 365 nm) to visible blue and green lights.<sup>170</sup> While it is not clear the nature of the platinum(II) species formed, they react readily with



nucleosides and DNA which are the putative target of platinum(II) drugs. More recently, Natile *et al.* reported the spontaneous photoreduction of platinum(IV)-Dach, *cis,cis,trans*,-[Pt(1,4-Dach)Cl<sub>2</sub>(OH)<sub>2</sub>], in visible light to yield parent platinum(II) complex *cis*-Pt(1,4-Dach)Cl<sub>2</sub> with concomitant dissociation of the axial hydroxide ligands to radicals without the presence of any photoactive agents such as azido or iodide ligands.<sup>171</sup> The hydroxide radicals quickly recombined to produce hydrogen peroxide and this phenomenon was observed on <sup>1</sup>H NMR spectroscopy.

Taken together, we hypothesize it will be possible for platinum(IV) bis-carboxylates to incontrovertibly yield cisplatin through cleavage of the axial Pt-O bonds upon photoreduction. The carboxylate ligands should have significant UV absorption cross-section and be able to stabilize departing radical species. Based on these considerations, we investigated the photoreactivatable properties of bis-carboxylated platinum(IV) complexes **1-3** under photolytic conditions using UV as a light source (Figure 23). Complexes **1** and **3** bear aromatic benzoate ligands in the axial positions which can act as chromophores to absorb the light while **2** does not contain any aromatic chromophore and was used as a control to validate our hypothesis. To investigate the tunable UV absorption parameter of this class of asymmetric platinum(IV) bis-carboxylates, complexes **I**, **20** and **21** were designed and studied (Figure 23).

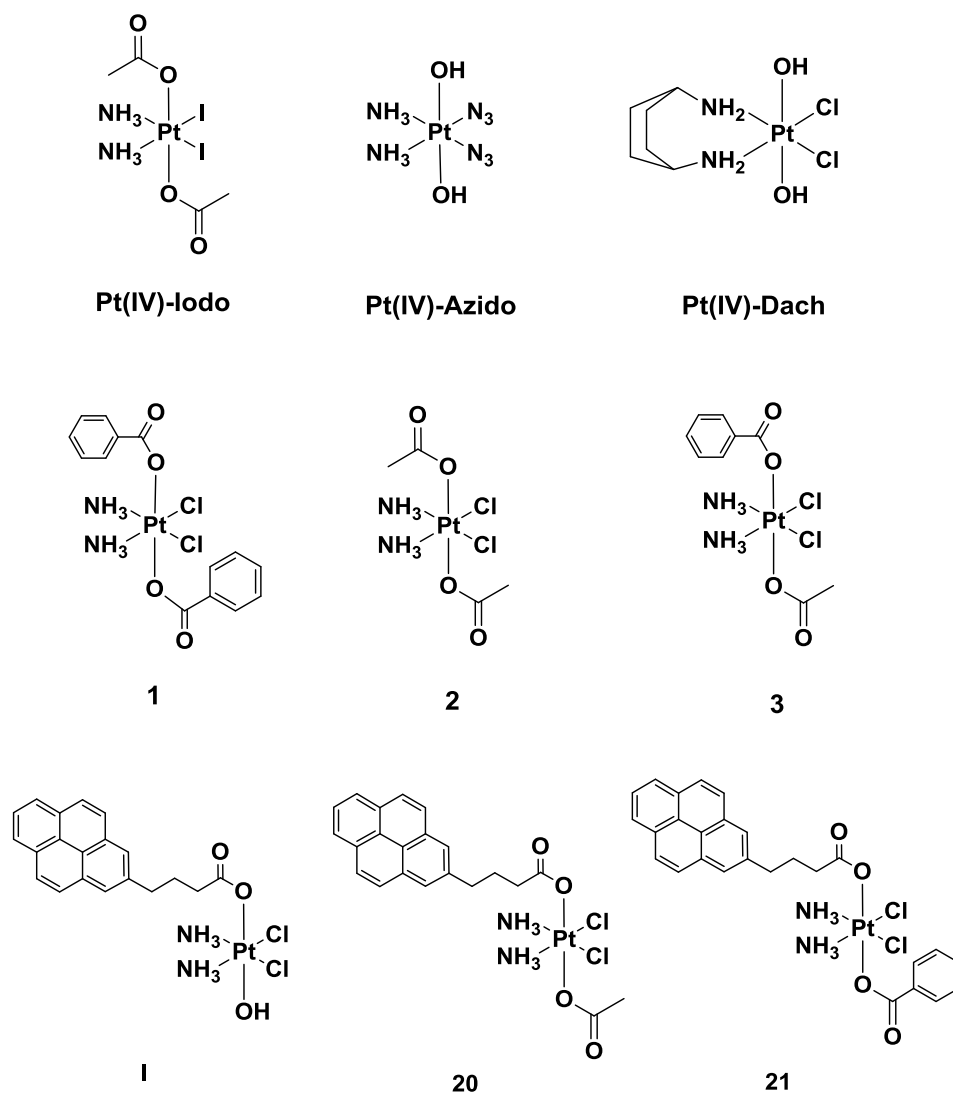


**Figure 23.** Chemical structure of platinum(IV) complexes investigated for their photoactivatable properties

## 5.2 Evaluating the Photoreducibility of Platinum(IV) Bis-Carboxylates

Structurally, **1** and **3** differ from **2** with the incorporation of at least an axial benzoate ligand. Due to its poor aqueous solubility, photoreduction of **1** was carried out in acetone by irradiating it at 365 nm using a standard handheld 16W laboratory UV lamp held 5 cm away. Within 5 min of irradiation, precipitation of

an off-white compound could be visually observed which was completed after 60 min. TLC analysis of the residual solvent phase indicated the conversion of **1** to a hydrophobic compound exhibiting a similar  $R_f$  to benzoic acid. The isolated precipitate, on the other hand, was highly polar and exhibited moderate aquatic solubility. The ESI-MS spectrum of the precipitate in aqueous solution showed distinct peaks at  $m/z$  335, 635 and 935 in the  $-ve$  mode, corresponding to molecular ions of cisplatin and its aggregates  $[\text{Cisplatin}+\text{Cl}]^-$ ,  $[2\times\text{Cisplatin}+\text{Cl}]^-$ , and  $[3\times\text{Cisplatin}+\text{Cl}]^-$  respectively. In order to confirm the identity of the isolated platinum precipitate, we carried out  $^{195}\text{Pt}$  NMR analyses of the sample in  $\text{DMSO-d}^6$ . Reduction of platinum(IV) to platinum(II) is accompanied by a change in the coordination sphere of complex **1** and decreases from 6 coordinated ligands to 4. The platinum chemical shift is highly sensitive to the ligand environment and platinum oxidation state with cisplatin and oxoplatin exhibiting resonances at ca. -2148 ppm and 853 ppm respectively. On the other hand, the resonance attributable to complex **1** was more deshielded and appeared at 1110 ppm due to the presence of the electron-withdrawing benzoate ligands. The isolated precipitate exhibited a resonance peak at -2144 ppm (Figure 24), which was consistent with the chemical shift of cisplatin and in stark contrast to **1**. These results support the initial hypothesis that platinum(IV) prodrugs of cisplatin bearing bis-aryl carboxylates in the axial positions will undergo reduction under UV irradiation to yield cisplatin. As far as we know, this represents the first example of a platinum(IV) prodrug which yields cisplatin after photoactivation.

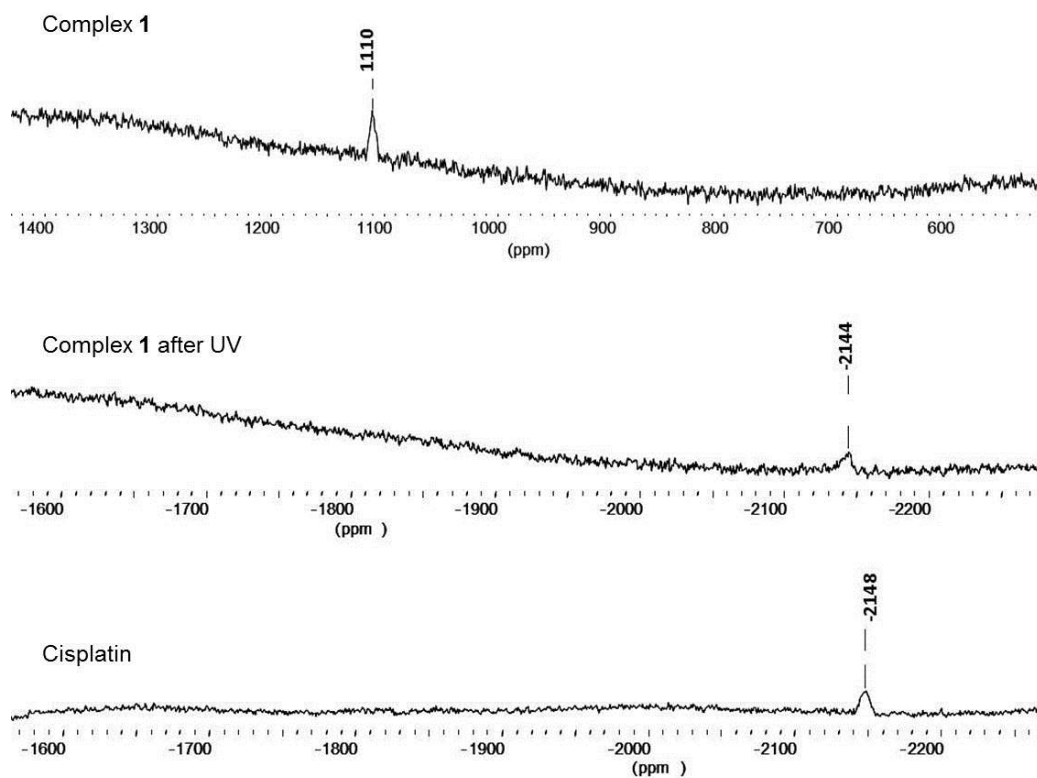


**Figure 24.**  $^{195}\text{Pt}$  NMR spectra of cisplatin, and complex **1** before and after UV

To further understand the nature of the photoactivation process, time-dependent  $^1\text{H}$  NMR studies was conducted to study the effect of UV irradiation on **1** at different time intervals in deuterated acetone solvent (Figure 25). Upon irradiation at 365 nm, the multiplet attributable to the  $\text{NH}_3$  ligands at ca. 6.5 ppm gradually diminished as the precipitate separated from the solvent. The most downfield peak at 7.99 ppm corresponding to the *ortho*-benzoate protons reduced in intensity with the appearance of two new sets of doublets that were more downfield. Of these two sets of doublets, one eventually dissipated leaving the other doublet at 8.04 ppm after prolonged irradiation. Resonances attributable to the *meta* and *para*-aryl protons underwent similar downfield shifts while the diammine peaks at 6.70

ppm gradually disappeared. Photoconversion was completed after 60 min of UV irradiation.

Based on these observations, we postulated that UV irradiation induced the dissociation of the axial benzoate ligands from the platinum(IV) scaffold. This could be accomplished via homolytic photocleavage of the Pt-O bond, yielding hydrophilic cisplatin as the precipitate, as well as two molar equivalents of benzoate radicals. These benzoate radical intermediate species formed were rapidly quenched by residual HOD to form the benzoic acid, evidenced by the decrease in intensity of the HOD resonance at c.a. 2.8 ppm and the appearance and dissipation of the most downfield peak corresponding to the *ortho*-benzoate radical protons over the course of the reaction. Formation of the benzoic acid product was also earlier observed using TLC analyses.

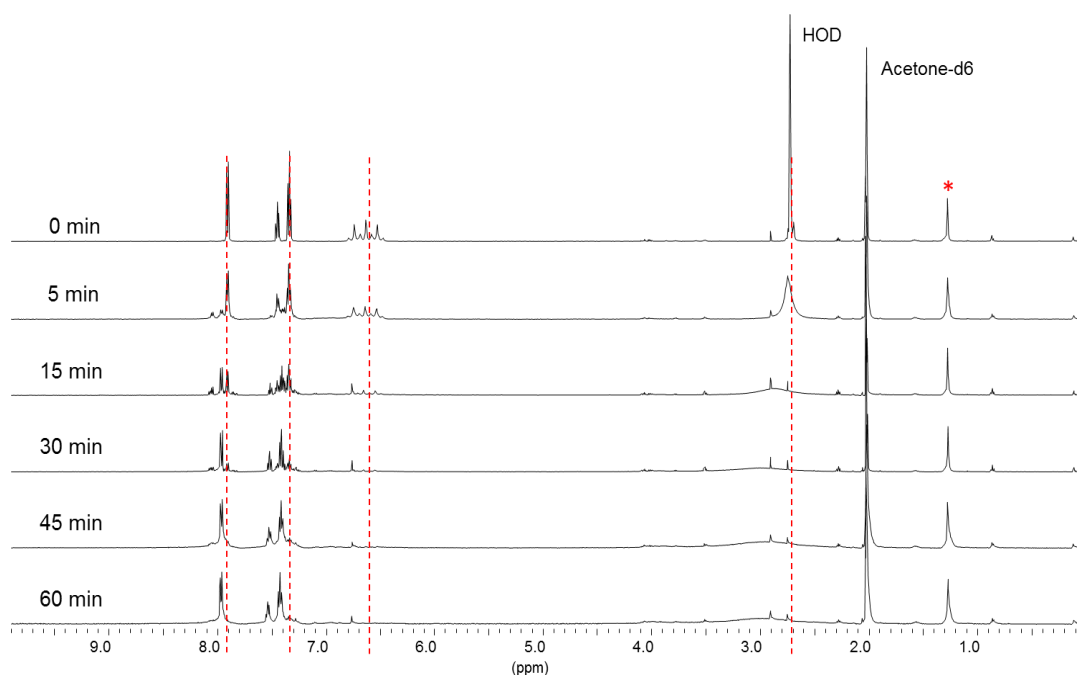


**Figure 25.** Effect of irradiation of UV light at 365 nm on  $^1\text{H}$  NMR spectra of complex **1** after 0, 5, 15, 30, 45, and 60 min

Asymmetric platinum(IV) bis-carboxylate **3** was also dissolved in deuterated water solvent and subjected to UV irradiation at 365 nm and the photoreduction was observed at regular time intervals on  $^1\text{H}$  NMR (Figure 26). The photoreduction was completed only after 120 min with no precipitate formed. A plausible argument could be during the photoreduction of **1** in acetone- $d_6$ , cisplatin was being precipitated as the by-product. Hence, the equilibrium was shifted right by Le Chatelier's principle which led to fast completion of the photoreduction. Another reason could be the presence of two benzoate ligands in **1** which were good chromophores for the UV irradiation while **3** only had one benzoate ligand, which resulted in **3** absorbing UV irradiation slower and hence photoreduced at a slower rate. In the  $^1\text{H}$  NMR spectra, the diammine protons which resonate at c.a. 6.5 ppm was absent due to deuterium exchange with the solvent. Upon irradiation, the most downfield peak at 7.86 ppm corresponding to the *ortho*-benzoate protons gradually diminished in intensity with the appearance of only one set of doublets at 7.92 ppm. Resonances attributable to the *meta* and *para*-aryl protons underwent a similar shift from 7.50 and 7.39 ppm to 7.57 and 7.45 ppm, respectively, while the acetyl protons peak at 2.06 ppm also decreased in intensity with the appearance of a new set of singlet at 2.00 ppm. The formation of radicals could occur during photoreduction. In the presence of water molecules in  $\text{D}_2\text{O}$  solvent, the benzoate and acetate radicals rapidly formed benzoic acid and acetic acid with the electrophilic  $\text{H}^+$ , which could explain why no radical intermediates were observable in the  $^1\text{H}$  NMR spectra. However, the reaction of the radicals with water molecules could be observed from the  $^1\text{H}$  NMR

where the peaks corresponding to D<sub>2</sub>O decreased in intensity as photoreduction proceeded.

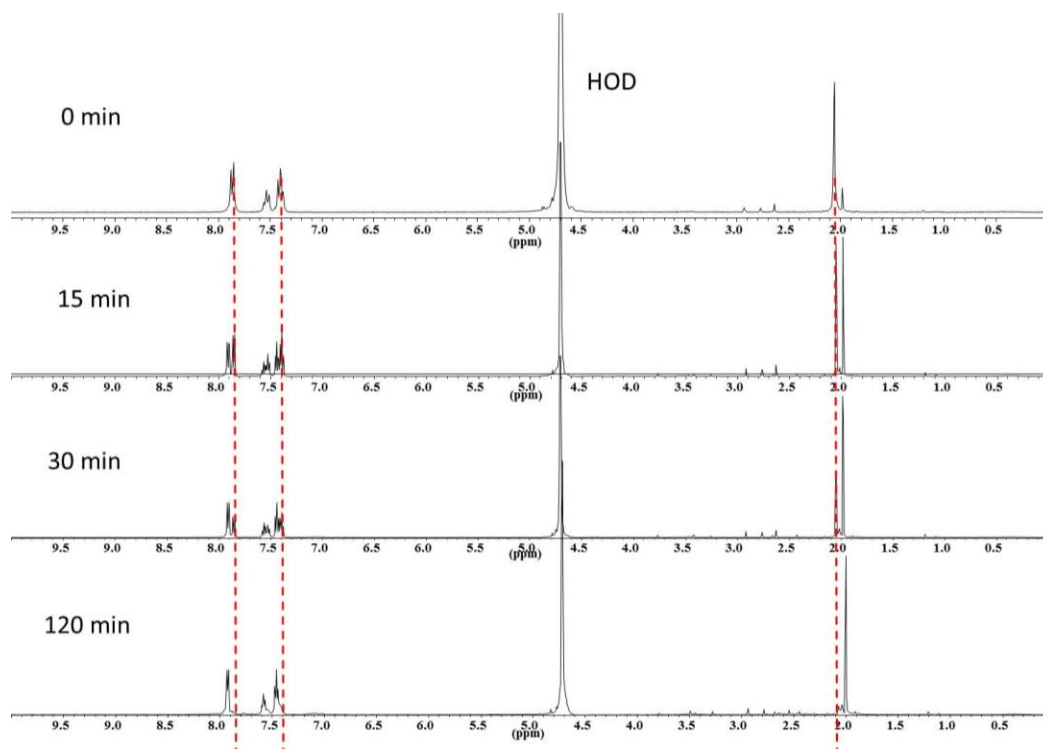


**Figure 26.** Effect of irradiation of UV light at 365 nm on <sup>1</sup>H NMR spectra of complex **3** after 0, 15, 30 and 120 min in D<sub>2</sub>O solvent

Complex **2** was also dissolved in D<sub>2</sub>O solvent and subjected to UV irradiation at 365 nm to prove our hypothesis that an aromatic chromophore is required for the photoreduction of platinum(IV) complexes to proceed. Surprisingly, it was found to undergo reduction under irradiation, albeit at a slower rate from the <sup>1</sup>H NMR studies. Similar to the previous observations, the singlet at 2.04 ppm corresponding to the acetyl protons of **2** gradually diminished in intensity with the appearance of a new singlet at 2.00 ppm. However, it was observed that the photoreduction of **2** was incomplete after 180 min of UV irradiation (Figure 27), leading to conclusion that having chromophoric ligands in the axial position of

platinum(IV) complexes do increase of rate of reduction, whereby the rate can be tuned by varying the number of chromophoric ligands.

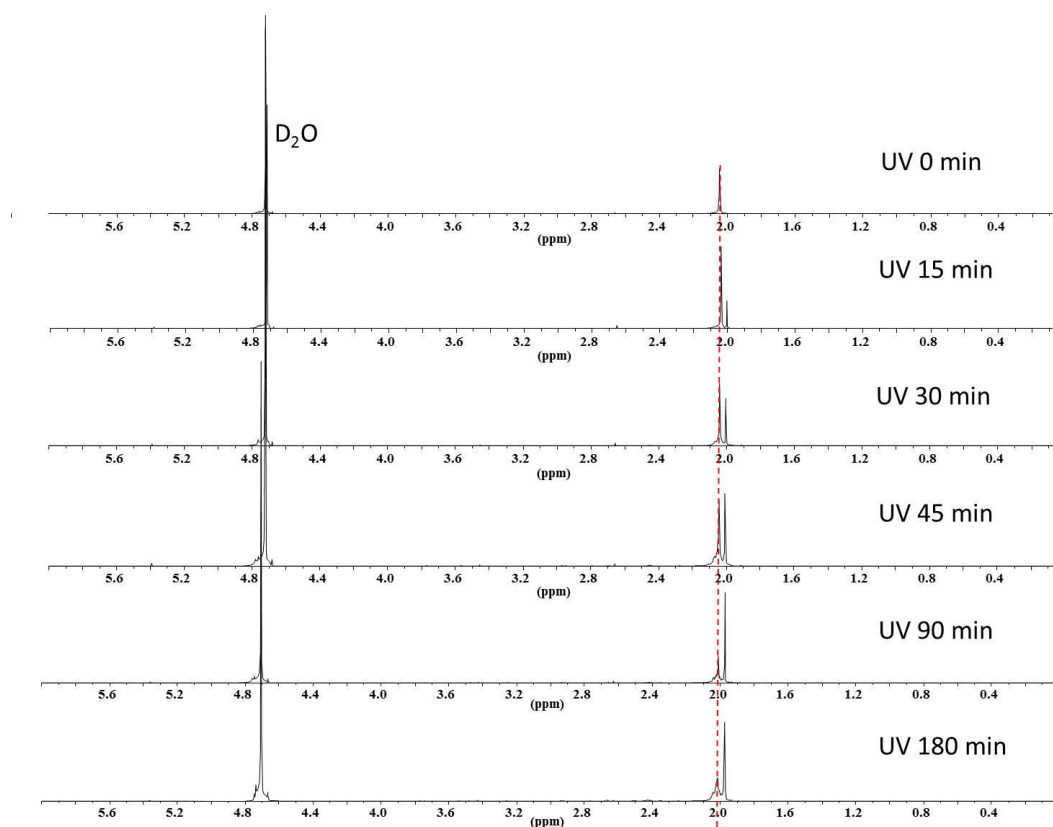


**Figure 27.** Effect of irradiation of UV light at 365 nm on  $^1\text{H}$  NMR spectra of complex **2** after 0, 15, 30, 45, 90 and 180 min in  $\text{D}_2\text{O}$  solvent

Unlike **1** where cisplatin was qualitatively isolated and analysed, we were unable to conclusively determine the identity of the reduced platinum(II) species formed for **2** and **3** as no cisplatin was observed from ESI-MS and  $^{195}\text{Pt}$  NMR. Nonetheless, we postulated that the platinum(II) species formed would either be cisplatin hydrolysed species or platinum(II) species bearing cisplatin pharmacophore [*cis*-Pt(NH<sub>3</sub>)<sub>2</sub>].



### 5.3 Evaluating the Photoactivation of Platinum(IV) Prodrugs by UV irradiation

To unanimously determine the formation of platinum(II) species upon photoreduction of platinum(IV) complexes, a fluorescent probe, Rho-DDTC, that was previously reported was used.<sup>172</sup> The fluorescent turn-on probe was found to be selective enough to distinguish between platinum(IV) and platinum(II) within a complex cellular environment as the probe only fluoresces when bound to platinum(II) species. A standard curve was obtained to quantify the amount of platinum(IV) reduced using cisplatin and 30  $\mu\text{M}$  of Rho-DDTC in HEPES buffer (20 mM, pH 7.4, 30% ethanol) (Figure 28). Various concentrations of cisplatin (0-90  $\mu\text{M}$ ) were mixed in 30  $\mu\text{M}$  of Rho-DDTC in HEPES buffer overnight and the fluorescence measured. The fluorescence intensity was found to increase linearly before reaching a plateau at 60  $\mu\text{M}$  of cisplatin concentration. Hence, 50  $\mu\text{M}$  of complexes **1-3** were subjected to photo-irradiation at 254 and 365 nm for up to 2 hours before mixing with Rho-DDTC at various time intervals to determine the amount of platinum(IV) reduced and the results depicted in Figure 29. All platinum(IV) complexes tested displayed little or no change in fluorescence intensity when stirred overnight with the Rho-DDTC. Upon UV irradiation to induce photoreduction of the platinum(IV) complexes, the Rho-DDTC showed an increased in fluorescence intensity.

From the data obtained, complex **1** was reduced to platinum(II) within 0.5 hour upon UV irradiation at 254 nm, and within an hour at 365 nm.  $58\pm 3$  % of

complex **2** was reduced to platinum(II) after 0.5 hour before proceeding to 96±4 % after 1.5 hours of UV irradiation at 254 nm. Upon UV irradiation at 365nm, only 28±5% of **2** was reduced to platinum(II) after 1 hour, before increasing to 32±2% after 2 hours (Figure 29). UV irradiation on **3** resulted in 92±2% reduced to platinum(II) after 0.5 hour before proceeding to 100% within 1 hour of UV irradiation at 254 nm, while 47±6% of **3** was reduced to Pt(II) species in 1 hour before proceeding to 100% after 2 hours when irradiated at 365 nm. The wavelength for maximum absorption ( $\lambda_{\text{max}}$ ) of the platinum(IV) complexes **1-3** were 232, 204 and 226 nm respectively, and their molar extinction coefficients ( $\epsilon$ ) at 6.0  $\mu\text{M}$  concentration were  $5.71 \times 10^5$ ,  $1.19 \times 10^5$  and  $1.93 \times 10^5 \text{ M}^{-1}\text{cm}^{-1}$  (Table 5).

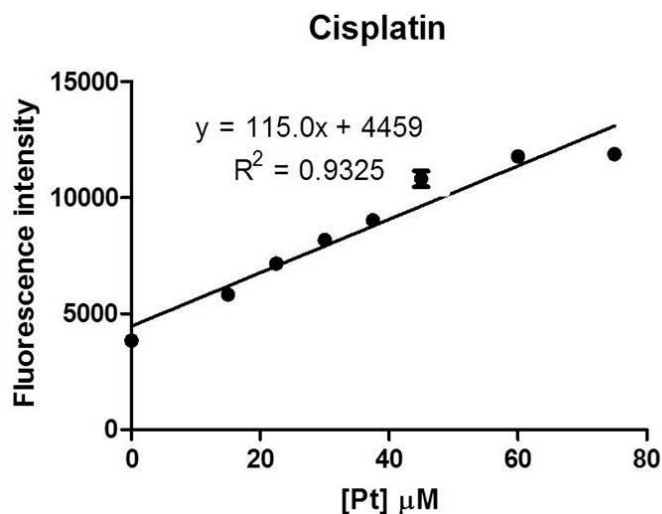


**Figure 28.** Standard curve depicting the increasing fluorescence intensity with increasing concentration of cisplatin

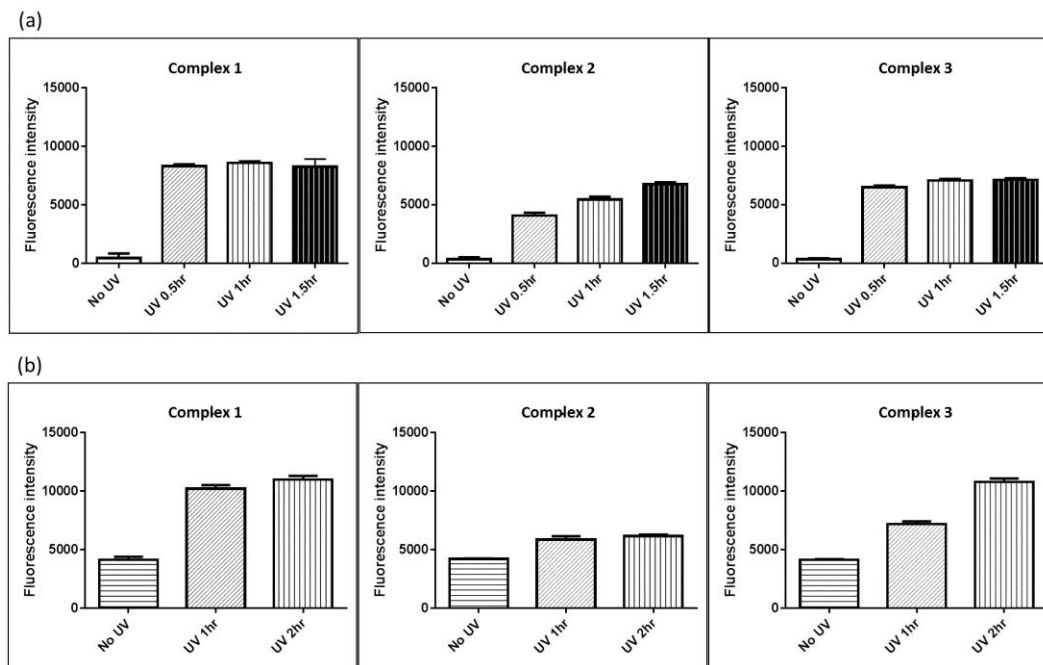


**Figure 29.** Chart depicting the increase in fluorescence intensity of platinum(IV) complexes 1-3 upon UV irradiation at (a) 254 nm and (b) 365 nm

These results indicate that the presence of aromatic pharmacophores are essential for photoreduction of platinum(IV) to platinum(II), especially when irradiated at wavelength significantly higher than their  $\lambda_{\max}$ . The photoreduction rates are faster when the compounds were irradiated at 254 nm than 365 nm. Evidently, increasing conjugation of the platinum(IV) complexes will lead to a red shift in the  $\lambda_{\max}$ , a better absorption of the UV irradiation and a faster rate of photoreduction. We postulate we can rationally design asymmetric platinum(IV) bis-carboxylates with  $\lambda_{\max}$  near 365 nm so as to tune their absorption spectrum and increase their rates of photoreduction.

**Table 5.** UV-Vis spectroscopy data of platinum(IV) complexes

| Complex              | $\lambda_{\max}$ (nm) | $\epsilon$ ( $M^{-1}cm^{-1}$ ) |
|----------------------|-----------------------|--------------------------------|
| <b>1</b>             | 232                   | $5.71 \times 10^5$             |
| <b>2<sup>b</sup></b> | 204                   | $1.19 \times 10^5$             |
| <b>3</b>             | 226                   | $1.93 \times 10^5$             |
| <b>I</b>             | 345                   | $6.18 \times 10^6$             |
| <b>20</b>            | 344                   | $6.31 \times 10^6$             |
| <b>21</b>            | 345                   | $6.36 \times 10^6$             |

<sup>b</sup>UV-Vis spectroscopy data was obtained in aqueous solution. The rest of the data were obtained in acetonitrile solution. Concentration of the platinum(IV) complexes were adjusted to 6.0  $\mu$ M before measurements.

#### 5.4 Evaluating the Tunable Photoactivatable Properties Asymmetric of Platinum(IV) Bis-Carboxylates

Platinum(IV) complexes **I** and **20-21** (Figure 23) containing a pyrene moiety in the axial position to increase their aromaticity and  $\lambda_{\max}$  were synthesized (Chapter 3) and investigated for their photoactivatable properties. The distance from the electron withdrawing pyrene moiety was increased with a propyl chain so as to decrease the rate of intracellular reduction, which was previously observed in Chapter 4. This was to ensure that majority of the platinum(IV) complexes **I** and **20-21** remained in their inert platinum(IV) forms, before photoactivated by UV irradiation to yield cytotoxic platinum(II) species at the tumor sites. The ligand in the other axial position was varied to investigate the effect on overall absorption spectrum and reduction rates of the prodrugs. Bearing the cisplatin core, the platinum(IV) prodrugs were expected to photoreduce to cisplatin upon UV irradiation.

Extensive conjugation in the pyrene functional group also allowed the platinum(IV) compounds to absorb strongly at ~345 nm ( $\lambda_{\text{max}}$ ) (Table 5), which was close to the UV irradiation at 365 nm. These absorption peaks corresponded to the  $\pi \rightarrow \pi^*$  electronic transition of pyrene with different vibrational energy levels at this electronic state. The presence of hydroxyl or carboxylate ligand on the other axial position had negligible effect on the  $\lambda_{\text{max}}$ . However, there was a slight increase in the molar extinction coefficient,  $\epsilon$ , of asymmetric platinum(IV) bis-carboxylates **20** and **21** when compared to platinum(IV) mono-carboxylate **I**. In comparison, platinum(IV) complexes **I** and **20-21** were able to exhibit significantly higher  $\lambda_{\text{max}}$  and  $\epsilon$  than **1-3** by substituting the axial ligand with a more conjugated aromatic molecule. This validated our approach of tuning the photoactivatable properties of platinum(IV) prodrugs through asymmetric carboxylation.

### **5.5 Evaluating the Photoactivation of Asymmetric Platinum(IV) Bis-Carboxylates by UV irradiation**

To ascertain that UV irradiation can photoreduce the platinum(IV) prodrugs, complexes **I** and **20-21** in DMF:H<sub>2</sub>O (1:1 v/v) solution were exposed to UV radiation (365 nm) for 0.5 hour. The UV absorption spectra of the complexes showed a decrease in the peaks corresponding to ~345 nm indicating the dissociation of the pyrene ligand upon photoactivation (Figure 30).

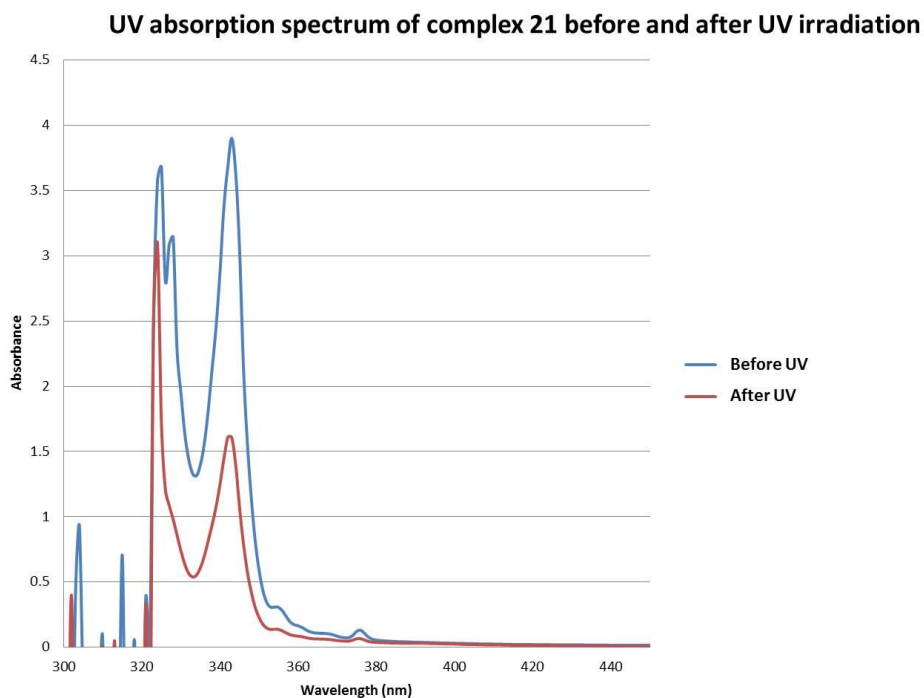


**Figure 30.** UV absorption spectrum of complex **21** before and after UV irradiation at 365 nm

Thin layer chromatography (TLC) was subsequently used to test for the presence of 1-pyrenebutyric acid formed upon reduction. Significant fluorescence intensity of 1-pyrenebutyric acid, which was initially quenched by platinum(IV) metal centre,<sup>173</sup> was observed on the TLC plate based on  $R_f$  value after photoreduction. Previously, the formation of benzoic acid that was observable on the TLC plate upon photoreduction of **1** did not exhibit any fluorescence. Hence, fluorescence measurements were taken to study the rate of reduction for complexes **I** and **20-21**. Equimolar solutions of **I** and **20-21** in 1:1 v/v ratio of DMF:H<sub>2</sub>O solutions were exposed to UV irradiation at 365 nm for 2 hours. At specified time intervals, the amount of 1-pyrenebutyric acid formed was monitored by fluorescence measurements using an excitation wavelength of 343 nm that corresponded to the

$\lambda_{\max}$  of pyrene. Fluorescence measurements of 1-pyrenebutyric acid showed complex **20** was photoreduced the fastest followed by **I** (Figure 31). The fluorescence intensity of 1-pyrenebutyric acid upon UV irradiation of **20** reached a plateau at 100 min. The plateau corresponded to the maximum amount of 1-pyrenebutyric acid that could be generated, which indicated complete reduction of the platinum(IV) complex. UV irradiation of **I** reached a similar level of fluorescence intensity at 100 min with a slower initial rate of reduction, while that of **21** had attained complete reduction after 2 hours. Surprisingly, the reduction rates of **I** and **20-21** were slower than **4** (Figure 29) despite having a stronger pyrene chromophore resulting in higher  $\lambda_{\max}$  and  $\epsilon$ . This was likely due to a more stable Pt-O<sub>pyrene</sub> bond as compared to Pt-O<sub>benzoate</sub> due to the presence of propyl hydrocarbon linker leading to increased bond distance between pyrene and platinum(IV) metal center.

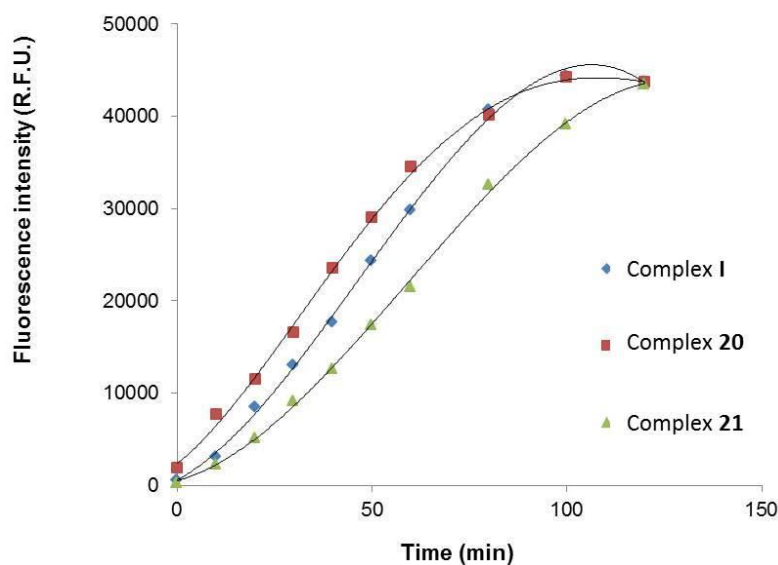


**Figure 31.** Fluorescence intensities at the maximum emission wavelength, 378nm, taken at specified times after initial UV irradiation of complexes **I** and **20-21**

One of the limitations using this class of platinum(IV) bis-carboxylate is the potential for them to undergo cellular reduction upon cell entry, although the reduction rate can be slowed significantly by increasing the bond distance between the electron withdrawing aryl moiety and platinum(IV) metal center. Another limitation will be the requirement of irradiation with shorter wavelength (365 nm) to photoactivate the platinum(IV) prodrugs which will limit its clinical applications,<sup>174</sup> as UV radiation has very limited penetration depth in biological tissues and can cause significant damage to DNA by inciting adjacent thymine pairs to form thymine dimers which replication polymerase cannot recognize.<sup>137</sup> However, this can be mitigated by further fine-tuning of the  $\lambda_{\max}$  with more conjugated chromophores. Nonetheless, a potential platinum(IV) prodrug strategy will be to encapsulate the platinum(IV) carboxylates in nano carriers which can



only be released as active platinum(II) species under photolytic conditions. As mentioned in Chapter 1, Xing *et al.* had conjugated a photoactivatable platinum(IV) complex to upconversion nanoparticles (UCNPs) that can convert NIR to UV light, leading to the reduction of the platinum(IV) complex (Scheme 10). Henceforth, the encapsulation of our series of platinum(IV) bis-carboxylates in UCNPs as a photoactivation of platinum(IV) prodrugs strategy will be of our main interest in overcoming the current limitations and is the subject of new ongoing investigation (Figure 32).

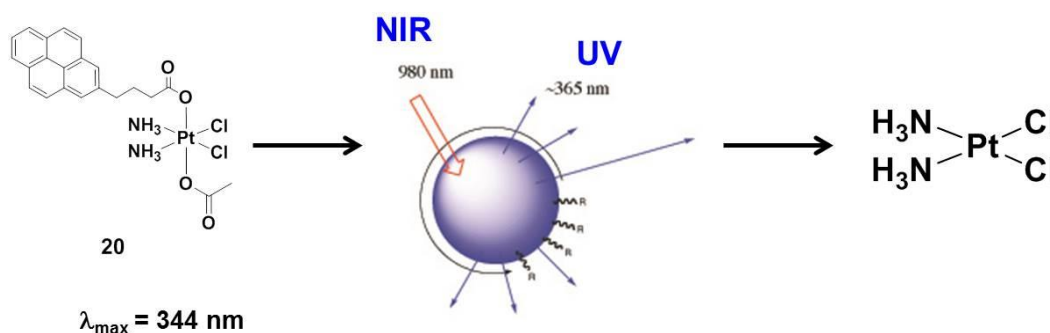


**Figure 32.** Photoactivation prodrug strategy using this class of asymmetric platinum(IV) bis-carboxylates

## 5.6 Summary

In summary, we have investigated a new class of photoactive platinum(IV) complexes containing benzoate ligands by design. The benzoate leaving groups are positioned at the axial ligand sites, in contrast to other examples, with the goal of yielding cisplatin upon ligands dissociation. Our evidences suggested that the

benzoate ligands on **1** were heterolytically cleaved from the platinum(IV) scaffold, resulting in its conversion to cisplatin, demonstrating for the first time that a photoreductive cisplatin-prodrug is possible. In addition, we showed that the photoreductive property of platinum(IV) complexes can be fine-tuned by replacing the benzoate ligands with a more conjugated pyrene moiety. We are optimistic that by further tuning the nature of the axial ligands, we can extend the strategy to identify other photoreductive platinum(IV) complexes that will generate exclusively cisplatin upon activation.

## 5.7 Experimental Procedures

Unless otherwise noted, all procedures were carried out without taking precautions to exclude air and moisture. All solvents and chemicals were used as received without further treatment. The platinum(IV) complexes used in the studies were synthesized as described in Chapter 3. The water used was of Milli-Q grade purified by a Milli-Q UV Purification System (Sartorius Stedim Biotech S.A., Aubagne Cedex, France). All other solvents and chemicals were of analytical grade or HPLC grade obtained from commercial sources.

**Instrumentation.**  $^1\text{H}$ , and  $^{195}\text{Pt}$  NMR spectra were recorded on a Bruker ACF 300 and Bruker AMX 500 spectrometer and the chemical shifts ( $\delta$ ) were internally referenced by the residual solvent signals relative to tetramethylsilane for  $^1\text{H}$  and externally referenced using  $\text{K}_2\text{PtCl}_4$  for  $^{195}\text{Pt}$ . Mass spectra were measured using a Bruker Ultimate 3000 ion trap ESI mass spectrometer. UV

spectra were recorded on a Shimadzu UV-1800 UV spectrophotometer using 1 cm path-length quartz cuvettes. Fluorescence measurements were performed using Synergy H1 hybrid multi-mode microplate reader from Biotek. The ultraviolet light source used for photochemical studies was a ZF-7A model handheld UV lamp with a power rating of 16W. It can operate with two different wavelengths of 254 nm and 365 nm respectively. The photochemical studies described were all conducted using UV light of 254 and 365 nm. The platinum(IV) complexes were irradiated at a distance of 5 cm from the UV lamp.

**Turn-on fluorescence probe by cisplatin.** Rho-DDTC was prepared as a 10 mM stock solution in DMSO and diluted in HEPES buffer (20 mM, pH 7.4, 30% ETOH) to obtain a concentration of 60  $\mu\text{M}$ . 50  $\mu\text{L}$  of the Rho-DDTC solution was mixed with 50  $\mu\text{L}$  of cisplatin to obtain 15.0, 22.5, 30.0, 37.5, 45.0, 60.0, 75.5 and 90.0  $\mu\text{M}$  of cisplatin respectively. The solution mixtures were incubate at 37°C overnight and the fluorescence intensity recorded at  $\lambda_{\text{em}} = 584 \text{ nm}$  ( $\lambda_{\text{ex}} = 490 \text{ nm}$ ). A standard curve of fluorescence intensity against concentration of cisplatin was plotted from the data obtained. This experiment was repeated in triplicates.

**Activation of Pt(IV) complexes.** Complex **1** was dissolved in acetone while **2** and **3** were dissolved in HEPES buffer solution respectively. These platinum(IV) solutions were irradiated with UV at 254 and 365 nm for up to 2 hours before mixing with prepared Rho-DDTC solution overnight at 37°C. The amount of platinum(II) species formed via photoreduction of platinum(IV) were determined

by measuring the fluorescence intensity and subsequently derived from the standard curve equation from cisplatin.

**Quantitative evaluation of the reduction of platinum(IV) complexes by UV irradiation.** Platinum(IV) complexes **I** and **20-21** (6.0  $\mu\text{mol}$  each) were dissolved in 1:1 v/v ratio of DMF:H<sub>2</sub>O solution (1.2 mL). The mixtures were contained in quartz cuvettes and subjected to UV irradiation (365nm). At regular time intervals (0, 10, 20, 30, 40, 50, 60, 80, 100, 120min upon UV irradiation), a fixed volume of platinum(IV) complexes solutions (2x100 $\mu\text{L}$  each for triplicate measurements) were pipetted out onto a 96-well plate. After 120 min, fluorescence measurements were performed on the 96-well plate with the solutions with a gain setting of 70, an excitation wavelength of 343nm and scanned emission wavelength from 360 to 450nm.

## Chapter 6

# Targeted Delivery of Dual-Drugs using Asymmetric Platinum(IV) Bis-Carboxylates Entrapped in Multi-Walled Carbon Nanotubes

### 6.1 Introduction

Cisplatin is limited by high toxicity and severe side-effects as well as incidences of platinum-associated drug resistance.<sup>22</sup> To overcome these limitations, cisplatin has been investigated in combination with anthracycline-based topoisomerase II (TOP2)-inhibitors against human lung cancer cell lines and found to greatly enhance the overall activity.<sup>175, 176</sup> TOP2 inhibitors intercalate duplex DNA and the resultant DNA-adducts formed inhibit the progression of TOP2 in the process of DNA remodelling. Because this pathway is independent of DNA alkylation damage induced by cisplatin, the cellular repair mechanisms can be overcome when TOP2 inhibitors are used together with cisplatin.<sup>177, 178, 179</sup> A recent Phase III clinical trials found that overall therapeutic efficacy was improved with a significantly higher response rate when cisplatin was co-administered with doxorubicin (Doxo, Figure 33), a TOP2 inhibitor, against endometrial adenocarcinoma.<sup>180</sup> Doxo:cisplatin combination regimens have also been evaluated in other clinical trials against several other malignancies with positive results. In these therapies, patients were dosed

---

with Doxo: cisplatin ratios of between ca. 0.9 to 3.0 molar equivalents cisplatin with respect to Doxo.<sup>180, 181, 182, 183, 184</sup>

There are however unique challenges involved in delivering drug combinations in a clinical setting,<sup>185</sup> as the drugs usually exhibit different pharmacokinetics properties resulting in uneven distribution of final concentrations at the intended target. Therefore, it is difficult to control the constituent drug levels of the combination regimen as well as coordinate their delivery to the site of action. . To ensure accurate control over the drug compositions, it is rationale to conjugate therapeutic drugs to the axial positions of platinum(IV) prodrug of cisplatin as a dual delivery of two drugs simultaneously. Upon reaching the tumor site, the platinum(IV) prodrug will undergo reduction to release cisplatin and therapeutic drug to yield the intended dosages. However classical synthetic strategy can only allow the development of symmetric platinum(IV) bis-carboxylates with no variation over the stoichiometric ratio of therapeutic drugs to cisplatin.<sup>72, 186</sup>

To demonstrate the viability of delivering ratiometric equivalent of cisplatin and doxorubicin, a novel asymmetric bis-carboxylate platinum(IV)-Doxo, **23**, was rationally designed (Figure 33). To achieve tumor-targeting, **23** was entrapped in multi-walled carbon nanotubes (MWCNT) whose surface were functionalized integrin-targeting cyclic peptide c(RGDfK). Previously, we reported the stable entrapment of lipophilic symmetric platinum(IV) bis-

carboxylate **1** with the MWCNT cavities through hydrophobic-hydrophobic interactions.<sup>122</sup> Henceforth, the lipophilicity of **23** was tuned by adding a hydrophobic benzoate moiety to the other axial position so as to achieve favourable drug loading into MWCNT.

This anticancer strategy is centred on the intracellular reduction of an inert platinum(IV) prodrug, that is stably entrapped within the MWCNT due to hydrophobic-hydrophobic interactions, which simultaneously releases exact ratiometric equivalent of hydrophilic cisplatin and Doxo upon cell entry (Figure 34). The formulation of MWCNT-platinum(IV) prodrug nanoconjugate capable of synchronous ratiometric delivery of two mechanistically complementary drugs and its anti-proliferative efficacy against ovarian and endometrial cancer cells will be discussed in greater details in the ensuing section.

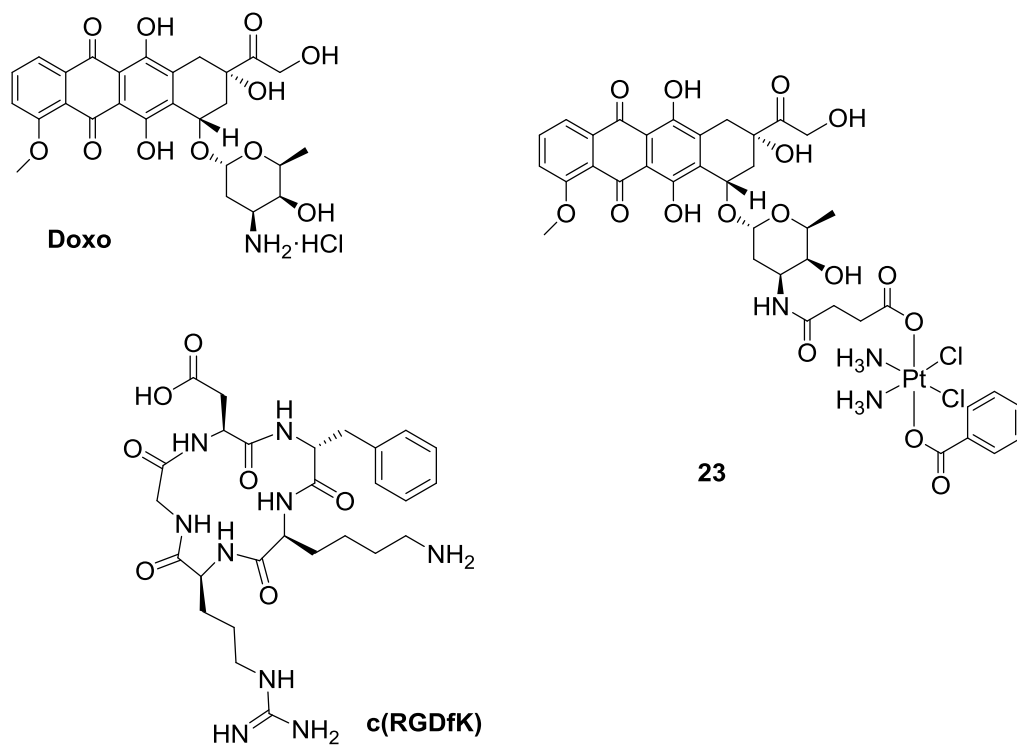


**Figure 33.** Chemical structure of doxorubicin (Doxo), c(RGDfK), and asymmetric carboxylate platinum(IV)-Doxo conjugate, **23**

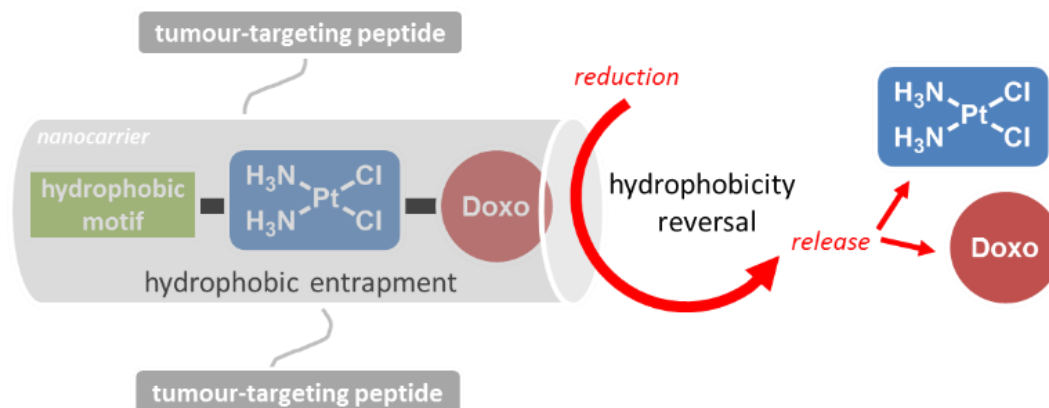


**Figure 34.** Concept of ratiometric dual-drug delivery via hydrophobic entrapment using MWCNT as nanocarrier



## 6.2 Synthesis and Characterization

### 6.2.1 Asymmetric Platinum(IV) Bis-Carboxylate **23**

To synthesize **23**, asymmetric platinum(IV) complex **22** bearing a free carboxylic function group in the axial position was prepared (Chapter 3). Complex precursor **22** was coupled to Doxo in DMF with *O*-benzotriazole-1-yl *N,N,N',N'*-tetramethyluronium hexafluoro-phosphate (HBTU) as a coupling reagent under room conditions to yield **23** (Scheme 14a). The product **23** was recovered from the crude reaction mixture *via* lyophilisation to remove the non-volatile DMF solvent, followed by repeated washing using water, acetone and diethyl ether. Previous attempts to synthesize **23** using *N,N'*-dicyclohexylcarbodiimide (DCC) and ethyl(dimethylaminopropyl)-carbodiimide (EDC) as coupling reagents resulted in poor yields. Complex **23** was characterized using ESI-MS and <sup>1</sup>H NMR spectroscopy, and its purity determined by elemental analysis. The parent molecular ions [M-H]<sup>-</sup> were readily observed using ESI-MS. Fragmentation analysis for **23** resulted in the loss of the Doxo ligand, consistent with the proposed structures. Characteristic resonances could be observed at ca. 6.6 ppm in <sup>1</sup>H NMR, assigned to the ammine ligands, which was consistent with previous platinum(IV) bis-carboxylates. The formation of **23** was also indicated by the disappearance of the -COOH proton at 12.0 ppm, which was present in <sup>1</sup>H NMR of **22**. In addition, the integral value in <sup>1</sup>H NMR showed that there was only one unit of Doxo with respect to the ammine ligands.

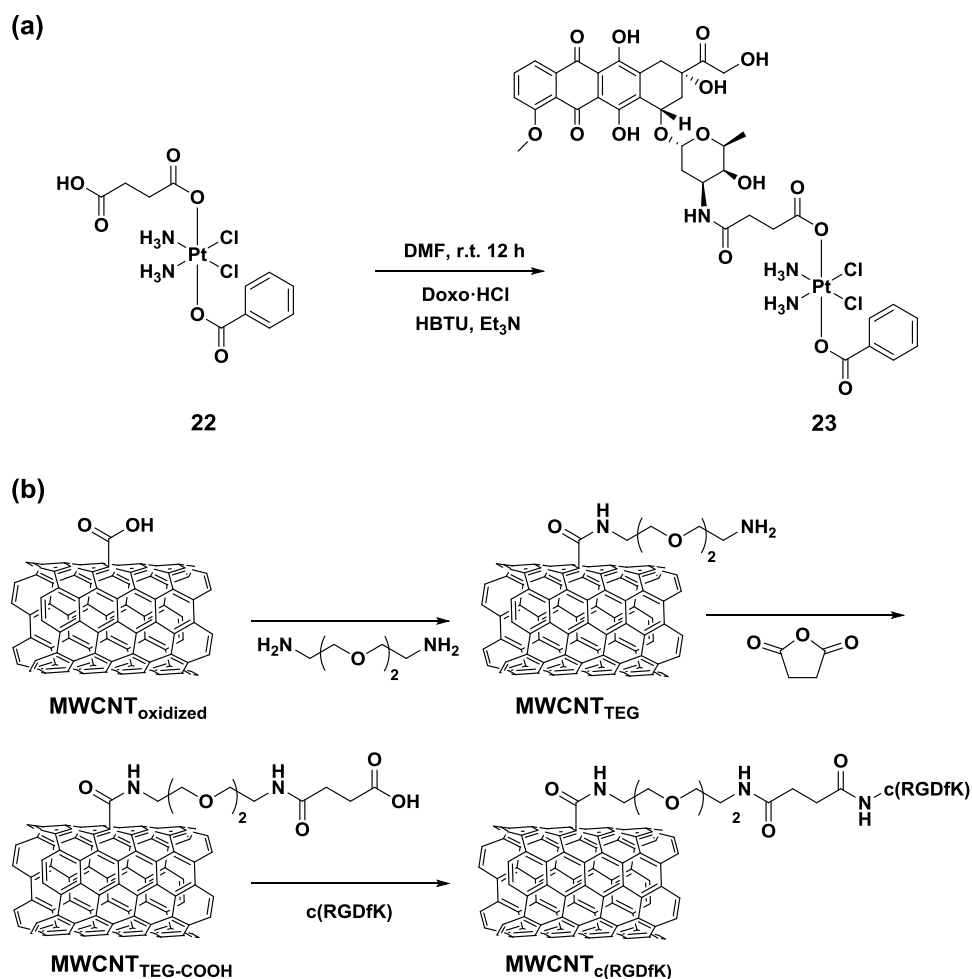
### 6.2.2 MWCNT-Platinum(IV) Prodrug Nanoconjugate [23·MWCNTc(RGDfK)]

To achieve tumour-targeting, c(RGDfK) peptide was conjugated to the MWCNT platform (Scheme 14b). These peptides recognize multiple ligands of  $\alpha_v$  integrin family,<sup>187</sup> and have been found to exhibit high affinity to  $\alpha_v\beta_3$  and  $\alpha_v\beta_5$  integrin receptors that are overexpressed in tumor angiogenic endothelial cells.<sup>188, 189</sup> Hence, they are particularly relevant for endometrial adenocarcinomas since vascular endothelial growth factor, which is correlated with angiogenesis, is the major stimulus for endothelial cell proliferation in these carcinomas.<sup>190</sup>

Ultrapure ( $\geq 98\%$ ) MWCNTs with a diameter of 30-40 nm and a length of up to a few  $\mu\text{m}$  were used given their higher internal loading capacity compared to single-walled CNTs (SWCNTs). These pristine MWCNTs were oxidized and purified in accordance to a reported procedure to yield MWCNT<sub>oxidized</sub> (Scheme 14b),<sup>191</sup> and coupled with bifunctional 2,2'-(ethylenedioxy)diethylamine (TEG) using EDC/DIPEA to obtain amine-terminated MWCNTs (MWCNT<sub>TEG</sub>). Quantitative Kaiser Test was performed to determine the degree of amino-functionalization on MWCNT<sub>TEG</sub> and ascertained to be 680  $\mu\text{mol}$  of  $-\text{NH}_2$  groups per gram of MWCNTs. The purified and dried MWCNTs were subsequently treated with excess of succinic anhydride in DMSO at r.t. for 3 days to form carboxylic acid-terminated MWCNTs (MWCNT<sub>TEG-COOH</sub>). A negative

Kaiser Test indicated that the amine groups on the MWCNTs were fully converted to carboxylic acid functional groups.

MWCNT<sub>TEG-COOH</sub> was subsequently coupled to c(RGDfK) peptide using HBTU/NEt<sub>3</sub> to obtain MWCNT<sub>c(RGDfK)</sub> (Scheme 14b). The formation of MWCNT<sub>c(RGDfK)</sub> was accompanied by a mass change of more than 50%. For hydrophobic entrapment, purified MWCNT<sub>c(RGDfK)</sub> was suspended with **23** in solvent and agitated for 3 days in accordance with a previously reported procedure.<sup>192</sup> Water or CHCl<sub>3</sub> was used as the drug entrapment solvent for nanoextraction since they poorly solubilized both **23** and MWCNT<sub>c(RGDfK)</sub> and would enhance their hydrophobic-hydrophobic interactions. The entrapped product [**23**·MWCNT<sub>c(RGDfK)</sub>] was filtered and washed extensively with a washing solvent mixture comprising water:CHCl<sub>3</sub>:MeOH (1:2:2.5 v/v). This washing step was essential to remove unbound **23** on the external MWCNT surface without displacing those entrapped within the core. Being intensely red in colour, complete removal of unbound **23** was indicated by clear washings and restoration of the MWCNTs as a black residue.



**Scheme 14.** Synthetic scheme for (a) preparation of **23** and (b) surface functionalization of MWCNT to yield MWCNT<sub>c(RGDfK)</sub>

Platinum content in [**23**·MWCNT<sub>c(RGDfK)</sub>] was determined using ICP-OES on samples that were incinerated at 1000°C and their residues reconstituted in 2% HNO<sub>3</sub>. Based on the platinum levels quantitated, the entrapment levels within MWCNT<sub>c(RGDfK)</sub> using CHCl<sub>3</sub> and water as solvent systems were ascertained to be 17.0±1.0% and 24.5±0.8% w/w of **23**, respectively. In previous reports, entrapment efficiencies of cisplatin and **1** in MWCNT<sub>oxidized</sub> were higher at 62.1±2.0% w/w and 51.7±2.0% w/w,

respectively.<sup>192</sup> The lower [**23**·MWCNT<sub>c(RGDfK)</sub>] loading was presumably due to its increased steric encumbrance, resulting in poorer mobility within the MWCNT cavity.

### **6.3 Evaluating the Anticancer Properties of [23·MWCNT<sub>c(RGDfK)</sub>]**

#### **6.3.1 Stability and Kinetic Properties**

To achieve targeted delivery, drug payload should only be released at the site of its intended target. To demonstrate that [**23**·MWCNT<sub>c(RGDfK)</sub>] can function effectively as a delivery platform for controlled release of its payload, we investigated the stability of **23** entrapped within MWCNT<sub>TEG</sub> under reducing and non-reducing aqueous conditions. For comparison, we prepared entrapped Doxo and monitored its release from MWCNT<sub>TEG</sub> using UV-vis spectroscopy ( $\lambda_{550}$ ). Under aqueous conditions, Doxo was released rapidly from MWCNT<sub>TEG</sub> with >50% of the payload released within 10 hours (Figure 35). Complete drug release was achieved after 4 days. Entrapped **23**, on the other hand, was stable within MWCNT<sub>amine</sub> and uncontrolled release of Doxo into the surrounding environment was not observed. Only after 4 days was ca. 10% Doxo w/w non-specifically released into the media. However, in the presence of chemical reductant, i.e. 3 mM ascorbic acid, release of Doxo was observed culminating with complete release after 4 days. In this manner, controlled release of the hydrophobically entrapped drug payload was achieved using reduction of

the platinum(IV) scaffold. Chemical reduction by ascorbic acid reduced the platinum(IV) prodrug to platinum(II) while liberating its axial ligands, namely benzoate and Doxo-succinate. Because these components are hydrophilic, they could not be stably entrapped within MWCNTs and were discharged.

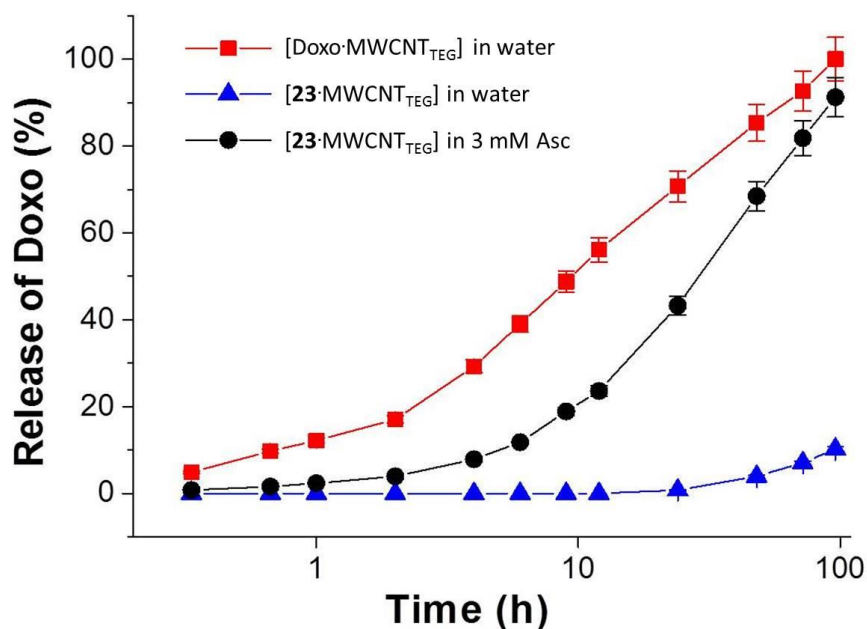


**Figure 35.** Release of Doxo from MWCNT<sub>TEG</sub> monitored using UV-vis spectroscopy ( $\lambda_{550}$ )

### 6.3.2 Anti-Proliferative Property

The anti-proliferative efficacy of the new constructs on the growth inhibition of Ishikawa endometrial adenocarcinoma as well as A2780 and A2780/Cis human ovarian carcinoma cells was investigated (Table 6). To mitigate the effects of contamination, platinum concentration of the stock solutions were determined using ICP-OES and the IC<sub>50</sub> values were adjusted to actual platinum concentration values for entries 1, 3, 4 and 6.

Cisplatin exerts its cytotoxic effects through DNA alkylation which yield primarily intrastrand platinated adducts on purine bases,<sup>161</sup> while Doxo, a DNA intercalator, prevents the progression of TOP2 during DNA remodelling leading to stalling of TOP2 at the adduct site.<sup>193</sup> Due to these complimentary mechanisms acting on the same biological target, we postulated that a combination of these drugs could lead to synergistic enhancement of cytotoxicity. As anticipated, Doxo exerted a strong cytotoxic effect against both A2780 and A2780/Cis indicating that its mode of action is independent of the cisplatin resistance pathway. We further noted that a 1:1 combination of cisplatin and Doxo was additive which could be due to differential uptakes of the two drugs. The construct [23·MWCNT<sub>c(RGDfK)</sub>] contained a platinum(IV) prodrug that was capable of delivering cisplatin and Doxo in stoichiometric-equivalent portions. [23·MWCNT<sub>c(RGDfK)</sub>] was more efficacious against the tested cell lines compared to cisplatin, Doxo or a physical mixture of cisplatin + Doxo (1:1). In keeping with Doxo, [23·MWCNT<sub>c(RGDfK)</sub>] was also able to overcome A2780/Cis. Strikingly, against target Ishikawa endometrial adenocarcinoma cells, [23·MWCNT<sub>c(RGDfK)</sub>] was ca. 2-fold more cytotoxic than either Doxo or cisplatin + Doxo 1:1 combination and 11-fold more than cisplatin alone. The IC<sub>50</sub> values of [23·MWCNT<sub>c(RGDfK)</sub>] was compared with pure 23 against these cell lines. We noted that at these concentrations, blank MWCNT<sub>c(RGDfK)</sub> was non-cytotoxic (Table 6, entry 5). In all instances, [23·MWCNT<sub>c(RGDfK)</sub>] was 4-7 fold more cytotoxic than the free 23,

indicating that the MWCNT<sub>c(RGDfK)</sub> platform was crucial for delivering the payload to the cancer cells.

### 6.3.3 Platinum Uptake in Ishikawa Cells

Therefore, we treated Ishikawa cells with **23** and [**23**·MWCNT<sub>c(RGDfK)</sub>] for 6 hours and quantitated the cellular platinum levels using ICP-MS to study the effect of the MWCNT construct on the drugs' efficacies. Cells treated with [**23**·MWCNT<sub>c(RGDfK)</sub>] exhibited ca. 3-fold higher platinum levels compared to those treated with **23** alone (Figure 36), demonstrating the excellent internalization of hydrophobic **23** by our MWCNT constructs.

**Table 6.** IC<sub>50</sub> values (μM) against cancer cell lines<sup>a</sup>

| Entry | Test compound <sup>b</sup>                | A2780       | A2780/Cis    | Ishikawa     |
|-------|---|-------------|--------------|--------------|
| 1     | Cisplatin                                 | 1.71 ± 0.42 | 13.11 ± 1.99 | 11.10 ± 0.80 |
| 2     | Doxo                                      | 0.92 ± 0.48 | 0.89 ± 0.15  | 2.96 ± 0.15  |
| 3     | Cisplatin + Doxo (1:1)                    | 0.84 ± 0.02 | 1.17 ± 0.11  | 2.35 ± 0.25  |
| 4     | <b>23</b>                                 | 3.29 ± 0.72 | 4.82 ± 0.28  | 6.76 ± 0.44  |
| 5     | [MWCNT <sub>c(RGDfK)</sub> ] <sup>c</sup> | >50         | >50          | >50          |
| 6     | [ <b>23</b> ·MWCNT <sub>c(RGDfK)</sub> ]  | 0.76 ± 0.17 | 0.90 ± 0.30  | 0.95 ± 0.06  |

<sup>a</sup>Concentration required to inhibit 50% of the cell growth with respect to control groups, measured by MTT assay after 72 h exposure. <sup>b</sup>Data obtained are based on the average of at least three independent experiments with the corresponding standard deviations. <sup>c</sup>Empty MWCNT<sub>c(RGDfK)</sub> were tested and inhibition of cell viability was not observed at >50 μg/mL which exceeded the concentrations tested for entry 6.



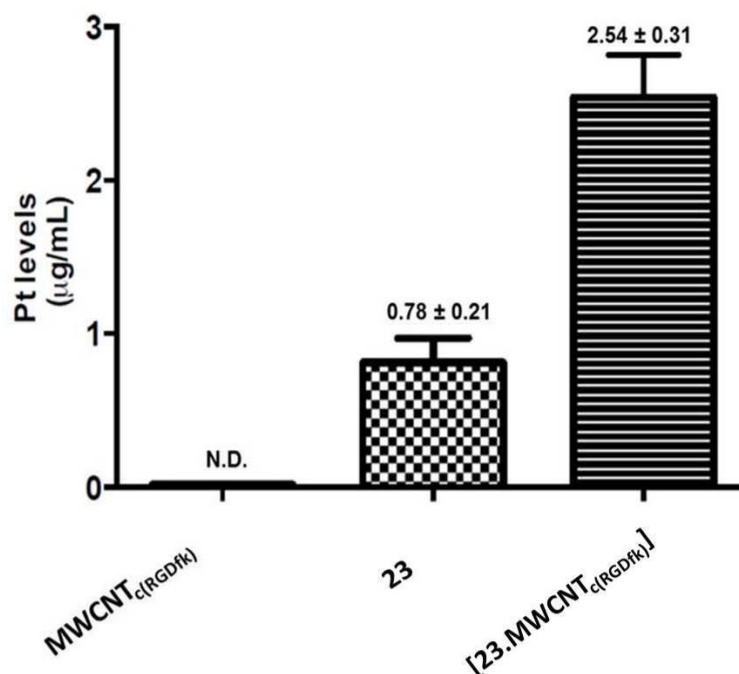


**Figure 36.** Platinum content of Ishikawa cell extracts after treatment with MWCNT<sub>c</sub>(RGDfK), **23** and [23·MWCNT<sub>c</sub>(RGDfK)]

#### 6.3.4 Evaluating the Internalization of [23·MWCNT<sub>c</sub>(RGDfK)] via Confocal Studies

In order to show that [23·MWCNT<sub>c</sub>(RGDfK)] was internalized by cells before releasing the payload, Ishikawa cells were treated with [23·MWCNT<sub>c</sub>(RGDfK)] for 6 hours before fixing and staining with Hoeschst 33342 nuclear dye. Although **23** was fluorescent by virtue of its Doxo motif, [23·MWCNT<sub>c</sub>(RGDfK)] did not exhibit fluorescence because it was obscured by its MWCNT carrier. This was shown by adding [23·MWCNT<sub>c</sub>(RGDfK)] onto untreated cells that had been fixed/stained before imaging (Figure 37d). Upon internalization and cellular reduction, Doxo was released into the cytoplasm resulting in characteristic fluorescence at  $\lambda_{Ex} = 488 \text{ nm}$ :  $\lambda_{Em}$

= 603 nm (Figure 37c). We observed that the Doxo released was distributed throughout the cytoplasm as well as the nucleus. In contrast, cells treated with Doxo were only localized within the nucleus (Figure 37b). Our hypothesis was that reduction of **23** yielded Doxo that was still conjugated to the succinate linker which imparted a negative charge to the conjugated entity instead of the free Doxo. This could delay the translocation of Doxo into the nucleus, leading to an altered distribution profile.

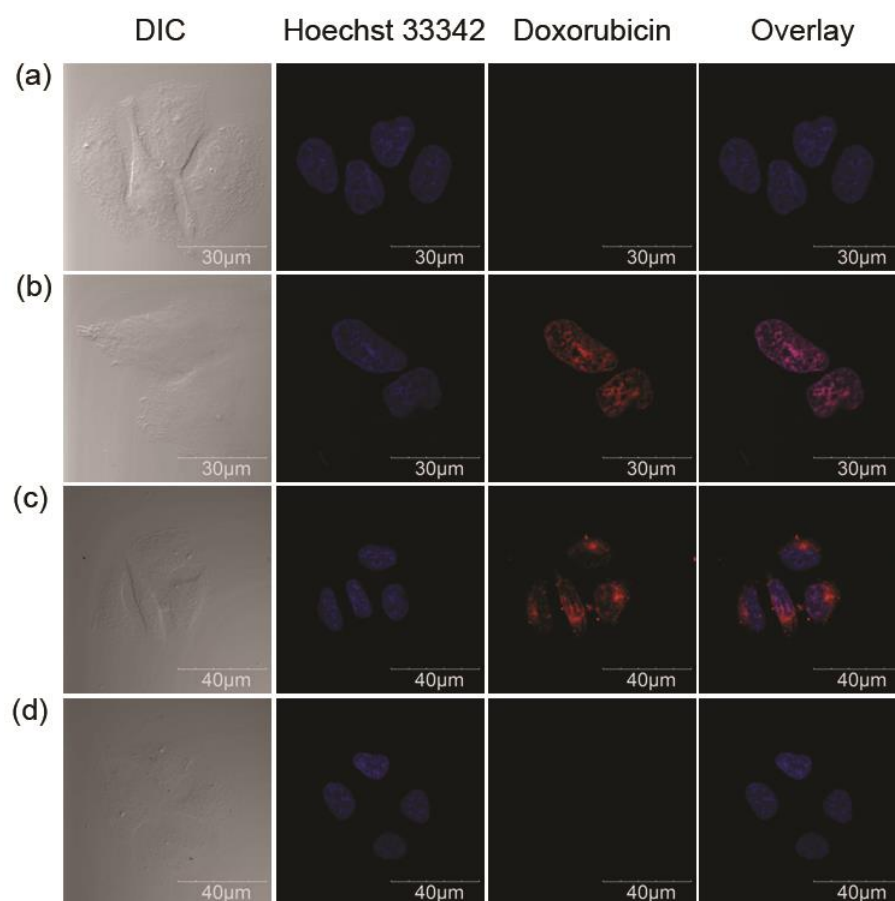


**Figure 37.** Merged fluorescence image of Ishikawa cells (a) untreated (control), and exposed to (b) Doxo, (c) [23·MWCNT<sub>c</sub>(RGDfK)] (d) [23·MWCNT<sub>c</sub>(RGDfK)] added to fixed/stained untreated cells as background control

### 6.3.5 Investigating the Reduction of Asymmetric Platinum(IV) Bis-Carboxylate **23**

To validate our hypothesis that complex **23** went through cellular reduction to yield Doxo-succinate conjugate resulting in a lower anti-proliferative profile, **23** was added to 3 mM ascorbic acid and monitored by RP-HPLC ( $\lambda_{500}$ ). The retention time of **23** was observed at 15.2 min on the HPLC chromatogram. Upon mixing with 3 mM ascorbic acid, a new peak with a retention time at 10.2 min appeared after 1 hour (Figure 38). ESI/MS analysis of the peak corresponding to retention time at 10.2 min showed the parent ion peak with m/z of 666 in the positive mode and 642 in the negative mode. These peaks corresponded to the  $[\text{Doxo-succinate} + \text{Na}]^+$  and  $[\text{Doxo-succinate} - \text{H}]^-$  respectively. The presence of the free carboxylic acid group would lead to the formation of a charged species upon dissociation of the acidic carboxylic proton and be repelled from the hydrophobic cellular membrane leading to lower efficacy, as observed previously for complexes **4** and **5** (Chapter 4, Table 2). To overcome this, a platinum(IV)-Doxo conjugate prodrug with a new linker that could allow the indiscriminate formation of free Doxo upon reduction could be designed and would be the subject of a new investigation.

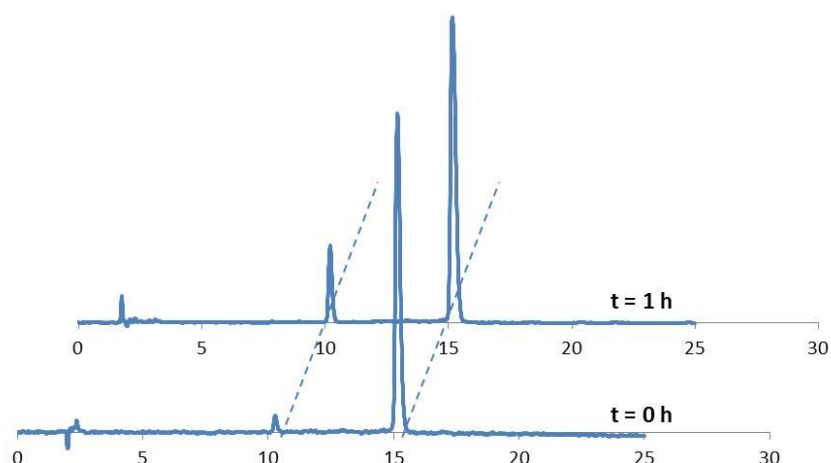


**Figure 38.** RP-HPLC Chromatograms depicting the reduction of complex **23** in 3 mM ascorbic acid

## 6.4 Summary

With the goal of delivering drug combinations in exact ratiometric proportions against targeted cancers, a nanodelivery platform that releases cisplatin and a Doxo-derivate when internalized in cancer cells has been developed. To accomplish this, we design a water-dispersible non-cytotoxic MWCNT-based drug delivery platform that is surface-functionalized with integrin-targeting peptide groups. We also develop a hydrophobic asymmetric platinum(IV) bis-carboxylate, based on the cisplatin template and conjugated to Doxo, that can be stably entrapped within the MWCNT interior cavity. To release the drug entities, we exploit the intracellular reductive environment to activate the platinum(IV) scaffold. Because the reduced product cisplatin and Doxo-derivate are intrinsically hydrophilic,

they are efficiently released from MWCNT platform. We have also demonstrated that controlled drug release can be triggered under reducing conditions particularly after the constructs are taken up in cells. These drug-loaded nano-constructs are also highly efficacious *in vitro* especially against endometrial adenocarcinoma cells. This strategy paves the way for the development of combination therapy regimens with precise molecular formulations at the target site for enhanced therapeutic effects.

## 6.5 Experimental Procedures

Unless otherwise noted, all procedures were carried out without taking precautions to exclude air and moisture. All solvents and chemicals were used as received without further treatment. Platinum(IV) complex **22** was synthesized as described in Chapter 3. Doxorubicin was purchased from Merlin Chemicals Ltd. c(RGDfK) peptide was purchased from ChinaPeptides Co. Ltd. RPMI 1640 medium was purchased from Invitrogen (Carlsbad, CA, USA). 2,2'-(Ethylenedioxy)diethylamine and dextran-coated charcoal were obtained from Sigma Aldrich. Penicillin, streptomycin and thiazolyl blue tetrazolium bromide (MTT) were all obtained from Sigma Chemical Co (St. Louis, MO, USA). Fetal bovine serum (FBS) was from Hyclone (Thermo Scientific Inc., Logan, UT, USA). DMEM nutrient mix F12 and antibiotic-antimycotic were obtained from Life Technologies. The water used was of Milli-Q grade purified by a Milli-Q UV Purification System (Sartorius Stedim Biotech S.A., Aubagne Cedex, France). All

other solvents and chemicals were of analytical grade or HPLC grade obtained from commercial sources.

**Instrumentation.**  $^1\text{H}$  NMR spectra were recorded on a Bruker AMX 500 spectrometer and the chemical shifts ( $\delta$ ) were internally referenced by the residual solvent signals relative to tetramethylsilane. Mass spectra were measured using a Finnigan MAT LCQ ion trap ESI mass spectrometer. UV spectra were recorded on a Shimadzu UV-1800 UV spectrophotometer using 1 cm path-length quartz cuvettes. Platinum concentration determination was performed using Inductively-Coupled Plasma Optical Emission Spectroscopy (ICP-OES) by CMMAC, NUS. Elemental analyses of selected platinum compounds were carried out on the Perkin-Elmer PE 2400 elemental analyzer by CMMAC, NUS.

**Synthesis of Complex 23.** Compound **22** (20 mg, 37.2  $\mu\text{mol}$ ) and Doxo-HCl (30 mg, 51.7  $\mu\text{mol}$ ) were stirred at r.t. in dried DMSO (5 mL) for 24 h. HBTU (21 mg, 55.8  $\mu\text{mol}$ ) was also added to the solution mixture followed by catalytic amounts of triethylamine. The crude solution mixture was concentrate to 2 mL and precipitated by adding to excess water (20 mL). The residue was washed with water (3x5 mL) and acetone (3x5 mL). The residue was re-dissolved in DMF (2 mL) and re-precipitated by adding to excess diethyl ether (20 mL). The precipitate was washed with diethyl ether (3x5 mL), dried *in vacuo*, to yield **23** as a dark red product. Yield: 27 mg (68%).  $^1\text{H}$  NMR (500 MHz, DMSO- $d_6$ ):  $\delta$  7.85 (br, 3 H, Ar-H), 7.61 (d, 2H, Ar-H), 7.50 (d, 1H, Ar-H), 7.40 (t, 2H, Ar-H), 6.59 (br, 6 H,

NH<sub>3</sub>), 5.43 (s, 1H, OCHO), 5.21 (s, 1H), 4.91 (s, 1H), 4.87 (t, 1H, CHCH<sub>3</sub>), 4.74 (d, 1H), 4.58 (d, 2H, CH<sub>2</sub>OH), 4.17 (d, 1H), 3.96 (s, 3H, OCH<sub>3</sub>; s, 1H), 2.99 (m, 2 H, CH<sub>2</sub>) 2.43 (t, 2H, CH<sub>2</sub>), 2.28 (t, 2H, CH<sub>2</sub>), 2.20 (d, 1 H), 2.09 (d, 1H), 1.85 (d, 1H), 1.42 (d, 1H), 1.12 (d, 3H, CH<sub>3</sub>). ESI-MS (-ve mode):  $m/z = 1061.99$  [M-H]<sup>-</sup>. Anal. Calcd.: C, 42.91; H, 4.07; N, 3.95. Found: C, 42.95; H, 4.20; N, 3.78.

**Preparation of MWCNT<sub>TEG</sub>.** Pristine MWCNTs were oxidised and purified as described in previous reported procedure.<sup>194</sup> As-prepared MWCNT<sub>oxidized</sub> (9.7 mg) were dispersed in DMF and sonicated for 5 min. TEG (111 μmol), NHS (45 μmol), EDC·HCl (112 μmol), and DIPEA (112 μmol) were added in the suspension. The mixture was heated at 60 °C for 24 h and filtered through a hydrophilic PTFE membrane (MWCO 0.22 μm). The residue was washed with DMF and deionized water, and dried *in vacuo* to yield MWCNT<sub>TEG</sub>. The degree of amino-functionalization per gram of MWCNT<sub>TEG</sub> (amino-loading) was calculated through quantitative Kaiser Test.<sup>195</sup> As-prepared MWCNT<sub>TEG</sub> (ca. 100 μg) was incubated with 75 μL of 4 g/mL phenol in EtOH, 100 μL of 0.02 mM KCN in pyridine, and 75 μL of ninhydrin in EtOH at 100°C for 7 min. After heating, the reaction was diluted with 60% EtOH to 5 mL, and the UV absorbance at 570 nm. The amount of -NH<sub>2</sub> groups (μmol/g in MWCNT<sub>amine</sub>) was calculated using the following equation:

$$\text{Amino amount } (\mu\text{mol/g}) = \frac{A_{570 \text{ nm}} \times 5 \times 10^6}{W \times 15000}$$

where  $A_{570 \text{ nm}}$  is the absorbance at the wavelength 570 nm; W is the weight of analysed nanotube sample (mg). Using this protocol,  $\text{MWCNT}_{\text{TEG}}$  was ascertained to contain 680  $\mu\text{mol}$  of  $\text{NH}_2$  groups/g  $\text{MWCNT}_{\text{TEG}}$ .

**Preparation of  $\text{MWCNT}_{\text{TEG-COOH}}$ .**  $\text{MWCNT}_{\text{TEG}}$  (10.0 mg) were dispersed in DMSO (3 mL) under sonication (5 min). Succinic anhydride (1.0 g) was then added to the suspension and the reaction mixture was allowed to stir at r.t. for 3 d. The reaction mixture was filtered, washed with DMSO (3 x 5 mL) and dialysed in water for 24 h to remove any unreacted succinic anhydride. Quantitative Kaiser Test (see preparation of  $\text{MWCNT}_{\text{TEG}}$ ) on  $\text{MWCNT}_{\text{TEG-COOH}}$  yielded a negative result indicating complete reaction of the amine groups.

**Preparation of  $\text{MWCNT}_{\text{c(RGDfk)}}$ .**  $\text{MWCNT}_{\text{TEG-COOH}}$  (5.0 mg) were dispersed in dried DMF (3 mL) under sonication (5 min). c(RGDfk) (30.0 mg, 50  $\mu\text{mol}$ ) was then added to the suspension followed by the addition of HBTU (19.0 mg, 50  $\mu\text{mol}$ ) and catalytic amounts of triethylamine. The reaction mixture was allowed to stir for 2 d at r.t., filtered, and washed with DMF (3 x 5 mL). The residue was then washed with diethyl ether (3 x 5 mL) and dried *in vacuo*. Final weight of the  $\text{MWCNT}_{\text{c(RGDfk)}}$  synthesized was found to be 7.7 mg.

**Entrapment of Doxo in  $\text{MWCNT}_{\text{TEG}}$  [ $\text{Doxo}\cdot\text{MWCNT}_{\text{TEG}}$ ].** 4.5 mg of Doxo and 2.2 mg of  $\text{MWCNT}_{\text{TEG}}$  were mixed in 1.5 mL of  $\text{CHCl}_3$  under a brief sonication. The mixture was stirred at room temperature for 5 d, filtered through PTFE membrane, and washed with deionized  $\text{H}_2\text{O}$  to remove unbound Doxo. The



product was recovered from PTFE membrane by dissolving in diethyl ether, and the suspension was centrifuged to discard the supernatant. The precipitating product  $\text{MWCNT}_{\text{TEG}}\text{-DOX}$  was dried *in vacuo* and found to be 2.9 mg. However, the exact loading of  $[\text{DOXO}\cdot\text{MWCNT}_{\text{TEG}}]$  could not be determined due to possible loss of materials through washing and presence of solvent molecules.

**Entrapment of 23 in  $\text{MWCNT}_{\text{TEG}}$  [ $23\cdot\text{MWCNT}_{\text{TEG}}$ ].** Complex **23** (5.0 mg) and  $\text{MWCNT}_{\text{TEG}}$  (1.9 mg) were suspended in  $\text{H}_2\text{O}$  (1.5 mL) under a brief sonication. The mixture was stirred at r.t. for 5 d, filtered through PTFE membrane, washed with  $\text{CHCl}_3\text{:MeOH:H}_2\text{O}$  (2:2.5:1 v/v). The product formed  $[23\cdot\text{MWCNT}_{\text{TEG}}]$  was dried *in vacuo*. The Pt content was ascertained to be  $24.3 \pm 0.8\%$  w/w as analysed using TGA and ICP-OES.

**Entrapment of 23 in  $\text{MWCNT}_{\text{c(RGDfK)}}$  [ $23\cdot\text{MWCNT}_{\text{c(RGDfK)}}$ ].** Complex **23** (3.0 mg) and  $\text{MWCNT}_{\text{TEG}}$  (2.0 mg) were suspended in  $\text{H}_2\text{O}$  (1.5 mL) under a brief sonication. The mixture was stirred at r.t. for 5 d, filtered through PTFE membrane, washed with  $\text{CHCl}_3\text{:MeOH:H}_2\text{O}$  (2:2.5:1 v/v). The product formed  $[23\cdot\text{MWCNT}_{\text{c(RGDfK)}}$ ] was dried *in vacuo*. The Pt content was ascertained to be  $24.5 \pm 1.0\%$  w/w as analysed using TGA and ICP-OES.

**Quantification of entrapped platinum complexes by TGA and ICP-OES.** The samples were heat in air at a heating rate of  $10^\circ\text{C}/\text{min}$  until a final temperature of

1000°C was reached. The remaining residue was dissolved in *aqua regia* and diluted with 2% HNO<sub>3</sub> for ICP-OES determination of Pt levels.

**Doxo Release Experiment.** [Doxo·MWCNT<sub>TEG</sub>] (< 0.1 mg) was suspended in deionized H<sub>2</sub>O (150 µL), transferred to a dialysis button, and immersed in deionized H<sub>2</sub>O (10 mL) to evaluate its stability in H<sub>2</sub>O. [23·MWCNT<sub>TEG</sub>] (1.5 mg) was suspended in deionized H<sub>2</sub>O (300 µL), transferred equally to two release buttons (150 µL each), followed by immersion in 10 deionized H<sub>2</sub>O (10 mL) and aq. ascorbic acid solution (3 mM, 10 mL), separately. For each experiment, the dialysis media was replaced at 20 min, 40 min, 1 h, 2 h, 4 h, 6 h, 9 h, 12 h, 24 h, 48 h, 72 h, 96 h after the immersion and their UV absorbance determined at 500 nm (corresponding to Doxo  $\lambda_{\max}$ ). Because loading of [Doxo·MWCNT<sub>TEG</sub>] could not be determined, the time-point at 96 h was approximated as terminal release.

**Tissue Culture.** A2780 and A2780/Cis were cultured in complete RPMI 1640 medium containing 100 units/mL penicillin, 100 µg/mL streptomycin and 10% fetal bovine serum (FBS). In order to maintain resistance, 1 µM cisplatin need to be added to the media for A2780/Cis every 2-3 passages. The endometrial carcinoma cells Ishikawa (ATCC) was cultured in complete DMEM F12 medium containing 10% FBS pretreated with dextran coated charcoal and 1% antimycotic (100x). The three cell lines were grown at 37°C in a humidified atmosphere of 95% air and 5% CO<sub>2</sub>. Experiments were performed on cells within 20 passages. Viable cells were counted using the Trypan Blue exclusion method.

**Inhibition of cell viability assay.** Drug effects on exponentially growing tumor cells were determined using MTT assay as described in Chapter 4. A2780, A2780/Cis and Ishikawa cells were seeded at a density of 6,000 cells per well in 96-well plates and incubated for 24 h. Cells were exposed to compounds at different concentrations in their respective medium without FBS and antibiotics. These compounds were prepared as DMSO stock solutions and serially diluted with DMSO to a series of decreasing concentrations, before diluting to the required concentrations in culture media. In this manner, all cells were exposed to 1% v/v DMSO, at which negligible cytotoxicity were observed. The cells were incubated with the test compounds for 6 h, replaced with fresh compound-free complete medium (with FBS and antibiotics) and incubated for 66 h. After 72 h following compound administration, the medium was aspirated, replaced with MTT assay solution (100  $\mu$ L, 0.5 mg/mL in PBS) and incubated for a further 4 h at 37°C. The medium was aspirated and the purple formazan precipitate dissolved in DMSO (100  $\mu$ L). Absorbance was measured at a 570 nm using a microplate reader (BioTek). Experiments were performed in triplicates for each concentration and carried out independently at least three times. Cytotoxicity was evaluated with reference to the  $IC_{50}$  value which was defined as the concentration needed for a 50% reduction of survival based on the survival curves.  $IC_{50}$  values were calculated from dose-response curves (cell survival vs. drug concentration) obtained in repeated experiments and adjusted to actual [Pt] administered which was separately determined using ICP-OES.

**Pt uptake in Ishikawa cells.** Ishikawa carcinoma cells were cultured DMEM F12 medium supplemented with 10% FBS and 1% antibiotics. Two samples were prepared namely, [23·MWCNT<sub>c(RGDfK)</sub>] and **23**, both of which are adjusted to 33.0 μM [Pt] concentrations determined from ICP-OES. Ishikawa cells were seeded in 30 mm cell culture dishes at a density of  $3.5 \times 10^6$  cells per dish and the dishes were incubated at 37°C with 5% CO<sub>2</sub> for 48 h prior to treatment with the samples. Cells were exposed to [23·MWCNT<sub>c(RGDfK)</sub>] or **23** in serum-free media for 3 h and replaced with fresh complete media for a further 3 h incubation. Control plates were also carried out during which cells were exposed to serum-free media without addition of the test compounds. After 6 h of incubation, the dishes were placed on ice and cell monolayer was washed with ice-cold PBS (2x5 mL). PBS (1 mL) was added to each dish, and cells were collected with a scraper and counted. The cells were pelleted by centrifugation for 15 min at 4°C. Concentrated HNO<sub>3</sub> (65% v/v, 150 μL) was added to the cells in an uncapped sample vial and heated at 90°C overnight to digest the cells. The digested solution was diluted with MilliQ water (3 mL) prior to ICP-MS analysis.

**Cell culture experiment for confocal studies.** Ishikawa cells were cultured in MEM medium supplemented with 2 mM glutamine, 1% non-essential amino acids (NEAA) and 5% FBS at 37°C with 5% CO<sub>2</sub>. Cells were seeded on cover slip in 6-well plates at a density of  $12 \times 10^4$  cells per mL and incubated 12 h before treatment. During treatment, the medium was replaced with incubation

media containing either blank MWCNT<sub>c(RGDfK)</sub>, (b) DOXO·HCl, (c) **23**, (d) [**23**·MWCNT<sub>c(RGDfK)</sub>] (3 μM [Pt]) in MEM at 37°C with 5% CO<sub>2</sub> for 6 h, as well as untreated controls. After 6 h incubation, the cells were washed twice with PBS, fixed with 4% paraformaldehyde for 15 min, stained with Hoechst 33342 nuclear stain (1.3 μg/mL) and then washed twice with PBS.

**Identification of the Doxo-derivative upon reduction of 23.** Complex **23** was dissolved in 1% DMSO of 3 mM ascorbic acid in 2 mL microtubes, centrifuged and analyzed. The reduction was monitored using analytical HPLC on a Shimadzu Prominence using an Agilent ZORBAX Eclipse Plus column (5 μm, 120 Å, 4.60 x 150 mm, 1.0 mL min<sup>-1</sup> flow) with UV detection at 500 nm. The isocratic eluent conditions were as follows: 60% water and 40% MeCN for 25 mins. The peak corresponding to the Doxo-derivative was collected using fraction collector and analyzed by ESI/MS.

## Chapter 7

### Conclusions

The strategies that have been presented in this dissertation represent a novel methodical approach in rational drug design and development to overcome the current limitations of classical symmetric platinum(IV) bis-carboxylates and FDA approved anticancer drug, cisplatin. Using a non-classical synthetic approach, asymmetric platinum(IV) bis-carboxylates bearing cisplatin pharmacophores were constructed via sequential carboxylation with the aim of being able to fine-tune the overall properties of the prodrugs by varying the ligands in the axial positions. Reduction of this novel class of compounds will result in the concomitant dissociation of the axial ligands leading to the formation of cisplatin. Most of the synthesized compounds represent “proof-of-concepts” based on specific design hypotheses.

The classical symmetric platinum(IV) bis-carboxylates are unable to exhibit good aqueous solubility and lipophilicity simultaneously, which undermine their clinical applications. The development of asymmetric platinum(IV) bis-carboxylates by introducing both lipophilic and hydrophilic ligands in the axial positions resulted in lipophilic prodrugs that are soluble in aqueous media and also exhibited cytotoxicity comparable to cisplatin against human ovarian carcinoma cell lines. Extensive studies on the series of finely-tuned asymmetric platinum(IV) complexes show an inter-properties dependency that affect the

overall efficacies of the prodrugs. These properties include lipophilicity, reduction rate, and cytotoxicity. Understanding these correlations will allow a more effective design and development of platinum(IV) prodrugs suitable for clinical evaluation. Based on our investigations, asymmetric platinum(IV) bis-carboxylate **7** has been selected for further in-depth analysis that include *in vivo* and pharmacokinetic studies due to its good aqueous solubility, lipophilicity, and anti-proliferative properties. In addition, we have also shown that the photoactivatable properties of platinum(IV) complexes can also be fine-tuned by constructing asymmetric platinum(IV) bis-carboxylates with varying axial ligands to achieve the desired  $\lambda_{\text{max}}$ . This represents a strategy of utilizing asymmetric platinum(IV) bis-carboxylate framework to customize anticancer prodrugs with engineered properties.

Other than small organic molecules, it is also possible to conjugate biomolecule in the axial position of platinum(IV) complexes for co-delivery of drugs to achieve synergism in a multi-functional approach. Through asymmetric carboxylation, we have successfully developed a platinum(IV) prodrug, **23**, which consists of exact equivalent of cisplatin and doxorubicin. The other axial ligand serves as a handle to fine-tune the overall property of the compound such as stability<sup>84</sup> and in our example, lipophilicity. The improve lipophilicity of **23** allows favorable entrapment into tumor-targeting MWCNT as delivery platform via hydrophobic-hydrophobic interaction. This increases the potency of **23** against a range of

human carcinoma cell lines, in particular the endometrial adenocarcinoma cells, due to increased drug accumulation arising from a more targeted perspective.

## **7.1 Future Prospect of Platinum-Based Anticancer Drugs**

Since the discovery of cisplatin, more than 10,000 platinum-based complexes have been developed but only 3 of them have obtained FDA-approval. They are cisplatin, carboplatin and oxaliplatin. This extremely low success ratio has fueled concerns over the prospect of platinum-based anticancer agents in the future, especially now that the more renowned platinum-based researchers have slowly shifted their focus to ruthenium-, rhodium- and even osmium-based anticancer agents. In addition, the overly reliance on *in vitro* model to evaluate the efficacies of these novel platinum-based agents with different pharmacophores and DNA-binding affinities reveal little about their mechanisms and does not give accurate and convincing analysis prior to clinical evaluations, resulting in a lack of progress for platinum-based complexes. The search for novel methodologies, chemistry and drug designs to create a niche for oneself in this academic driven field has often neglected existing ones that could be useful in rational drug design against cancers and compromised progress, resulting in a lack of clinical applications.

Moving forward, it is likely we will, or have already, seen a shift of research focus from platinum(II) to platinum(IV) based anticancer complexes. Prodrugs of cisplatin have undergone intensive studies to improve its efficacies, overcome its limitations and even increase its functionalities. Given the well-studied and



established advantages of platinum(IV) prodrugs over their platinum(II) counterparts, the next FDA-approved platinum-based anti-cancer agent may potentially be a platinum(IV) prodrug of cisplatin other than satraplatin, which is still undergoing various clinical evaluations.

In the near future, there could be an increased interest in developing platinum(IV) prodrugs of carboplatin and oxaliplatin, the other two platinum-based FDA approved anticancer drugs. This is especially so for oxaliplatin, which has been recently found to give rise to immunogenic cell deaths, a process whereby cell death leads to the release of damage-associated molecular pattern molecules and triggers the immune system.<sup>196</sup> The ability to fine-tune the pharmacological properties of oxaliplatin prodrugs to further enhance anti-proliferative efficacies against tumor cells would certainly be beneficial for future clinical applications.

Today, the development of platinum-based anticancer drugs stands at a crossroad. The limitations and inadequacies of platinum(II)-based anti-cancer drugs and classical drug development of symmetric platinum(IV) prodrugs are clear, while the non-classical approach in the development of symmetric platinum(IV) complexes is still at its infancy stage. Nonetheless, given the strong interest in this area, advancement in scientific knowledge and analytical tools and an ever increasing cancer population, we are likely to witness greater development in platinum-based anticancer drugs. Whether we see the development of a new class of FDA-approved platinum-based anticancer drugs remain to be seen.

## Bibliography

1. Rosenberg, B.; Van Camp, L.; Krigas, T., Inhibition of Cell Division in *Escherichia coli* by Electrolysis Products from a Platinum Electrode. *Nature* **1965**, *205* (4972), 698-699.
2. Gibson, D., The mechanism of action of platinum anticancer agents-what do we really know about it? *Dalton Trans.*, **2009**, (48), 10681-10689.
3. Galanski, M.; Keppler, B. K., Searching for the Magic Bullet: Anticancer Platinum Drugs Which Can Be Accumulated or Activated in the Tumor Tissue. *Anti-Cancer Agents Med. Chem.*, **2007**, *7*, 55-73.
4. Bosl, G. J.; Motzer, R. J., Testicular Germ-Cell Cancer. *New Engl. J. Med.*, **1997**, *337* (4), 242-254.
5. Horwich, A.; Shipley, J.; Huddart, R., Testicular germ-cell cancer. *Lancet* **2006**, *367* (9512), 754-765.
6. von der Maase, H.; Andersen, L.; Crinò, L.; Weinknecht, S.; Dogliotti, L., Weekly gemcitabine and cisplatin combination therapy in patients with transitional cell carcinoma of the urothelium: A phase II clinical trial. *Ann. Oncol.* **1999**, *10* (12), 1461-1465.
7. Colucci, G.; Labianca, R.; Di Costanzo, F.; Gebbia, V.; Carteni, G.; Massidda, B.; Dapretto, E.; Manzione, L.; Piazza, E.; Sannicolò, M.; Ciaparrone, M.; Cavanna, L.; Giuliani, F.; Maiello, E.; Testa, A.; Pederzoli, P.; Falconi, M.; Gallo, C.; Di Maio, M.; Perrone, F., Randomized Phase III Trial of Gemcitabine Plus Cisplatin Compared With Single-Agent Gemcitabine As First-Line

Treatment of Patients With Advanced Pancreatic Cancer: The GIP-1 Study. *J. Clin. Oncol.* **2010**, *28* (10), 1645-1651.

8. von der Maase, H.; Sengelov, L.; Roberts, J. T.; Ricci, S.; Dogliotti, L.; Oliver, T.; Moore, M. J.; Zimmermann, A.; Arning, M., Long-Term Survival Results of a Randomized Trial Comparing Gemcitabine Plus Cisplatin, With Methotrexate, Vinblastine, Doxorubicin, Plus Cisplatin in Patients With Bladder Cancer. *J. Clin. Oncol.* **2005**, *23* (21), 4602-4608.

9. Giaccone, G.; Ardizzoni, A.; Kirkpatrick, A.; Clerico, M.; Sahnoud, T.; van Zandwijk, N., Cisplatin and etoposide combination chemotherapy for locally advanced or metastatic thymoma. A phase II study of the European Organization for Research and Treatment of Cancer Lung Cancer Cooperative Group. *J. Clin. Oncol.* **1996**, *14* (3), 814-20.

10. Schrijvers, D.; Van Herpen, C.; Kerger, J.; Joosens, E.; Van Laer, C.; Awada, A.; Van den Weyngaert, D.; Nguyen, H.; Le Boudier, C.; Castelijns, J. A.; Kaanders, J.; De Mulder, P.; Vermorken, J. B., Docetaxel, cisplatin and 5-fluorouracil in patients with locally advanced unresectable head and neck cancer: a phase I-II feasibility study. *Ann. Oncol.* **2004**, *15* (4), 638-645.

11. Keil, F.; Selzer, E.; Berghold, A.; Reinisch, S.; Kapp, K. S.; De Vries, A.; Greil, R.; Bachtary, B.; Tinchon, C.; Anderhuber, W.; Burian, M.; Kasperek, A.-K.; Elsässer, W.; Kainz, H.; Riedl, R.; Kopp, M.; Kornek, G., Induction chemotherapy with docetaxel, cisplatin and 5-fluorouracil followed by radiotherapy with cetuximab for locally advanced squamous cell carcinoma of the head and neck. *Eur. J. Cancer* **2013**, *49* (2), 352-359.

12. Hall, M. D.; Okabe, M.; Shen, D.-W.; Liang, X.-J.; Gottesman, M. M., The Role of Cellular Accumulation in Determining Sensitivity to Platinum-Based Chemotherapy\*. *Ann. Rev. Pharm. Toxicol.*, **2008**, *48* (1), 495-535.
13. Jamieson, E. R.; Lippard, S. J., Structure, Recognition, and Processing of Cisplatin–DNA Adducts. *Chem. Rev.*, **1999**, *99* (9), 2467-2498.
14. Fuertes, M. A.; Alonso, C.; Pérez, J. M., Biochemical Modulation of Cisplatin Mechanisms of Action: Enhancement of Antitumor Activity and Circumvention of Drug Resistance. *Chem. Rev.*, **2003**, *103* (3), 645-662.
15. Coste, F.; Malinge, J.-M.; Serre, L.; Leng, M.; Zelwer, C.; Shepard, W.; Roth, M., Crystal structure of a double-stranded DNA containing a cisplatin interstrand cross-link at 1.63 Å resolution: Hydration at the platinated site. *Nucleic Acids Res.*, **1999**, *27* (8), 1837-1846.
16. Takahara, P. M.; Rosenzweig, A. C.; Frederick, C. A.; Lippard, S. J., Crystal structure of double-stranded DNA containing the major adduct of the anticancer drug cisplatin. *Nature* **1995**, *377* (6550), 649-652.
17. Ang, W. H.; Myint, M.; Lippard, S. J., Transcription Inhibition by Platinum–DNA Cross-Links in Live Mammalian Cells. *J. Am. Chem. Soc.*, **2010**, *132* (21), 7429-7435.
18. Jung, Y.; Lippard, S. J., Direct Cellular Responses to Platinum-Induced DNA Damage. *ChemInform* **2007**, *38* (31), no-no.
19. Timerbaev, A. R.; Hartinger, C. G.; Aleksenko, S. S.; Keppler, B. K., Interactions of Antitumor Metallodrugs with Serum Proteins: Advances in

Characterization Using Modern Analytical Methodology. *Chem. Rev.*, **2006**, *106* (6), 2224-2248.

20. Galanski, M.; Jakupec, M. A.; Keppler, B. K., Update of the Preclinical Situation of Anticancer Platinum Complexes: Novel Design Strategies and Innovative Analytical Approaches. *Curr. Med. Chem.*, **2005**, *12* (18), 2075-2094.

21. Kelland, L., The resurgence of platinum-based cancer chemotherapy. *Nat Rev Cancer* **2007**, *7* (8), 573-584.

22. Fuertes, M. A.; Alonso, C.; Pérez, J. M., Biochemical Modulation of Cisplatin Mechanisms of Action: Enhancement of Antitumor Activity and Circumvention of Drug Resistance. *Chem. Rev.* **2003**, *103* (3), 645-662.

23. Judson, I.; Kelland, L., New Developments and Approaches in the Platinum Arena. *Drugs* **2000**, *59* (4), 29-36.

24. Wheate, N. J.; Walker, S.; Craig, G. E.; Oun, R., The status of platinum anticancer drugs in the clinic and in clinical trials. *Dalton Trans.*, **2010**, *39* (35), 8113-8127.

25. Wilson, J. J.; Lippard, S. J., In Vitro Anticancer Activity of cis-Diammineplatinum(II) Complexes with  $\beta$ -Diketonate Leaving Group Ligands. *J. Med. Chem.*, **2012**, *55* (11), 5326-5336.

26. Vijgh, W. F., Clinical Pharmacokinetics of Carboplatin. *Clin. Pharmacokinet.* **1991**, *21* (4), 242-261.

27. Knox, R. J.; Friedlos, F.; Lydall, D. A.; Roberts, J. J., Mechanism of Cytotoxicity of Anticancer Platinum Drugs: Evidence That cis-Diamminedichloroplatinum(II) and cis-Diammine-(1,1-

cyclobutanedicarboxylato)platinum(II) Differ Only in the Kinetics of Their Interaction with DNA. *Cancer Res.*, **1986**, *46* (4 Part 2), 1972-1979.

28. Rixe, O.; Ortuzar, W.; Alvarez, M.; Parker, R.; Reed, E.; Paull, K.; Fojo, T., Oxaliplatin, tetraplatin, cisplatin, and carboplatin: Spectrum of activity in drug-resistant cell lines and in the cell lines of the national cancer institute's anticancer drug screen panel. *Biochem. Pharmacol.*, **1996**, *52* (12), 1855-1865.

29. Hector, S.; Bolanowska-Higdon, W.; Zdanowicz, J.; Hitt, S.; Pendyala, L., In vitro studies on the mechanisms of oxaliplatin resistance. *Cancer Chemother. Pharmacol.* **2001**, *48* (5), 398-406.

30. Fink, D.; Nebel, S.; Aebi, S.; Zheng, H.; Cenni, B.; Nehmé, A.; Christen, R. D.; Howell, S. B., The Role of DNA Mismatch Repair in Platinum Drug Resistance. *Cancer Res.*, **1996**, *56* (21), 4881-4886.

31. Spingler, B.; Whittington, D. A.; Lippard, S. J., 2.4 Å Crystal Structure of an Oxaliplatin 1,2-d(GpG) Intrastrand Cross-Link in a DNA Dodecamer Duplex. *Inorg. Chem.*, **2001**, *40* (22), 5596-5602.

32. Reedijk, J., Improved understanding in platinum antitumour chemistry. *Chem. Commun.*, **1996**, (7), 801-806.

33. Reedijk, J., Why Does Cisplatin Reach Guanine-N7 with Competing S-Donor Ligands Available in the Cell? *Chem. Rev.*, **1999**, *99* (9), 2499-2510.

34. Chin, C.F.; Wong Y. Q. D.; Jothibas, R.; Ang, W.H., Anticancer Platinum (IV) Prodrugs with Novel Modes of Activity. *Curr. Top. Med. Chem.*, **2011**, *11* (21), 2602-2612.

35. Hall, M. D.; Hambley, T. W., Platinum(IV) antitumour compounds: their bioinorganic chemistry. *Coord. Chem. Rev.*, **2002**, 232 (1-2), 49-67.
36. Hall, M. D.; Mellor, H. R.; Callaghan, R.; Hambley, T. W., Basis for Design and Development of Platinum(IV) Anticancer Complexes. *J. Med. Chem.*, **2007**, 50 (15), 3403-3411.
37. Ellis, L.; Er, H.; Hambley, T., The Influence of the Axial Ligands of a Series of Platinum(IV) Anti-Cancer Complexes on Their Reduction to Platinum(II) and Reaction With DNA. *Aust. J. Chem.*, **1995**, 48 (4), 793-806.
38. Battle, A. R.; Deacon, G. B.; Dolman, R. C.; Hambley, T. W., Electrochemistry, Protein Binding and Crystal Structures of Platinum(II) and Platinum(IV) Carboxylato Complexes. *Aust. J. Chem.*, **2002**, 55 (11), 699-704.
39. Choi, S.; Filotto, C.; Bisanzo, M.; Delaney, S.; Lagasee, D.; Whitworth, J. L.; Jusko, A.; Li, C.; Wood, N. A.; Willingham, J.; Schwenker, A.; Spaulding, K., Reduction and Anticancer Activity of Platinum(IV) Complexes. *Inorg. Chem.*, **1998**, 37 (10), 2500-2504.
40. Hall, M. D.; Amjadi, S.; Zhang, M.; Beale, P. J.; Hambley, T. W., The mechanism of action of platinum(IV) complexes in ovarian cancer cell lines. *J. Inorg. Biochem.*, **2004**, 98 (10), 1614-1624.
41. Friedman, H. S.; Krischer, J. P.; Burger, P.; Oakes, W. J.; Hockenberger, B.; Weiner, M. D.; Falletta, J. M.; Norris, D.; Ragab, A. H.; Mahoney, D. H., Treatment of children with progressive or recurrent brain tumors with carboplatin or iproplatin: a Pediatric Oncology Group randomized phase II study. *J. Clin. Oncol.*, **1992**, 10 (2), 249-56.

42. Goldenberg, A.; Kelsen, D.; Dougherty, J.; Magill, G., Phase II study of CHIP chemotherapy in advanced adenocarcinomas of the upper gastrointestinal tract. *Invest New Drug*, **1990**, *8* (1), 71-75.
43. McGuire, W.; Blessing, J.; Hatch, K.; DiSaia, P., A Phase II study of CHIP in advanced squamous cell carcinoma of the cervix (a Gynecologic Oncology Group study). *Invest New Drug*, **1986**, *4* (2), 181-186.
44. Lira-Puerto, V.; Silva, A.; Morris, M.; Martinez, R.; Groshen, S.; Morales-Canfield, F.; Tenorio, F.; Muggia, F., Phase II trial of carboplatin or iproplatin in cervical cancer. *Cancer Chemother. Pharmacol.*, **1991**, *28* (5), 391-396.
45. Kelland, L. R.; Abel, G.; McKeage, M. J.; Jones, M.; Goddard, P. M.; Valenti, M.; Murrer, B. A.; Harrap, K. R., Preclinical Antitumor Evaluation of Bis-acetato-ammine-dichloro-cyclohexylamine Platinum(IV): an Orally Active Platinum Drug. *Cancer Res.*, **1993**, *53* (11), 2581-2586.
46. Samimi, G.; Howell, S., Modulation of the cellular pharmacology of JM118, the major metabolite of satraplatin, by copper influx and efflux transporters. *Cancer Chemother. Pharmacol.*, **2006**, *57* (6), 781-788.
47. Choy, H., Satraplatin: an orally available platinum analog for the treatment of cancer. *Expert Rev. Anticancer Ther.*, **2006**, *6* (7), 973-982.
48. Sternberg CN, W. P., Hetherington J, Paluchowska B, Slee PH, Vekemans K, Van Erps P, Theodore C, Koriakine O, Oliver T, Lebwohl D, Debois M, Zurlo A, Collette L, Phase III trial of satraplatin, an oral platinum plus prednisone vs. prednisone alone in patients with hormone-refractory prostate cancer. *Oncology* **2005**, *68* (1), 2-9.



49. Kauffman, G. B.; Slusarczuk, G.; Kirschner, S., cis- and trans-Tetrachlorodiammineplatinum(IV). In *Inorganic Syntheses*, John Wiley & Sons, Inc.: 2007; pp 236-238.
50. Bulten, E. J.; Verbeek, F., *U.S. Patent 4482569* **1984**.
51. Tschugájeff, L.; Chlopin, W.; Fritzmann, E., Über Oxydation von Komplexverbindungen des Platins. Abhandlung I. Oxydation durch Wasserstoffsperoxyd und Ozon. *Z. Anorg. Allg. Chem.*, **1926**, *151* (1), 253-268.
52. Wilson, J. J.; Lippard, S. J., Synthetic Methods for the Preparation of Platinum Anticancer Complexes. *Chem. Rev.*, **2013**, *114* (8), 4470-4495.
53. Shamsuddin, S.; van Hal, J. W.; Stark, J. L.; Whitmire, K. H.; Khokhar, A. R., Synthesis and Characterization of Novel Axial Dichloroplatinum(IV) Cisplatin Analogues: Crystal Structure of an Axial Dichloro Complex [Pt(cis-1,4-DACH)(trans-Cl<sub>2</sub>)(CBDCA)]·1/2MeOH. *Inorg. Chem.*, **1997**, *36* (25), 5969-5971.
54. Chung, T.; Na, Y.; Kang, S.; Jung, O.-S.; Lee, Y.-A., Facile generation of platinum(IV) compounds with mixed labile moieties. Hydrogen peroxide oxidation of platinum(II) to platinum(IV) compounds. *Transition Met. Chem.*, **2005**, *30* (5), 541-545.
55. Feazell, R. P.; Nakayama-Ratchford, N.; Dai, H.; Lippard, S. J., Soluble Single-Walled Carbon Nanotubes as Longboat Delivery Systems for Platinum(IV) Anticancer Drug Design. *J. Am. Chem. Soc.*, **2007**, *129* (27), 8438-8439.

56. Lee, Y.-A.; Ho Yoo, K.; Jung, O.-S., Oxidation of Pt(II) to Pt(IV) complex with hydrogen peroxide in glycols. *Inorg. Chem. Commun.*, **2003**, 6 (3), 249-251.
57. Pichler, V.; Heffeter, P.; Valiahdi, S. M.; Kowol, C. R.; Egger, A.; Berger, W.; Jakupec, M. A.; Galanski, M.; Keppler, B. K., Unsymmetric Mono- and Dinuclear Platinum(IV) Complexes Featuring an Ethylene Glycol Moiety: Synthesis, Characterization, and Biological Activity. *J. Med. Chem.*, **2012**, 55 (24), 11052-11061.
58. Lee, Y.-a.; Myung jung, S.; Won kang, S.; Jung, O.-s., Hydrogen peroxide oxidation of di(hydroxo)platinum(II) species in carboxylic acids. *Transition Met. Chem.*, **2004**, 29 (7), 710-713.
59. Zhang, J. Z.; Bonnitca, P.; Wexselblatt, E.; Klein, A. V.; Najajreh, Y.; Gibson, D.; Hambley, T. W., Facile Preparation of Mono-, Di- and Mixed-Carboxylato Platinum(IV) Complexes for Versatile Anticancer Prodrug Design. *Chem. Eur. J.*, **2013**, 19 (5), 1672-1676.
60. Johnstone, T. C.; Wilson, J. J.; Lippard, S. J., Monofunctional and Higher-Valent Platinum Anticancer Agents. *Inorg. Chem.*, **2013**, 52 (21), 12234-12249.
61. Barnard, C. F. J.; Vollano, J. F.; Chaloner, P. A.; Dewa, S. Z., Studies on the Oral Anticancer Drug JM-216: Synthesis and Characterization of Isomers and Related Complexes. *Inorg. Chem.*, **1996**, 35 (11), 3280-3284.
62. Littlefield, S. L.; Baird, M. C.; Anagnostopoulou, A.; Raptis, L., Synthesis, Characterization and Stat3 Inhibitory Properties of the Prototypical

Platinum(IV) Anticancer Drug, [PtCl<sub>3</sub>(NO<sub>2</sub>)(NH<sub>3</sub>)<sub>2</sub>] (CPA-7). *Inorg. Chem.*, **2008**, *47* (7), 2798-2804.

63. Ravera, M.; Gabano, E.; Pelosi, G.; Fregonese, F.; Tinello, S.; Osella, D., A New Entry to Asymmetric Platinum(IV) Complexes via Oxidative Chlorination. *Inorg. Chem.*, **2014**, *53* (17), 9326-9335.

64. Giandomenico, C. M.; Abrams, M. J.; Murrer, B. A.; Vollano, J. F.; Rheinheimer, M. I.; Wyer, S. B.; Bossard, G. E.; Higgins, J. D., Carboxylation of Kinetically Inert Platinum(IV) Hydroxy Complexes. An Entry into Orally Active Platinum(IV) Antitumor Agents. *Inorg. Chem.*, **1995**, *34* (5), 1015-1021.

65. Galanski, M.; Keppler, B. K., Carboxylation of Dihydroxoplatinum(IV) Complexes via a New Synthetic Pathway. *Inorg. Chem.*, **1996**, *35* (6), 1709-1711.

66. Wilson, J. J.; Lippard, S. J., Synthesis, Characterization, and Cytotoxicity of Platinum(IV) Carbamate Complexes. *Inorg. Chem.*, **2011**, *50* (7), 3103-3115.

67. Cowens, J. W.; Stevie, F. A.; Alderfer, J. L.; Hansen, G. E.; Pendyala, L.; Creaven, P. J., Synthesis and identification of derivatives of a platinum containing complex. *Int. J. Mass Spec. Ion Phy.*, **1983**, *48* (0), 177-180.

68. Perez, J. M.; Camazón, M.; Alvarez-Valdes, A.; Quiroga, A. G.; Kelland, L. R.; Alonso, C.; Navarro-Ranninger, M. C., Synthesis, characterization and DNA modification induced by a novel Pt(IV)-bis(monoglutarate) complex which induces apoptosis in glioma cells. *Chem.-Biol. Interact.*, **1999**, *117* (2), 99-115.

69. Alvarez-Valdés, A.; Pérez, J. M.; López-Solera, I.; Lannegrand, R.; Contente, J. M.; Amo-Ochoa, P.; Camazón, M. J.; Solans, X.; Font-Bardía, M.; Navarro-Ranninger, C., Preparation and Characterization of Platinum(II) and (IV)

Complexes of 1,3-Diaminepropane and 1,4-Diaminebutane: Circumvention of Cisplatin Resistance and DNA Interstrand Cross-Link Formation in CH1cisR Ovarian Tumor Cells. *J. Med. Chem.*, **2002**, *45* (9), 1835-1844.

70. Reithofer, M.; Galanski, M.; Roller, A.; Keppler, B. K., An Entry to Novel Platinum Complexes: Carboxylation of Dihydroxoplatinum(IV) Complexes with Succinic Anhydride and Subsequent Derivatization. *Eur. J. Inorg. Chem.*, **2006**, *2006* (13), 2612-2617.

71. Reithofer, M. R.; Bytzek, A. K.; Valiahdhi, S. M.; Kowol, C. R.; Groessl, M.; Hartinger, C. G.; Jakupec, M. A.; Galanski, M.; Keppler, B. K., Tuning of lipophilicity and cytotoxic potency by structural variation of anticancer platinum(IV) complexes. *J. Inorg. Biochem.*, **2011**, *105* (1), 46-51.

72. Barnes, K. R.; Kutikov, A.; Lippard, S. J., Synthesis, Characterization, and Cytotoxicity of a Series of Estrogen-Tethered Platinum(IV) Complexes. *Chembiol.*, **2004**, *11* (4), 557-564.

73. Mukhopadhyay, S.; Barnés, C. M.; Haskel, A.; Short, S. M.; Barnes, K. R.; Lippard, S. J., Conjugated Platinum(IV)-Peptide Complexes for Targeting Angiogenic Tumor Vasculature. *Bioconjugate Chem.*, **2007**, *19* (1), 39-49.

74. Wong, D. Y. Q.; Lau, J. Y.; Ang, W. H., Harnessing chemoselective imine ligation for tethering bioactive molecules to platinum(iv) prodrugs. *Dalton Trans.*, **2012**, *41* (20), 6104-6111.

75. Aryal, S.; Hu, C.-M. J.; Zhang, L., Polymer-Cisplatin Conjugate Nanoparticles for Acid-Responsive Drug Delivery. *ACS Nano*, **2009**, *4* (1), 251-258.

76. Pichler, V.; Mayr, J.; Heffeter, P.; Domotor, O.; Enyedy, E. A.; Hermann, G.; Groza, D.; Kollensperger, G.; Galanski, M.; Berger, W.; Keppler, B. K.; Kowol, C. R., Maleimide-functionalised platinum(IV) complexes as a synthetic platform for targeted drug delivery. *Chem. Commun.*, **2013**, 49 (22), 2249-2251.
77. Kizu, R.; Nakanishi, T.; Hayakawa, K.; Matsuzawa, A.; Eriguchi, M.; Takeda, Y.; Akiyama, N.; Tashiro, T.; Kidani, Y., A new orally active antitumor 1R,2R-cyclohexanediamine-platinum(IV) complex: trans-(n-valerato)chloro(1R,2R-cyclohexanediamine) (oxalato)platinum(IV). *Cancer Chemother. Pharmacol.* **1999**, 43 (2), 97-105.
78. Wang, D.; Lippard, S. J., Cellular processing of platinum anticancer drugs. *Nat. Rev. Drug Discov.*, **2005**, 4 (4), 307-320.
79. Chin, C. F.; Tian, Q.; Setyawati, M. I.; Fang, W.; Tan, E. S. Q.; Leong, D. T.; Ang, W. H., Tuning the Activity of Platinum(IV) Anticancer Complexes through Asymmetric Acylation. *J. Med. Chem.*, **2012**, 55 (17), 7571-7582.
80. Pichler, V.; Valiahdi, S. M.; Jakupec, M. A.; Arion, V. B.; Galanski, M.; Keppler, B. K., Mono-carboxylated diaminedichloridoplatinum(IV) complexes - selective synthesis, characterization, and cytotoxicity. *Dalton Trans.*, **2011**, 40 (32), 8187-8192.
81. Chin, C. F.; Yap, S. Q.; Li, J.; Pastorin, G.; Ang, W. H., Ratiometric delivery of cisplatin and doxorubicin using tumour-targeting carbon-nanotubes entrapping platinum(IV) prodrugs. *Chem. Sci.*, **2014**, 5 (6), 2265-2270.

82. Dhar, S.; Daniel, W. L.; Giljohann, D. A.; Mirkin, C. A.; Lippard, S. J., Polyvalent Oligonucleotide Gold Nanoparticle Conjugates as Delivery Vehicles for Platinum(IV) Warheads. *J. Am. Chem. Soc.*, **2009**, *131* (41), 14652-14653.
83. Xiao, H.; Yan, L.; Zhang, Y.; Qi, R.; Li, W.; Wang, R.; Liu, S.; Huang, Y.; Li, Y.; Jing, X., A dual-targeting hybrid platinum(iv) prodrug for enhancing efficacy. *Chem. Commun.*, **2012**, *48* (87), 10730-10732.
84. Wong, D. Y. Q.; Yeo, C. H. F.; Ang, W. H., Immuno-Chemotherapeutic Platinum(IV) Prodrugs of Cisplatin as Multimodal Anticancer Agents. *Angew. Chem. Int. Ed.*, **2014**, *53* (26), 6752-6756.
85. Arnott, J. A.; Planey, S. L., The influence of lipophilicity in drug discovery and design. *Exp. Opin. Drug Discov.*, **2012**, *7* (10), 863-875.
86. Hanessian, S.; Zhan, L.; Bovey, R.; Saavedra, O. M.; Juillerat-Jeanneret, L., Functionalized Glycomers as Growth Inhibitors and Inducers of Apoptosis in Human Glioblastoma Cells. *J. Med. Chem.*, **2003**, *46* (17), 3600-3611.
87. Fiaux, H.; Popowycz, F.; Favre, S.; Schütz, C.; Vogel, P.; Gerber-Lemaire, S.; Juillerat-Jeanneret, L., Functionalized Pyrrolidines Inhibit  $\alpha$ -Mannosidase Activity and Growth of Human Glioblastoma and Melanoma Cells. *J. Med. Chem.*, **2005**, *48* (13), 4237-4246.
88. Platts, J. A.; Hibbs, D. E.; Hambley, T. W.; Hall, M. D., Calculation of the Hydrophobicity of Platinum Drugs. *J. Med. Chem.*, **2000**, *44* (3), 472-474.
89. Reithofer, M. R.; Valiahdi, S. M.; Jakupec, M. A.; Arion, V. B.; Egger, A.; Galanski, M.; Keppler, B. K., Novel Di- and Tetracarboxylatoplatinum(IV)

Complexes. Synthesis, Characterization, Cytotoxic Activity, and DNA Platination. *J. Med. Chem.*, **2007**, *50* (26), 6692-6699.

90. Reithofer, M. R.; Schwarzinger, A.; Valiahdi, S. M.; Galanski, M.; Jakupec, M. A.; Keppler, B. K., Novel bis(carboxylato)dichlorido(ethane-1,2-diamine)platinum(IV) complexes with exceptionally high cytotoxicity. *J. Inorg. Biochem.*, **2008**, *102* (12), 2072-2077.

91. Kostova, I., Platinum Complexes as Anticancer Agents. *Recent Pat. Anti-Canc.*, **2006**, *1* (1), 1-22.

92. Jolley, J. N.; Yanovsky, A. I.; Kelland, L. R.; Nolan, K. B., Synthesis and antitumour activity of platinum(II) and platinum(IV) complexes containing ethylenediamine-derived ligands having alcohol, carboxylic acid and acetate substituents: Crystal and molecular structure of [PtL4Cl2]·H2O where L4 is ethylenediamine-N,N'-diacetate. *J. Inorg. Biochem.*, **2001**, *83* (2-3), 91-100.

93. Choi, S.; Filotto, C.; Bisanzo, M.; Delaney, S.; Lagasee, D.; Whitworth, J. L.; Jusko, A.; Li, C.; Wood, N. A.; Willingham, J.; Schwenker, A.; Spaulding, K., Reduction and Anticancer Activity of Platinum(IV) Complexes. *Inorg. Chem.*, **1998**, *37* (10), 2500-2504.

94. Battle, A. R.; Deacon, G. B.; Dolman, R. C.; Hambley, T. W., Electrochemistry, Protein Binding and Crystal Structures of Platinum(II) and Platinum(IV) Carboxylato Complexes. *Aust. J. Chem.*, **2002**, *55* (11), 699-704.

95. Reithofer, M. R.; Bytzek, A. K.; Valiahdi, S. M.; Kowol, C. R.; Groessl, M.; Hartinger, C. G.; Jakupec, M. A.; Galanski, M.; Keppler, B. K., Tuning of

Lipophilicity and Cytotoxic Potency by Structural Variation of Anticancer Platinum(IV) Complexes. *J. Inorg. Biochem.*, **2011**, *105* (1), 46-51.

96. Wilson, J. J.; Lippard, S. J., Synthesis, Characterization, and Cytotoxicity of Platinum(IV) Carbamate Complexes. *Inorg. Chem.*, **2011**, *50* (7), 3103-3115.

97. Kizu, R.; Nakanishi, T.; Miyazaki, M.; Tashiro, T.; Noji, M.; Matsuzawa, A.; Eriguchi, M.; Takeda, Y.; Akiyama, N.; Kidani, Y., An orally active antitumor cyclohexanediamine-Pt(IV) complex: trans,cis,cis-bis(n-valerato)(oxalato)(1R,2R-cyclohexane diamine)Pt(IV). *Anti-cancer drugs*, **1996**, *7* (3), 248-56.

98. Scagliotti, G. V.; Novello, S.; Selvaggi, G., Multidrug resistance in non-small-cell lung cancer. *Ann. Oncol.*, **1999**, *10* (suppl 5), S83-S86.

99. P.V. Shekhar, M., Drug Resistance: Challenges to Effective Therapy. *Curr. Cancer Drug Targets*, **2011**, *11* (5), 613-623.

100. Gottesman, M. M., MECHANISMS OF CANCER DRUG RESISTANCE. *Annu. Rev. Med.*, **2002**, *53* (1), 615-627.

101. Persidis, A., Cancer multidrug resistance. *Nat. Biotech.*, **1999**, *17* (1), 94-95.

102. Bozic, I.; Reiter, J. G.; Allen, B.; Antal, T.; Chatterjee, K.; Shah, P.; Moon, Y. S.; Yaqubie, A.; Kelly, N.; Le, D. T.; Lipson, E. J.; Chapman, P. B.; Diaz, L. A.; Vogelstein, B.; Nowak, M. A., *Evolutionary dynamics of cancer in response to targeted combination therapy*. **2013**; Vol. 2.

103. Agarwal, R.; Kaye, S. B., Ovarian cancer: strategies for overcoming resistance to chemotherapy. *Nat. Rev. Cancer*, **2003**, *3* (7), 502-516.



104. van Iersel, M. L. P. S.; Ploemen, J.-P. H. T. M.; Struik, I.; van Amersfoort, C.; Keyzer, A. E.; Schefferlie, J. G.; van Bladeren, P. J., Inhibition of glutathione S-transferase activity in human melanoma cells by  $\alpha,\beta$ -unsaturated carbonyl derivatives. Effects of acrolein, cinnamaldehyde, citral, crotonaldehyde, curcumin, ethacrynic acid, and trans-2-hexenal. *Chem.-Biol. Interact.*, **1996**, *102* (2), 117-132.
105. Aizawa, S.; Ookawa, K.; Kudo, T.; Asano, J.; Hayakari, M.; Tsuchida, S., Characterization of cell death induced by ethacrynic acid in a human colon cancer cell line DLD-1 and suppression by N-acetyl-l-cysteine. *Cancer Sci.*, **2003**, *94* (10), 886-893.
106. Graf, N.; Mokhtari, T. E.; Papayannopoulos, I. A.; Lippard, S. J., Platinum(IV)-chlorotoxin (CTX) conjugates for targeting cancer cells. *J. Inorg. Biochem.*, **2012**, *110* (0), 58-63.
107. Ruoslahti, E., RGD AND OTHER RECOGNITION SEQUENCES FOR INTEGRINS. *Ann. Rev. Cell Dev. Biol.*, **1996**, *12* (1), 697-715.
108. Quail, D. F.; Joyce, J. A., Microenvironmental regulation of tumor progression and metastasis. *Nat. Med.*, **2013**, *19* (11), 1423-1437.
109. Erdreich-Epstein, A.; Shimada, H.; Groshen, S.; Liu, M.; Metelitsa, L. S.; Kim, K. S.; Stins, M. F.; Seeger, R. C.; Durden, D. L., Integrins  $\alpha\beta 3$  and  $\alpha\beta 5$  Are Expressed by Endothelium of High-Risk Neuroblastoma and Their Inhibition Is Associated with Increased Endogenous Ceramide. *Cancer Res.*, **2000**, *60* (3), 712-721.

110. Ndinguri, M. W.; Solipuram, R.; Gambrell, R. P.; Aggarwal, S.; Hammer, R. P., Peptide Targeting of Platinum Anti-Cancer Drugs. *Bioconjugate Chem.*, **2009**, *20* (10), 1869-1878.
111. Abramkin, S.; Valiahdi, S. M.; Jakupec, M. A.; Galanski, M.; Metzler-Nolte, N.; Keppler, B. K., Solid-phase synthesis of oxaliplatin-TAT peptide bioconjugates. *Dalton Trans.*, **2012**, *41* (10), 3001-3005.
112. Dhar, S.; Lippard, S. J., Mitaplatin, a potent fusion of cisplatin and the orphan drug dichloroacetate. *Proc. Nat. Acad. Sci.*, **2009**, *106* (52), 22199-22204.
113. Wexselblatt, E.; Yavin, E.; Gibson, D., Platinum(IV) Prodrugs with Haloacetato Ligands in the Axial Positions can Undergo Hydrolysis under Biologically Relevant Conditions. *Angew. Chem. Int. Ed.*, **2013**, *52* (23), 6059-6062.
114. Yang, J.; Sun, X.; Mao, W.; Sui, M.; Tang, J.; Shen, Y., Conjugate of Pt(IV)–Histone Deacetylase Inhibitor as a Prodrug for Cancer Chemotherapy. *Mol. Pharm.*, **2012**, *9* (10), 2793-2800.
115. Neumann, W.; Crews, B. C.; Marnett, L. J.; Hey-Hawkins, E., Conjugates of Cisplatin and Cyclooxygenase Inhibitors as Potent Antitumor Agents Overcoming Cisplatin Resistance. *ChemMedChem* **2014**, *9* (6), 1150-1153.
116. Aapro, M. S.; van Wijk, F. H.; Bolis, G.; Chevallier, B.; van der Burg, M. E. L.; Poveda, A.; de Oliveira, C. F.; Tumolo, S.; Scotto di Palumbo, V.; Piccart, M.; Franchi, M.; Zanaboni, F.; Lacave, A. J.; Fontanelli, R.; Favalli, G.; Zola, P.; Guastalla, J. P.; Rosso, R.; Marth, C.; Nooij, M.; Presti, M.; Scarabelli, C.; Splinter, T. A. W.; Ploch, E.; Beex, L. V. A.; ten Bokkel Huinink, W.; Forni, M.;

Melpignano, M.; Blake, P.; Kerbrat, P.; Mendiola, C.; Cervantes, A.; Goupil, A.; Harper, P. G.; Madronal, C.; Namer, M.; Scarfone, G.; Stoot, J. E. G. M.; Teodorovic, I.; Coens, C.; Vergote, I.; Vermorken, J. B., Doxorubicin versus doxorubicin and cisplatin in endometrial carcinoma: definitive results of a randomised study (55872) by the EORTC Gynaecological Cancer Group. *Ann. Oncol.*, **2003**, *14* (3), 441-448.

117. Haag, R.; Kratz, F., Polymer Therapeutics: Concepts and Applications. *Angew. Chem. Int. Ed.*, **2006**, *45* (8), 1198-1215.

118. Duong, H. T. T.; Huynh, V. T.; de Souza, P.; Stenzel, M. H., Core-Cross-Linked Micelles Synthesized by Clicking Bifunctional Pt(IV) Anticancer Drugs to Isocyanates. *Biomacromolecules* **2010**, *11* (9), 2290-2299.

119. Brown, S. D.; Nativo, P.; Smith, J.-A.; Stirling, D.; Edwards, P. R.; Venugopal, B.; Flint, D. J.; Plumb, J. A.; Graham, D.; Wheate, N. J., Gold Nanoparticles for the Improved Anticancer Drug Delivery of the Active Component of Oxaliplatin. *J. Am. Chem. Soc.*, **2010**, *132* (13), 4678-4684.

120. Rieter, W. J.; Pott, K. M.; Taylor, K. M. L.; Lin, W., Nanoscale Coordination Polymers for Platinum-Based Anticancer Drug Delivery. *J. Am. Chem. Soc.*, **2008**, *130* (35), 11584-11585.

121. Chen, H.; Pazicni, S.; Krett, N. L.; Ahn, R. W.; Penner-Hahn, J. E.; Rosen, S. T.; O'Halloran, T. V., Coencapsulation of Arsenic- and Platinum-based Drugs for Targeted Cancer Treatment. *Angew. Chem. Int. Ed.*, **2009**, *48* (49), 9295-9299.

122. Li, J.; Yap, S. Q.; Chin, C. F.; Tian, Q.; Yoong, S. L.; Pastorin, G.; Ang, W. H., Platinum(IV) prodrugs entrapped within multiwalled carbon nanotubes:

Selective release by chemical reduction and hydrophobicity reversal. *Chem. Sci.*, **2012**, 3 (6), 2083-2087.

123. Aryal, S.; Hu, C.-M. J.; Zhang, L., Polymeric Nanoparticles with Precise Ratiometric Control over Drug Loading for Combination Therapy. *Mol. Pharm.*, **2011**, 8 (4), 1401-1407.

124. Nie, S.; Xing, Y.; Kim, G. J.; Simons, J. W., Nanotechnology Applications in Cancer. *Ann. Rev. Biomed. Engin.*, **2007**, 9 (1), 257-288.

125. Dhar, S.; Gu, F. X.; Langer, R.; Farokhzad, O. C.; Lippard, S. J., Targeted delivery of cisplatin to prostate cancer cells by aptamer functionalized Pt(IV) prodrug-PLGA-PEG nanoparticles. *Proc. Nat. Acad. Sci.*, **2008**, 105 (45), 17356-17361.

126. Sanchez-Cano, C.; Hannon, M. J., Novel and emerging approaches for the delivery of metallo-drugs. *Dalton Trans.*, **2009**, (48), 10702-10711.

127. Ajima, K.; Yudasaka, M.; Murakami, T.; Maigné, A.; Shiba, K.; Iijima, S., Carbon Nanohorns as Anticancer Drug Carriers. *Mol. Pharm.*, **2005**, 2 (6), 475-480.

128. Li, J.; Pant, A.; Chin, C. F.; Ang, W. H.; Ménard-Moyon, C.; Nayak, T. R.; Gibson, D.; Ramaprabhu, S.; Panczyk, T.; Bianco, A.; Pastorin, G., In vivo biodistribution of platinum-based drugs encapsulated into multi-walled carbon nanotubes. *Nanomedicine*, **2014**, in press.

129. Yoong, S. L.; Wong, B. S.; Zhou, Q. L.; Chin, C. F.; Li, J.; Venkatesan, T.; Ho, H. K.; Yu, V.; Ang, W. H.; Pastorin, G., Enhanced cytotoxicity to cancer

cells by mitochondria-targeting MWCNTs containing platinum(IV) prodrug of cisplatin. *Biomaterials* **2014**, 35 (2), 748-759.

130. Dhar, S.; Liu, Z.; Thomale, J.; Dai, H.; Lippard, S. J., Targeted Single-Wall Carbon Nanotube-Mediated Pt(IV) Prodrug Delivery Using Folate as a Homing Device. *J. Am. Chem. Soc.*, **2008**, 130 (34), 11467-11476.

131. Aryal, S.; Jack Hu, C.-M.; Fu, V.; Zhang, L., Nanoparticle drug delivery enhances the cytotoxicity of hydrophobic-hydrophilic drug conjugates. *J. Mat. Chem.*, **2012**, 22 (3), 994-999.

132. Min, Y.; Li, J.; Liu, F.; Yeow, E. K. L.; Xing, B., Near-Infrared Light-Mediated Photoactivation of a Platinum Antitumor Prodrug and Simultaneous Cellular Apoptosis Imaging by Upconversion-Luminescent Nanoparticles. *Angew. Chem. Int. Ed.*, **2014**, 53 (4), 1012-1016.

133. British Society for Investigative Dermatology Annual Meeting University of Cambridge 11-13 April 2005 Programme and Abstracts Monday 11 April. *Br. J. Dermatol.*, **2005**, 152 (4), 830-858.

134. Kratochwil, N. A.; Zabel, M.; Range, K.-J.; Bednarski, P. J., Synthesis and X-ray Crystal Structure of trans,cis-[Pt(OAc)<sub>2</sub>I<sub>2</sub>(en)]: A Novel Type of Cisplatin Analog That Can Be Photolyzed by Visible Light to DNA-Binding and Cytotoxic Species in Vitro. *J. Med. Chem.*, **1996**, 39 (13), 2499-2507.

135. Müller, P.; Schröder, B.; Parkinson, J. A.; Kratochwil, N. A.; Coxall, R. A.; Parkin, A.; Parsons, S.; Sadler, P. J., Nucleotide Cross-Linking Induced by Photoreactions of Platinum(IV)-Azide Complexes. *Angew. Chem. Int. Ed.*, **2003**, 42 (3), 335-339.

136. Mackay, F. S.; Woods, J. A.; Moseley, H.; Ferguson, J.; Dawson, A.; Parsons, S.; Sadler, P. J., A Photoactivated trans-Diammine Platinum Complex as Cytotoxic as Cisplatin. *Chem. Eur. J.*, **2006**, *12* (11), 3155-3161.
137. Ley, R. D.; Applegate, L. A.; Stuart, T. D.; Fry, R. J. M., Uv Radiation-Induced Skin Tumors in Monodelphis-Domestica. *Photodermatology* **1987**, *4* (3), 144-147.
138. Ang, W. H.; Pilet, S.; Scopelliti, R.; Bussy, F.; Juillerat-Jeanneret, L.; Dyson, P. J., Synthesis and Characterization of Platinum(IV) Anticancer Drugs with Functionalized Aromatic Carboxylate Ligands: Influence of the Ligands on Drug Efficacies and Uptake. *J. Med. Chem.*, **2005**, *48* (25), 8060-8069.
139. Wexselblatt, E.; Gibson, D., What do we know about the reduction of Pt(IV) pro-drugs? *J. Inorg. Biochem.*, **2012**, *117*, 220-229.
140. Ang, W. H.; Pilet, S.; Scopelliti, R.; Bussy, F.; Juillerat-Jeanneret, L.; Dyson, P. J., Synthesis and Characterization of Platinum(IV) Anticancer Drugs with Functionalized Aromatic Carboxylate Ligands: Influence of the Ligands on Drug Efficacies and Uptake. *J. Med. Chem.*, **2005**, *48* (25), 8060-8069.
141. Galanski, M.; Keppler, B. K., Carboxylation of Dihydroxoplatinum(IV) Complexes via a New Synthetic Pathway. *Inorg. Chem.*, **1996**, *35* (6), 1709-1711.
142. Shi, Y.; Liu, S. A.; Kerwood, D. J.; Goodisman, J.; Dabrowiak, J. C., Pt(IV) Complexes as Prodrugs for Cisplatin. *J. Inorg. Biochem.*, **2012**, *107* (1), 6-14.
143. Still, B. M.; Kumar, P. G. A.; Aldrich-Wright, J. R.; Price, W. S., 195Pt NMR-theory and Application. *Chem. Soc. Rev.*, **2007**, *36* (4), 665-686.

144. Pregosin, P. S., Platinum-195 Nuclear Magnetic Resonance. *Coord. Chem. Rev.*, **1982**, *44* (2), 247-291.
145. Chen, L.; Foo Lee, P.; D. Ranford, J.; J. Vittal, J.; Ying Wong, S., Reduction of the Anti-cancer Drug Analogue *cis,trans,cis*-[PtCl<sub>2</sub>(OCOCH<sub>3</sub>)<sub>2</sub>(NH<sub>3</sub>)<sub>2</sub>] by L-cysteine and L-methionine and its Crystal Structure. *Dalton Trans.*, **1999**, (8), 1209-1212.
146. Perez, J. M.; Camazón, M.; Alvarez-Valdes, A.; Quiroga, A. G.; Kelland, L. R.; Alonso, C.; Navarro-Ranninger, M. C., Synthesis, Characterization and DNA Modification Induced by a Novel Pt(IV)-bis(monoglutarate) Complex which Induces Apoptosis in Glioma Cells. *Chem.-Biol. Interact.*, **1999**, *117* (2), 99-115.
147. Dhara, S., A Rapid Method for the Synthesis of *cis*-[Pt(NH<sub>3</sub>)<sub>2</sub>Cl<sub>2</sub>]. *Indian J. Chem.*, **1970**, *8*, 193-194.
148. *SMART ver. 5.628*, Bruker AXS Inc.: Madison, WI, 2001.
149. *SAINT+ ver. 6.22a*, Bruker AXS Inc.: Madison, WI, 2001.
150. *SADABS ver. 2.10*, Sheldrick G. W.: University of Gottingen, Gottingen, Germany, 2001.
151. *SHELXTL ver. 6.14*, Bruker AXS Inc.: Madison, WI, 2000.
152. Leo, A. J., Calculating Log *P*<sub>oct</sub> from Structures. *Chem. Rev.*, **1993**, *93* (4), 1281-1306.
153. Oldfield, S. P.; Hall, M. D.; Platts, J. A., Calculation of Lipophilicity of a Large, Diverse Dataset of Anticancer Platinum Complexes and the Relation to Cellular Uptake. *J. Med. Chem.*, **2007**, *50* (21), 5227-5237.

154. Platts, J. A.; Hibbs, D. E.; Hambley, T. W.; Hall, M. D., Calculation of the Hydrophobicity of Platinum Drugs. *J. Med. Chem.*, **2000**, *44* (3), 472-474.
155. Song, R.; Kim, K. M.; Sohn, Y. S., Lipophilicity vs. Antitumor Activity of Carboxylatoplatinum(IV) Complexes. *Bull. Kor. Chem. Soc.*, **2000**, *21* (10), 1000-1004.
156. Hansch, C.; Fujita, T.,  $\rho$ - $\sigma$ - $\pi$  Analysis. A Method for the Correlation of Biological Activity and Chemical Structure. *J. Am. Chem. Soc.*, **1964**, *86* (8), 1616-1626.
157. Kaliszan, R.; Haber, P.; Baczek, T.; Siluk, D., Gradient HPLC in the determination of drug lipophilicity and acidity. *Pure Appl. Chem.*, **2001**, *73* (9), 1465-1475.
158. Jones, N. A.; Turner, J.; McIlwrath, A. J.; Brown, R.; Dive, C., Cisplatin- and Paclitaxel-induced Apoptosis of Ovarian Carcinoma Cells and the Relationship between Bax and Bak Up-regulation and the Functional Status of p53. *Mol. Pharmacol.*, **1998**, *53* (5), 819-826.
159. Hall, M. D.; Amjadi, S.; Zhang, M.; Beale, P. J.; Hambley, T. W., The mechanism of action of platinum(IV) complexes in ovarian cancer cell lines. *J. Inorg. Biochem.*, **2004**, *98* (10), 1614-1624.
160. Andrews, P. A.; Wung, W. E.; Howell, S. B., A High-Performance Liquid-Chromatographic Assay with Improved Selectivity for Cisplatin and Active Platinum(II) Complexes in Plasma Ultrafiltrate. *Anal. Biochem.*, **1984**, *143* (1), 46-56.



161. Todd, R. C.; Lippard, S. J., Inhibition of transcription by platinum antitumor compounds. *Metallomics*, **2009**, *1* (4), 280-291.
162. Warnke, U.; Rappel, C.; Meier, H.; Kloft, C.; Galanski, M.; Hartinger, C. G.; Keppler, B. K.; Jaehde, U., Analysis of Platinum Adducts with DNA Nucleotides and Nucleosides by Capillary Electrophoresis Coupled to ESI-MS: Indications of Guanosine 5'-Monophosphate O6-N7 Chelation. *ChemBioChem*, **2004**, *5* (11), 1543-1549.
163. van der Veer, J. L.; Peters, A. R.; Reedijk, J., Reaction Products from Platinum(IV) Amine Compounds and 5'-GMP are Mainly bis(5'-GMP)Platinum(II) Amine Adducts. *J. Inorg. Biochem.*, **1986**, *26* (2), 137-142.
164. Zhang, J. Z.; Wexselblatt, E.; Hambley, T. W.; Gibson, D., Pt(IV) analogs of oxaliplatin that do not follow the expected correlation between electrochemical reduction potential and rate of reduction by ascorbate. *Chem. Commun.*, **2012**, *48* (6), 847-849.
165. Ocde, *Test No. 107: Partition Coefficient (n-octanol/water): Shake Flask Method*. Éditions OCDE.
166. Olszewski, U.; Ach, F.; Ulsperger, E.; Baumgartner, G.; Zeillinger, R.; Bednarski, P.; Hamilton, G., In Vitro Evaluation of Oxoplatin: An Oral Platinum(IV) Anticancer Agent. *Met. Based Drugs*, **2009**, *2009*, 348916.
167. Burkitt, K.; Ljungman, M., Phenylbutyrate interferes with the Fanconi anemia and BRCA pathway and sensitizes head and neck cancer cells to cisplatin. *Mol. Cancer*, **2008**, *7* (1), 24.

168. OECD, *Test No. 107: Partition Coefficient (n-octanol/water): Shake Flask Method*. OECD Publishing.
169. Carmichael, J.; DeGraff, W. G.; Gazdar, A. F.; Minna, J. D.; Mitchell, J. B., Evaluation of a Tetrazolium-based Semiautomated Colorimetric Assay: Assessment of Chemosensitivity Testing. *Cancer Res.*, **1987**, *47* (4), 936-942.
170. Farrer, N. J.; Woods, J. A.; Salassa, L.; Zhao, Y.; Robinson, K. S.; Clarkson, G.; Mackay, F. S.; Sadler, P. J., A Potent Trans-Diimine Platinum Anticancer Complex Photoactivated by Visible Light. *Angew. Chem. Int. Ed.*, **2010**, *49* (47), 8905-8908.
171. Petruzzella, E.; Margiotta, N.; Ravera, M.; Natile, G., NMR Investigation of the Spontaneous Thermal- and/or Photoinduced Reduction of trans Dihydroxido Pt(IV) Derivatives. *Inorg. Chem.*, **2013**, *52* (5), 2393-2403.
172. Montagner, D.; Yap, S. Q.; Ang, W. H., A Fluorescent Probe for Investigating the Activation of Anticancer Platinum(IV) Prodrugs Based on the Cisplatin Scaffold. *Angew. Chem. Int. Ed.*, **2013**, *52*, 11785-11789.
173. Wilson, J. J.; Lippard, S. J., Modulation of Ligand Fluorescence by the Pt(II)/Pt(IV) Redox Couple. *Inorg. Chim. Acta*, **2012**, *389*, 77-84.
174. Bonnett, R., 9.22 - Metal Complexes for Photodynamic Therapy. In *Comprehensive Coordination Chemistry II*, Meyer, J. A. M. J., Ed. Pergamon: Oxford, 2003; pp 945-1003.
175. Bigioni, M.; Benzo, A.; Irrissuto, C.; Lopez, G.; Curatella, B.; Maggi, C. A.; Manzini, S.; Crea, A.; Caroli, S.; Cubadda, F.; Binaschi, M., Antitumour effect of combination treatment with Sabarubicin (MEN 10755) and cis-platin

(DDP) in human lung tumour xenograft. *Cancer Chemother. Pharmacol.*, **2008**, 62 (4), 621-629.

176. Nitiss, J. L., Targeting DNA topoisomerase II in cancer chemotherapy. *Nat. Rev. Cancer.*, **2009**, 9 (5), 338-350.

177. Eder, J.; Teicher, B.; Holden, S.; Senator, L.; Cathcart, K. S.; Schnipper, L., Ability of four potential topoisomerase II inhibitors to enhance the cytotoxicity of cis-diamminedichloroplatinum (II) in Chinese hamster ovary cells and in an epipodophyllotoxin-resistant subline. *Cancer Chemother. Pharmacol.*, **1990**, 26 (6), 423-428.

178. Ali-Osman, F.; Berger, M. S.; Rajagopal, S.; Spence, A.; Livingston, R. B., Topoisomerase II Inhibition and Altered Kinetics of Formation and Repair of Nitrosourea and Cisplatin-induced DNA Interstrand Cross-Links and Cytotoxicity in Human Glioblastoma Cells. *Cancer Res.*, **1993**, 53 (23), 5663-5668.

179. Saleem, A.; Ibrahim, n.; Patel, M.; Li, X.-G.; Gupta, E.; Mendoza, J.; Pantazis, P.; Rubin, E. H., Mechanisms of Resistance in a Human Cell Line Exposed to Sequential Topoisomerase Poisoning. *Cancer Res.*, **1997**, 57 (22), 5100-5106.

180. Aapro, M. S.; van Wijk, F. H.; Bolis, G.; Chevallier, B.; van der Burg, M. E. L.; Poveda, A.; de Oliveira, C. F.; Tumolo, S.; Scotto di Palumbo, V.; Piccart, M.; Franchi, M.; Zanaboni, F.; Lacave, A. J.; Fontanelli, R.; Favalli, G.; Zola, P.; Guastalla, J. P.; Rosso, R.; Marth, C.; Nooij, M.; Presti, M.; Scarabelli, C.; Splinter, T. A. W.; Ploch, E.; Beex, L. V. A.; ten Bokkel Huinink, W.; Forni, M.; Melpignano, M.; Blake, P.; Kerbrat, P.; Mendiola, C.; Cervantes, A.; Goupil, A.;

Harper, P. G.; Madronal, C.; Namer, M.; Scarfone, G.; Stoot, J. E. G. M.; Teodorovic, I.; Coens, C.; Vergote, I.; Vermorken, J. B., Doxorubicin versus doxorubicin and cisplatin in endometrial carcinoma: definitive results of a randomised study (55872) by the EORTC Gynaecological Cancer Group. *Ann. Oncol.*, **2003**, *14* (3), 441-448.

181. Guthrie, T. H., Jr.; McElveen, L. J.; Porubsky, E. S.; Harmon, J. D., Cisplatin and doxorubicin. An effective chemotherapy combination in the treatment of advanced basal cell and squamous carcinoma of the skin. *Cancer*, **1985**, *55* (8), 1629-32.

182. Lyass, O.; Hubert, A.; Gabizon, A. A., Phase I Study of Doxil-Cisplatin Combination Chemotherapy in Patients with Advanced Malignancies. *Clin. Cancer Res.*, **2001**, *7* (10), 3040-3046.

183. Honda, M.; Miura, A.; Izumi, Y.; Kato, T.; Ryotokuji, T.; Monma, K.; Fujiwara, J.; Egashira, H.; Nemoto, T., Doxorubicin, cisplatin, and fluorouracil combination therapy for metastatic esophageal squamous cell carcinoma. *Dis. Esophagus*, **2010**, *23* (8), 641-5.

184. Fleming, G. F.; Brunetto, V. L.; Cella, D.; Look, K. Y.; Reid, G. C.; Munkarah, A. R.; Kline, R.; Burger, R. A.; Goodman, A.; Burks, R. T., Phase III Trial of Doxorubicin Plus Cisplatin With or Without Paclitaxel Plus Filgrastim in Advanced Endometrial Carcinoma: A Gynecologic Oncology Group Study. *J. Clin. Oncol.*, **2004**, *22* (11), 2159-2166.

185. Hu, C. M.; Aryal, S.; Zhang, L., Nanoparticle-assisted combination therapies for effective cancer treatment. *Ther. Deliv.*, **2010**, *1* (2), 323-34.

186. Ang, W. H.; Khalaila, I.; Allardyce, C. S.; Juillerat-Jeanneret, L.; Dyson, P. J., Rational Design of Platinum(IV) Compounds to Overcome Glutathione-S-Transferase Mediated Drug Resistance. *J. Am. Chem. Soc.*, **2005**, *127* (5), 1382-1383.
187. Pierschbacher, M. D.; Ruoslahti, E., Cell attachment activity of fibronectin can be duplicated by small synthetic fragments of the molecule. *Nature*, **1984**, *309* (5963), 30-33.
188. Erdreich-Epstein, A.; Shimada, H.; Groshen, S.; Liu, M.; Metelitsa, L. S.; Kim, K. S.; Stins, M. F.; Seeger, R. C.; Durden, D. L., Integrins  $\alpha(v)\beta_3$  and  $\alpha(v)\beta_5$  are expressed by endothelium of high-risk neuroblastoma and their inhibition is associated with increased endogenous ceramide. *Cancer Res.*, **2000**, *60* (3), 712-21.
189. Haubner, R.; Gratias, R.; Diefenbach, B.; Goodman, S. L.; Jonczyk, A.; Kessler, H., Structural and Functional Aspects of RGD-Containing Cyclic Pentapeptides as Highly Potent and Selective Integrin  $\alpha V\beta_3$  Antagonists. *J. Am. Chem. Soc.*, **1996**, *118* (32), 7461-7472.
190. Sivridis, E., Angiogenesis and endometrial cancer. *Anticancer Res.*, **2001**, *21* (6B), 4383-8.
191. Nayak, T. R.; Leow, P. C.; Ee, P.-L. R.; Arockiadoss, T.; Ramaprabhu, S.; Pastorin, G., Crucial Parameters Responsible for Carbon Nanotubes Toxicity. *Curr. Nanosci.*, **2010**, *6* (2), 141-154.
192. Li, J.; Yap, S. Q.; Chin, C. F.; Tian, Q.; Yoong, S. L.; Pastorin, G.; Ang, W. H., Platinum(IV) prodrugs entrapped within multiwalled carbon nanotubes:

Selective release by chemical reduction and hydrophobicity reversal. *Chem. Sci.*, **2012**, *3* (6), 2083-2087.

193. Zwellig, L. A.; Bales, E.; Altschuler, E.; Mayes, J., Circumvention of resistance by doxorubicin, but not by idarubicin, in a human leukemia cell line containing an intercalator-resistant form of topoisomerase II: evidence for a non-topoisomerase II-mediated mechanism of doxorubicin cytotoxicity. *Biochem. Pharmacol.*, **1993**, *45* (2), 516-20.

194. Nayak, T. R.; Leow, P. C. h. i. n.; Ee, P.-L. R. a. c. h. e. l.; Arockiadoss, T.; Ramaprabhu, S.; Pastorin, G., Crucial Parameters Responsible for Carbon Nanotubes Toxicity. *Curr. Nanosci.*, **2010**, *6* (2), 141-154.

195. Sarin, V. K.; Kent, S. B. H.; Tam, J. P.; Merrifield, R. B., Quantitative monitoring of solid-phase peptide synthesis by the ninhydrin reaction. *Anal. Biochem.*, **1981**, *117* (1), 147-157.

196. Bianchi, M. E., Killing cancer cells, twice with one shot. *Cell Death Differ.*, **2014**, *21* (1), 1-2.

## Appendix

**Table 7.** Selected X-ray crystallographic data for **A** and **3**

| Complex                                   | (Compound <b>A</b> )·DMSO   | 2×(Compound <b>3</b> )·acetone   |
|---|---|--|
| Formula                                   | [Pt(NH <sub>3</sub> ) <sub>2</sub> Cl <sub>2</sub> (CO <sub>2</sub> C <sub>6</sub> H <sub>5</sub> )(OH)]·C <sub>2</sub> H <sub>6</sub> OS | [Pt(NH <sub>3</sub> ) <sub>2</sub> Cl <sub>2</sub> (CO <sub>2</sub> C <sub>6</sub> H <sub>5</sub> )(CO <sub>2</sub> CH <sub>3</sub> )] <sub>2</sub> ·CH <sub>3</sub> COCH <sub>3</sub> |
| Formula weight                            | 516.3   | 1018.50  |
| Temperature [K]                           | 100(2)  | 293(2)   |
| Wavelength [Å]                            | 0.71073   | 0.71073  |
| Crystal size [mm <sup>3</sup> ]           | 0.33 × 0.24 × 0.18  | 0.50 × 0.14 × 0.08   |
| Crystal system                            | monoclinic  | monoclinic   |
| Space group                               | <i>C2/m</i>   | <i>P2<sub>1</sub>/c</i>  |
| <i>a</i> [Å]                              | 17.064(3)   | 13.660(3)  |
| <i>b</i> [Å]                              | 7.2554(12)  | 9.867(2)   |
| <i>c</i> [Å]                              | 12.642(2)   | 23.937(6)  |
| $\alpha$ [deg]                            | 90  | 90   |
| $\beta$ [deg]                             | 102.211(3)  | 98.520(5)  |
| $\gamma$ [deg]                            | 90  | 90   |
| <i>V</i> [Å <sup>3</sup> ]                | 1529.8(4)   | 3190.6(13)   |
| <i>Z</i>                                  | 4   | 8  |
| <i>D<sub>c</sub></i> [Mg/m <sup>3</sup> ] | 2.242   | 2.120  |
| $\mu$ [mm <sup>-1</sup> ]                 | 9.667   | 9.145  |
| $\theta$ range [deg]                      | 2.44 – 27.45  | 2.11 to 27.50  |
| no. of unique data                        | 5357  | 22207  |
| max., min. transmn                        | 0.2750 and 0.1426   | 0.5282 and 0.0918  |
| final R indices                           | R1 = 0.0261   | R1 = 0.0427  |
| [I > 2 $\sigma$ (I)]                      | wR2 = 0.0711  | wR2 = 0.0953   |
| R indices (all data)                      | R1 = 0.0273   | R1 = 0.0514  |
|   | wR2 = 0.0720  | wR2 = 0.0988   |
| goodness-of-fit on F <sup>2</sup>         | 1.099   | 1.100  |
| peak/hole [e Å <sup>-3</sup> ]            | 2.070 and -0.922  | 4.522 and -1.310   |

<sup>a</sup>R =  $\Sigma||F_o| - |F_c||/\Sigma|F_o|$ , wR<sup>2</sup> =  $\{\Sigma[w(F_o^2 - F_c^2)^2]/\Sigma[w(F_o^2)^2]\}^{1/2}$ . Goodness-of-fit (GOF) =  $\{\Sigma[w(F_o^2 - F_c^2)^2]/(n - p)\}^{1/2}$ , where n is the number of data and p is the number of parameters refined.

# Curriculum Vitae

Chin Chee Fei (Mr.)

National University of Singapore  
Faculty of Science, Department of Chemistry

3 Science Drive 3, Singapore 117543

Telephone: +65 96211065

Email: [a0031131@nus.edu.sg](mailto:a0031131@nus.edu.sg)

## Education

2010-2014 National University of Singapore. Ph.D., Chemistry

2006-2010 National University of Singapore. Bachelor of Science, Chemistry,

*Honors.*

## Work Experience

2006-2006 *Sales Assistant*, Panasonic Singapore.

2003-2004 *Sales Assistant*, F&N Singapore

## Awards and Fellowships

2013 Solvay Graduate Fellowship in Science, National University of  
Singapore

2010 NUS Research Scholarship

2010 Dean's List, National University of Singapore, Science.

## Teaching Experience

2011-2012 *Teaching Assistant*, National University of Singapore.

2010-2014 *BSc Research Project Mentor*, National University of Singapore.



**Submitted patent**

1. C. A. Davey, W. H. Ang, C. F. Chin, Platinum anticancer agents that allow control of nucleosome targeting, **2014**, *patent pending*.

**Published/accepted articles or articles submitted for publication**

1. C. F. Chin, D. Y. Q. Wong, R. Jothibas, W. H. Ang\*. Platinum(IV) anticancer complex with novel modes of activity, *Curr. Op. Med. Chem.*, **2011**, 11, 2602-2612.
2. C. F. Chin, Q. Tian, M. I. Setyawati, W. Fang, E. S. Q. Tan, D. T. Leong, W. H. Ang\*. Tuning the activity of platinum(IV) anticancer complexes through asymmetric acylation, *J. Med. Chem.*, **2012**, 55, 7571-7582.
3. C. F. Chin, S. Q. Yap, J. Li, G. Pastorin\*, W. H. Ang\*. Ratiometric delivery of cisplatin and doxorubicin using tumour-targeting carbon-nanotubes entrapping platinum(IV) prodrugs, *Chem. Sci.*, **2014**, 5, 2265-2270.
4. E. Y. D. Chua, G. E. Davey, C. F. Chin, P. Dröge, W. H. Ang\*, C. A. Davey\*. Modulating antitumor activity through stereochemical control of nucleosome targeting by platinum-intercalator agents. **2015**, *Nucleic Acids Res.*, accepted for publications.
5. J. Li, S. Q. Yap, C. F. Chin, G. Pastorin\*, W. H. Ang\*. Platinum(IV) prodrugs entrapped within multiwalled carbon nanotubes: Selective release by chemical reduction and hydrophobicity reversal. *Chem. Sci.* **2012**, 3, 2083-2087.
6. S. L. Yoong, B. S. Wong, Q. L. Zhou, C. F. Chin, J. Li, T. Venkatesan, H. K. Ho, V. Yu, W. H. Ang\*, G. Pastorin\*. Enhanced cytotoxicity to cancer cells by mitochondria-targeting MWCNTs containing platinum(IV) prodrug of cisplatin, *Biomaterials*, **2014**, 35, 748-753.

7. J. Li, A. Pant, C. F. Chin, W. H. Ang\*, C. Ménard-Moyon, T. R. Nayak, D. Gibson, S. Ramaprabhu, T. Panczyk, A. Bianco, G. Pastorin\*. In vivo biodistribution of platinum-based drugs encapsulated into multi-walled carbon nanotubes, *Nanomedicine*, **2014**, in press.
8. Z. Tay, S. H. Koo, N. T. T. Trang, T. S. Tan, M. L. Chen, C. F. Chin, K. K. Lim, W. H. Ang, B. H. Bay, E. J. D. Lee, E. S. Chen\*. P-glycoprotein and vacuolar ATPase synergistically confer anthracycline resistance to fission yeast and human cells, *Curr. Med. Chem.*, **2014**, 21, 251-260.
9. L. Muzi, C. M.-Moyon, J. Russier, J. Li, C. F. Chin, W. H. Ang, G. Pastorin\*, G. Risuleo, A. Bianco\*. The diameter of functionalized multi-walled carbon nanotubes filled with a cisplatin prodrug allows to control the release of the drug prolonging its anticancer efficacy, **2015**, *Nanoscale*, 2015, 7, 5383-5394.  
2015,7, 5383-5394
10. J. X. Ong, S. Q. Yap, D. Y. Q. Wong, C. F. Chin, W. H. Ang\*, Platinum(IV) carboxylate prodrug complexes as versatile platforms for targeted chemotherapy, *CHIMIA Int. J. Chem.*, **2015**, 69, 100-103(4).
11. H. V. Huynh\*, W. H. Sim, C. F. Chin. [2]Rotaxanes with Palladium(II)-NHC stoppers, *Dalton Trans.*, **2011**, 40, 11690–11692.